EFFECT OF HEPARIN ON THE IMMUNOBIOLOGY OF INTERLEUKIN 12

Khue Gia Nguyen

A dissertation submitted to the faculty of the University of North Carolina at Chapel Hill in partial fulfillment of the requirements for the degree of Doctor of Philosophy in the Department of Microbiology and Immunology.

Chapel Hill
2018

Approved by:

David Zaharoff

Jason Whitmire

Jian Liu

Roland Tisch

Yisong Wan

ABSTRACT

Khue Gia Nguyen: Effect of heparin on the immunobiology of interleukin-12
(Under the direction of David Alexander Zaharoff)

IL-12 is a potent pro-inflammatory cytokine that plays a central role in cellular immunity. Recently, we have shown that IL-12 is a specific heparin-binding protein. However, the interaction of heparin and IL-12 at the molecular level and the mechanisms by which heparin modulates the biological functions of IL-12 are unknown. For the first time, we described the unique ability of heparin to enhance the bioactivity of IL-12. Heparin was found to enhance binding of IL-12 to cell surfaces while modestly protecting the cytokine from proteolytic degradation. An exploration of critical heparin characteristics revealed that IL-12 binding and activity increased were dependent on heparin chain length and sulfation level. Based on our bioactivity data, we developed a model of stabilization showing that heparin likely serves as a co-receptor that enhances the interaction of IL-12 with its subunit receptors. Finally, we examined the effect of heparin on IL-12 bioactivity in IL-12Rβ1 deficient cells. In both PBMCs isolated from patients of Mendelian susceptibility to mycobacterial diseases (MSMD) and IL-12Rβ1 mutant NK-92MI cell line, heparin was found to partially recover IL-12 signaling as measured via IFN-γ production. Taken together, these studies define a new role for heparin as a modulator of the immunobiology of IL-12 and potentially other IL-12 family cytokines.

DEDICATION

This dissertation is dedicated to my beloved family (Khai Nguyen and Thu Tran – my parents,
Huong Le and Maggie Nguyen – my wife and my little daughter)
I couldn't make it this far without you all.

ACKNOWLEDGEMENTS

I would like to express my special thanks of gratitude to my respected advisor Dr. David A. Zaharoff for all the things he has done for me. He patiently supported me to do this wonderful project as well as trained me with all of his enthusiasm.

I am grateful to members of my dissertation committee Dr. Roland Tisch, Dr. Jason Whitmire, Dr. Jian Liu, and Dr. Yisong Wan for every valuable feedback on my dissertation.

I would like to express my thanks to my lab-mates Bhanu Koppolu, Sean Smith, Sruthi Ravindranathan, Jared Hopkins, Frank Gilliam, and Maura Vrabel who helped me during the time I worked on this project.

I take this opportunity to record sincere gratefulness to my parents, my parents-in-law, for supporting and encouraging me to pursue my dream.

Specially, I would like to thank my lovely wife Huong Le who is always by my side to take care of me, support, and energize me, and thank my little daughter Maggie Nguyen who always brings happiness to our family so that I was in the best mood to study and completed this project.

TABLE OF CONTENTS

LIST OF TABLES

LIST OF FIGURES

LIST OF ABBREVIATIONS

Arg	Arginine
BSA	Bovine serum albumin
CAR	Chimeric Antigen Receptor
CBA	Cytometric bead array
CD	Cluster of differentiation
CTLs	Cytotoxic T lymphocytes
DCs	Dendritic cells
DNA	Deoxyribonucleic acid
EBI3	Epstein-Barr virus induced gene 3
EC_{50}	Half maximal effective concentration
ECDs	Extracellular domains
ELISA	Enzyme-linked immunosorbent assay
FGF	Fibroblast growth factor
GAGs	Glycosaminoglycans
GM-CSF	Granulocyte-macrophage colony-stimulating factor
gp130	Glycoprotein 130
His	Histidine
HIV	Human immunodeficiency virus
HS	Heparan sulfate
HSV	Herpes simplex virus
IC_{50}	Half maximal inhibitory concentration
IFN-γ	Interferon gamma
IL	Interleukin

IL-12	Interleukin 12
hIL-12	Human interleukin 12
mIL-12	Mouse interleukin 12
IL-12R	Interleukin 12 receptors
IL-12Rβ1	Interleukin 12 receptor subunit β 1
IL-12Rβ2	Interleukin 12 receptor subunit β 2
ITC	Isothermal titration calorimetry
JAK	Janus kinase
LMWH	Low molecular weight heparin
LPS	Lipopolysaccharides
Lys	Lysine
MAPK	Mitogen-activated protein kinase
MHC	Major histocompatibility complex
MSMD	Mendelian susceptibility to mycobacterial diseases
NMR	Nuclear magnetic resonance
PBMCs	Peripheral blood mononuclear cells
RANKL	Receptor activator of nuclear factor–β ligand
SEAP	Secreted embryonic alkaline phosphatase
STAT	Signal transducer and activator of transcription
T_H	T helper cells
TLRs	Toll-like receptors
TNFα	Tumor necrosis factor α
TYK	Tyrosine kinase

CHAPTER 1: INTRODUCTION

1.1. The structure and production of IL-12

IL-12 is a potent pro-inflammatory cytokine that plays a central role in cellular immunity. IL-12 is composed of two subunits, p35 and p40, that are linked by three disulfide bridges to form a p70 heterodimer (1-4). The structure of p35 is similar to other single-chain cytokines, such as IL-6, whereas p40 shares homology to the hematopoietic receptor family, particularly the extracellular domain of the IL-6Rα chain (5). It has been suggested, therefore, that IL-12 arose from a combination of an IL-6 family member and its receptor (6).

p35 is constitutively expressed by various cell types while the expression of p40 is induced mainly by TLR ligands and generally limited to antigen presenting cells, such as dendritic cells, monocytes and macrophages (7). p40 is produced in excess while p35 is only secreted when linked to the p40 chain to form a complete IL-12 molecule (3). p40 is secreted in two forms, a monomer and a disulfide linked homodimer (8). Both p40 monomer and p40 homodimer have been shown to compete with IL-12 for binding to IL-12R (8-10). In mice, p40 homodimers have been detected *in vivo* during inflammatory events and have been shown to antagonize the functions of IL-12 (11). p40 homodimers overexpressed in human cells have been shown to bind to IL-12R and act as an antagonist of IL-12 in Kit225/K6 cells, a human T cell line that expresses IL-12R (12). Heparin, a negatively charged GAG, was found to inhibit the antagonist activity of p40 monomer and p40 homodimer on IL-12 (Appendix 3). Unlike in mice, p40 homodimers have not been detected in humans or produced by non-transfected human cells even in the presence of large amounts of p40 monomer (13).

1

As mentioned above, IL-12 is mainly produced by phagocytic cells, such as monocytes, macrophages, neutrophils, microglia and DCs in response to TLR stimulation with structural or released components of bacteria, parasites, or fungi, including LPS, CpG oligonucleotides, bacterial DNA, or double-stranded RNA (14). For example, 2 research groups led by Mashayekhi and Reise-Sousa have shown that CD8α^+ DCs are the first cell population to synthesize IL-12 *in vivo* in response to soluble extracts of *Toxoplasma gondii* or to LPS (15, 16). Other pathogens, such as *Brucella abortus* or CpG containing bacterial DNA, have been shown to trigger production of IL-12 by both CD8α^+ and CD8α^- DCs (17-19). In response to several types of viral infection, plasmacytoid DCs are another source of IL-12 (20). Macrophages and monocytes are strong producers of IL-12 in response to bacterial peptidoglycans (21, 22).

The production of IL-12 is controlled by positive and negative feedback mechanisms. The diversity and quantity of TLRs expressed in phagocytic cells will determine the relative efficiency of IL-12 production in response to pathogenic components (23, 24). However, TLR stimulation alone is insufficient to maximize the production of IL-12. The presence of IFN-γ enhances IL-12 production by augmenting the transcription of both p40 and p35 (25, 26). IFN-γ functions as a positive feedback factor for IL-12 production in inflammation and T_H1 responses. Interleukin-10 (IL-10), which is also induced by pathogenic stimulation, is immunosuppressive and inhibits p35 and p40 transcription (27).

1.2. IL-12 receptors and signaling

IL-12R consists of 2 receptor subunit chains, IL-12Rβ1 and IL-12Rβ2. The receptor subunits share similar morphologies with the type-I cytokine receptor superfamily and are homologous to gp130 (28). IL-12Rβ1 binds p40 with a K_d of 6 nM, IL-12Rβ2 binds p35 with a K_d of 5 nM while the p70 heterodimer binds both subunits with a K_d of 65 pM (29). IL-12Rβ2,

normally expressed on NK cells and activated T cells, plays a vital role in triggering IL-12

signaling (30). IL-12Rβ2 is up-regulated by T_H1-related cytokines and down-regulated by T_H2-

related cytokines (31). IL-12Rβ1, a type I transmembrane protein with a disulfide linked

oligomer, is constitutively expressed at low levels in lymphocyte and can be upregulated by T

cell activation (32). Upon the binding of IL-12 to IL-12R, IL-12 recruits 2 important kinases

including JAK2 and TYK2. These kinases phosphorylate themselves and IL-12R leading to the

recruitment of STAT3 and STAT4 to the intracellular domain of IL-12R. STAT3 and STAT4

binds to the phosphorylated receptor and are phosphorylated by the activated JAK2 and TYK2.

Phosphorylated STATs form dimers and translocate into the nucleus to induce expression of the

transcription factor family of interferon regulatory factors. These transcription factors then

regulate target genes that are important for the effector functions of T_H1 cells (33-37).

Individuals with defects in IL-12 signaling exhibit profound immunodeficiencies. In

particular, patients with mutations in IL-12Rβ1, IL-12β2 or TYK2 lack sufficient production of

IFN-γ. These patients are unable to mount immune responses against intracellular infections (38,

39).

IL-12 has a number of proinflammatory biological functions. Chief among these is IL-

12's ability to activate cell-mediated effectors, including NK, NKT and $CD8^+$ T lymphocytes

(40, 41). Specifically, IL-12 promotes the proliferation, cytotoxic activity and IFN-γ production

of activated NK and $CD8^+$ T cells. IL-12 also induces the differentiation of naïve $CD4^+$ T

lymphocytes into T_H1 effectors that produce IFN-γ (42-45). In addition, IL-12 recruits NK cells

to tissues by serving as a direct chemotactic factor (46). Furthermore, IL-12 has been found to

mediate the activation of human and murine B cells (47, 48). B lymphocytes can be developed

into IFN-γ producing cells when they are synergically stimulated with IL-12 and IL-18 *in vivo* (49).

1.3. IL-12-based cancer immunotherapy

1.3.1. The use of IL-12 as an antitumor reagent

The pleiotropic functions of IL-12 which drive cellular immunity support its exploration as an antitumor agent. In addition to the biological activities of IL-12 mentioned in the previous section, IFN-γ, which is strongly induced by IL-12 has been shown to be directly cytotoxic/cytostatic to some tumor cells, upregulates MHC class I on tumor cells, has anti-angiogenic activity, and enhances T cell infiltration into tumors (50-53). Not surprisingly then, in numerous preclinical studies, the systemic administration of recombinant IL-12 triggers tumor regression and increases survival rate in mice bearing a wide range of transplantable, spontaneous, or carcinogen-induced tumors (54-57). Antitumor effects of IL-12 were found to be largely dependent on CD8^{+} T cells, NK and NK T cells (55, 58, 59).

In clinical studies, IL-12 has been evaluated as an experimental treatment for numerous malignancies (60-70). Unfortunately, the efficacy of IL-12 at tolerated doses was minimal (61, 62, 65). Atkins and colleagues were the first to employ IL-12 immunotherapy in a clinical trial (60). This phase I study enrolled 40 patients, including 20 with renal cancer and 12 with melanoma, to investigate intravenous administration of recombinant hIL-12. One melanoma patient had a transient complete response and one renal cancer patient had a partial response with recombinant hIL-12 (60). In a separate study, ten pretreated patients with advanced melanoma were enrolled in a pilot study of subcutaneous recombinant hIL-12 (61). A fixed dose of recombinant hIL-12 (0.5 μg/kg) was given to patients on days 1, 8, and 15 for two sequential cycles of 28 days. No partial or complete responses were reported. Minor tumor shrinkages

involving some subcutaneous metastases and hepatic metastases were observed.(61). In yet another study in melanoma patients, the administration of IL-12 was found to induce a striking burst, in the periphery, of HLA-restricted CTL precursors directed to autologous tumors and to multiple immunogenic tumor-associated antigens (71). Significantly, the infiltration of CD8^{+} T cells with a memory and cytolytic phenotype was identified in posttreatment metastatic lesions, but not in pretreatment metastatic lesions of three patients (71). IL-12 has induced more productive antitumor responses against cutaneous T cell lymphoma variants (70), AIDS-related Kaposi sarcoma (76) and non–Hodgkin's lymphoma (77), however, it has never progressed past phase II studies.

Although IL-12 has demonstrated robust antitumor activity in preclinical studies and potent immune-stimulating potential in humans, systemic administrations of IL-12 have been shown to be exceedingly toxic. In a phase II trial sponsored by Genetics Institute, a maximal dose of 0.5 µg/kg per day resulted in severe side effects in 12 out of 17 enrolled patients and the deaths of two patients (72). Interestingly, the dose of 0.5 µg/kg IL-12 per day was found to be well-tolerated in patients that were enrolled in a previous phase I study. A difference in dosing schedule accounted for the differences in toxicity between the phase I and phase II trials. In the phase I trial, a single tester dose of IL-12 was administered one week before a multiple-dose regimen. The tester dose was found to blunt the toxicity associated with the multiple doses (73).

1.3.2. Advances of IL-12 based cancer immunotherapy

Due to the toxic effects of IL-12, recent efforts have focused on delivery strategies with potential to target tumors directly and/or restrict the systemic dissemination of IL-12. (59, 60). Numerous technologies involving gene delivery, IL-12-encapsulation, injectable hydrogels, and targeted IL-12-fusion proteins are under investigation (54, 61-66).

1.3.2.1. Gene-based delivery of IL-12

Gene-based delivery of IL-12 is attractive for several reasons. First, in vivo expression of IL-12 can provide sustained cytokine levels that overcomes the need for multiple administrations due to rapid IL-12 clearance. Second, if the plasmid containing IL-12 gene is locally delivered, i.e. directly within a tumor, more of the IL-12 will be retained at the desired site/tissue compared to systemic delivery of recombinant IL-12. High local levels of IL-12 are capable of triggering antitumor responses. Intratumoral (i.t.) injections of plasmid DNA encoding IL-12 have demonstrated significant antitumor activity against melanoma (74), colorectal adenocarcinoma (75-78) and renal cell carcinoma (76) in preclinical models. In the clinic, i.t. injections of IL-12 plasmid were found to reduce the size of treated lesions by at least 30% in 5 of 12 patients enrolled in a Phase I/IB study (79). In another Phase I/II trial, 3 of 9 and 8 of 9 patients with stage IV malignant melanoma experienced clinical and local responses, respectively, following intralesional injections with IL-12 plasmid (80). IL-12 plasmid injections were well tolerated as no patient in either study experienced a significant treatment related adverse event.

Several technologies are under investigation to enhance the delivery and antitumor activity of IL-12-encoding DNA. The application of pulsed, high electric fields to facilitate cellular uptake and expression of a therapeutic gene is called electro-gene therapy (EGT). EGT with cytokine-encoding genes injected i.t. has been explored in range of tumor models (81-85); SCCVII (85), CT26 (86), RENCA (86-88). EGT with i.t. IL-12 plasmid induced tumor regression in up to 80% of mice, whereas i.t. injections of IL-12 plasmid alone delayed but could not eliminate primary tumors (84). In other tumor models, EGT with i.t. IL-12 plasmid suppressed the growth of murine SA-1 sarcomas leading to complete regression in approximately 50-90% of treated mice (87, 89). Importantly, i.t. IL-12 EGT was able to inhibit the growth of

distant untreated tumors (89). In a study using dogs presenting with mast cell tumors, i.t. IL-12 EGT resulted in a 13 to 83% reduction in tumor volume (90). Treated nodules displayed increases in leukocytic inflammation and decreases in the number of malignant mast cells (90). In beagles with canine transmissible venereal tumors (CTVTs), i.t. IL-12 plasmid followed by electroporation induced complete regression of treated lesions (91). Contralateral untreated tumors were also significantly inhibited. Serum IL-12 peaked 7 days after treatment however, blood chemistries and cell counts were not different from those of control dogs (91).

Reports conflict on whether i.t. IL-12 EGT does (89-94) or does not (83, 87, 95) produce significant increases in serum IL-12 and IFN-γ. One study that i.t. IL-12 EGT of subcutaneous (s.c.) MH134 hepatocellular carcinomas resulted in elevated serum IL-12 and IFN-γ for at least one month (93).

Recently, a Phase I study using electroporation immediately following i.t. injection of IL-12 plasmid demonstrated that 53% of patients with stage III or IV melanoma experienced a systemic response defined as either stable disease or regression of untreated lesions (96). Most notably, 2 of 19 patients showed complete regression of all metastases. The importance of electric-field assisted delivery of plasmid was obvious as the aforementioned Phase I/IB study by Mahvi et al. used the same IL-12 vector without electric-field but found no differences in untreated lesions (79)..

Complexes of polymers or lipids with DNA, are under investigation to enhance the delivery and transfection efficiency of cytokine-encoding plasmids. IL-12 plasmid/PVP polyplexes eliminated half of RENCA and CT26 tumors following 4 i.t. injections (97). Antitumor responses were dependent on CD8$^+$ T cell. Overt signs of toxicity normally associated with systemic IL-12 administration were not observed. IL-12/PVP was more effective than

IFNα/PVP in controlling preclinical tumors while the combination of IL-12/PVP and IFNα/PVP synergized to eliminate 100% of RENCA and 50% of CT26 tumors (98). Plasmids complexed with poly-a-(4-aminobutyl)-L-glycolic acid (PAGA) enhanced transfection efficiency and expression of IL-12 in vitro and in vivo (77, 99). However, T cell infiltration of injected CT26 colon adenocarcinomas and antitumor activities following repeated injections of PAGA/IL-12 and naked IL-12 were similar (77). IL-12 DNA complexed with a cationic lipid and injected i.t. was found to inhibit and eliminate CT26 and RENCA tumors and protected mice from re-challenge (76). Interesting, a direct comparison between naked IL-12 DNA and lipid complexed IL-12 DNA revealed no difference in antitumor activity (76).

Currently, there are 5 ongoing clinical trials evaluating gene-based delivery of IL-12 in cancer treatment that are listed on the cllinicaltrials.gov website provided by the National Library of Medicine at the National Institutes of Health (NCT03281382, NCT02555397, NCT02531425, NCT03132675, NCT03567720. Key words used for searching included "IL-12 gene therapy", "cancer").

Although no serious IL-12-related toxicities have been reported in any of the above studies, the use of IL-12 DNA raises concerns over the possibilities of uncontrolled IL-12 production and genetic recombination. In addition, a major disadvantage of this approach is the inherent variability of IL-12 transfection in vivo.

1.3.2.2 Oncolytic Viruses

Oncolytic viruses expressing IL-12 have become a promising trend in cancer therapy. Recently, T-VEC, a genetically engineered herpes simplex virus producing GM-CSF, was the first oncolytic virus to receive by the FDA approval. Oncolytic viruses were first discovered in the late 19th century in cancer patients who simultaneously developed viral infections (100, 101).

Oncolytic viruses are able to selectively lyse cancer cells expressing low level of proteins that play important roles in both tumor suppression and viral infection, e.g. p53 protein. A genetically engineered HSV-1 expressing IL-12 is currently being tested in patients with recurrent/progressive glioblastoma multiforme, anaplastic astrocytoma, or gliosarcoma in a phase I study (102). In the study, M032 oncolytic HSV-1 was infused via a catheter at a single dose into tumor sites defined by magnetic resonance imaging. The results showed that M032 oncolytic HSV-1 selectively infected and lysed tumor cells but not normal cells. Local secretion of IL-12 promoted specific antitumor responses at the tumor sites. In another study, oncolytic adenovirus encoding non-secreting IL-12 was effective in enhancing survival of animals bearing pancreatic tumors with no toxic side effect (103). Removing the signal peptide sequence of IL-12 led to the accumulation of IL-12 inside cancer cells with minimal systemic release.

1.3.2.3 Immunocytokines

Immunocytokines, also known as antibody-cytokine fusion proteins, allow potentially toxic cytokines, such as IL-12, to be targeted to a tumor following systemic administration (104). The targeted element, usually an antibody fragment, can be engineered to bind tumor cells directly via mutant or overexpressed proteins or indirectly by targeting tumor vasculature or stromal components.

The monoclonal antibody, BC-1, which recognizes the oncofetal fibronectin isoform, B-FN. B-FN is highly expressed in tumor tissues but undetectable in normal adult tissues with the exception of endometrium (105). The immunocytokine, huBC1-IL12, is comprised of two molecules of IL-12 linked to each of the IgG heavy chains of BC-1 (105). Systemic administration of huBC1-IL12 was found to eliminate experimental PC3 metastases and suppress

the growth of multiple human tumor lines in immunocompromised mice more effectively than IL-12 alone (105).

Another IL-12 fusion cytokine, NHS-IL12 capitalizes on the specificity of the NHS76 antibody for extracellular DNA often found in necrotic tumors. NHS-IL12 has been shown to delay the growth of colorectal carcinomas in mice (106). Furthermore, tumor-bearing mice treated with NHS-IL12 developed CD8^{+} T cell responses against endogenous tumor antigens. In vivo imaging studies showed that NHS-IL12 was localized to flank tumors following a s.c. injection. NHS-IL12 is currently in Phase I clinical studies (NCT01417546)

IL-12 has also been fused with the two F8 antibodies in single-chain variable fragment format specific to the extra domain A of fibronectin, a marker of tumor neovasculature (107). The novel molecule named IL-12-F8-F8 could be produced in mammalian cells at high yield. This immunocytokine inhibited tumor growth in three different murine tumor models, including subcutaneous teratocarcinoma, colon carcinoma, and lymphoma (107).

One limitation of immunocytokines is that all targeting moieties are susceptible to non-specific binding and distribution in normal, untargeted tissues. Radiolabeled NHS76 has been found in all major tissues in mice for 2-3 days after intravenous administration (108). In the case of neovasculature targeting moieties, angiogenesis is a normal process of wound healing and provides for atherosclerotic blood vessels. As a result, hypertension is a frequent adverse event for bevacizumab. Further complicating DNA-targeting agents, cancer patients have high levels of circulating cell-free DNA that is shed from tumors. It is not clear how circulating DNA impacts NHS targeting.

Another concern is that systemically administered immunocytokines can still be expected to interact with immune cells in circulation. NK cells in particular are capable of producing large

amounts of IFN-γ which can lead to severe toxicities. The hope of this approach is that the use of

targeting moieties may improve biodistribution enough to enhance IL-12's therapeutic window.

1.3.2.4 Sustained release platforms for localized delivery of recombinant IL-12

Local administration of recombinant IL-12 protein is the most direct and most

quantifiable strategy in terms of ensuring the accuracy and reproducibility of a delivered dose.

However, recombinant cytokines disseminate rapidly from local injection sites (109). In fact, as

mentioned above, s.c. injections of IL-12 caused dose-limiting toxicities in early clinical trials

(62, 110). In order to maintain high levels of cytokines in the tumor microenvironment while

minimizing systemic exposure, several delivery strategies are being investigated. The two most

promising approaches are highlighted here.

First, encapsulation of IL-12 in polycaprolactone:polylactic acid (PCL) and polylactic

acid (PLA) microparticles has shown promise for i.t. immunotherapy of murine (111) and human

tumors (112, 113). However, differences in antitumor efficacy have been noted in different

models. For example, Egilmez et al. report that IL-12 encapsulated in PLA microspheres and

injected i.t. can eradicate 70% of Line-1 tumors and 80% of CT26 tumors (111), however, others

have found that the same immunotherapy regimen could not prevent the growth of B16

melanoma (114) or MT-901 mammary carcinomas (115). Another concern of microsphere

encapsulation of IL-12, is the required use of organic solvents during formulation. These

solvents can denature IL-12 immediately or adversely affect long term storage if they are not

completely removed. In fact, more than 80% of the bioactivity of IL-12 was lost when PLA/IL-

12 microsphere were stored for three weeks.

The second approach involves development of injectable hydrogels and matrices capable

of co-formulation with, and sustained, local release of IL-12. Our group has pioneered the use of

chitosan-based solutions and hydrogels for the local delivery of immunomodulatory agents, such as IL-12 (55, 116-118). Chitosan is a bioadhesive polysaccharide derived primarily from the exoskeletons of crustaceans. It is an unbranched copolymer of glucosamine and N-acetylglucosamine units linked by β(1-4) glycosidic bonds. Chitosan is non-toxic, biodegradable, and non-immunoreactive with an established safety profile in humans. It is used as a pharmaceutical excipient, a weight loss supplement and as active component of FDA-approved hemostatic dressings. In vivo, chitosan is safely degraded into excretable glucosamine and N-acetylglucosamine fragments by lysozyme, glucosaminidase, lipase and other endogenous human enzymes. Importantly, chitosan is formulable in mild aqueous solutions which enables it to maintain bioactivities of fragile cytokines.

Co-formulations of IL-12 with chitosan (CS/IL-12), when administered intratumorally, causes complete tumor regression in 80-100% of mice bearing established colorectal and pancreatic2 tumors (55). In an aggressive triple negative breast cancer model, neoadjuvant CS/IL-12 immunotherapy eliminated metastases in two-thirds of treated mice (117). In an orthotopic bladder cancer model, intravesical administration of CS/IL-12 induced complete tumor regression in 88-100% of mice. More importantly, in a dual tumor model, mice could be cured of a flank MB49 tumor if an orthotopic MB49 tumor was treated intravesically with CS/IL-12 (116, 118). In the absence of an orthotopic tumor, treated mice did not eliminate flank tumors. Thus, CS/IL-12 is capable of inducing an in situ vaccination leading to abscopal responses.

Mechanistic studies revealed that CD8^{+} T cells were required for tumor regression while CD4^{+} T cells played a minor role. Tumors treated with CS/IL-12 became heavily infiltrated by

both $CD4^+$ and $CD8^+$ effector-memory T cells. Ongoing work with this platform is aimed at elucidating the neoantigen specificity of the cytotoxic T cell response.

1.4. Heparin as a cytokine modulator

Heparin is a naturally occurring polymer of the glycosaminoglycan (GAG) molecular family (119-121). Heparin is well known as the highest negatively charged polysaccharide of any known biological molecule (122). Heparin, which binds antithrombin, a critical protein in regulating coagulation, was the first anticoagulant drug to be discovered and approved for human useb (119). Additional biological functions of heparin include inhibition of angiogenesis and tumor growth (123, 124), antiviral activity (125-130), and inhibition of complement activation (131, 132). Heparin's biological functions derive from its interaction with numerous proteins. The binding of proteins by heparin is mostly electrostatic, involving interactions between cationic groups of proteins with anionic sites on heparin.

During the past several decades, more than 400 proteins, including many cytokines, have been shown to bind to heparin (133). Of particular interest to this dissertation research are the effects of heparin on the biological activities of interleukins. Heparin has been found to enhance the functions of some interleukins, while inhibiting others. On yet other interleukins, heparin has shown not any modulatory activity. These seemingly contradictory effects might be explained by the location of heparin binding sites on each interleukin. On the one hand, the binding of heparin may block the interaction of an interleukin with its receptor thus inhibiting interleukin bioactivity. On the other hand, heparin may cause oligomerization of interleukins leading to enhanced IL/ILR interactions, similar to FGF. Heparin may also stabilize the interaction of interleukin and its receptors to enhance interleukin signaling. The sections below will describe heparin or heparan sulfate-induced modulation of interleukin activity.

1.5. The binding of heparin-interleukin has no effect on interleukin bioactivity

1.5.1. Interleukin 2 (IL-2)

IL-2 is synthesized and secreted by antigen- or mitogen-activated T-cells. This glycoprotein promotes the proliferation of T cells and has an immunomodulatory effect on cytotoxic T-cells, natural killer cells, activated B-cells, and lymphokine activated cells (134, 135). Najjam and colleagues showed a concentration-dependent interaction between human IL-2 and heparin by ELISA (136). They reported two putative heparin binding sites on human IL-2. The first binding site consists of four basic amino acids, Lys48, Lys49, Lys54, and His55, whereas the other binding site contains a discontinuous region including Lys43, Lys64, Arg81, and Arg83. The binding of heparin to human IL-2 does not influence the latter's bioactivity. Interestingly, the binding of heparin to human IL-2 was found to be dependent on heparin chain length while heparin did not bind to murine IL-2 (137). They also showed that the putative binding sites for heparin on IL-2 are well separated from the receptor binding sites (137).

1.5.2. Interleukin 6 (IL-6)

IL-6 plays diverse and important roles in various cell types (138). IL-6 is involved in host immune defense as well as modulation of growth and differentiation of many types of malignant tumors (139-141). Mummery and colleagues showed that IL-6 is a heparin-binding cytokine using an ELISA approach (142). It was suggested that the interaction with heparin could help localize pro-inflammatory IL-6 in or near a tissue of interest, thus favoring a paracrine mechanism of action. This study showed that the binding of heparin protects IL-6 from proteolytic degradation. By analyzing the effects of heparin on anti-IL-6 antibody binding, the authors concluded that heparin does not bind to epitopes that are critical for engagement of IL-6R (142).

1.6. The binding of heparin-interleukin inhibits the bioactivity of interleukins

1.6.1. Interleukin 4 (IL-4)

IL-4 is a pleiotropic cytokine that was originally described as a B-cell growth factor (143). It produces both stimulatory and inhibitory effects on growth, differentiation and functional activity of B cells and T cells (144). Using different binding experiments, Lortat-Jacob and colleagues investigated the interaction of IL-4 and an array of GAGs, including heparin, heparan sulfate, dermatan sulfate, chondroitin sulfate (145). IL-4 exhibits a stronger binding interaction to heparin and heparan sulfate compared to less sulfated GAGs. In another study, the bioactivity of IL-4 was shown to be inhibited by heparin/heparan sulfate (146). The interaction of IL-4 and heparin was assessed by IL-4 binding to a heparin sepharose column. After incubation on a heparin sepharose column for 30 minutes, IL-4 was eluted and then tested on human peripheral blood monocytes. The effect of GAGs on IL-4 activity was then investigated by incubating IL-4 with dermatan sulfate and heparan sulfate (other GAGs that shared similar structure with heparin) for 30 minutes prior to treatment of IL-4 on human monocytes. The results revealed that IL-4-mediated suppression of LPS-induced TNFα was significantly inhibited by these types of GAGs (146).

1.6.2. Interleukin 7 (IL-7)

IL-7 is a hematopoietic growth factor that influences development, proliferation and homeostasis of B and T cells (147). Clarke and colleagues proposed that heparin acts as a carrier for IL-7 to block its effect on target cells while preventing degradation from proteolysis (148). They found that heparin could inhibit the proliferation of an IL-7 dependent pre-B cell line (2E8) and protect IL-7 from serine protease digestion.

Zhang and colleagues dissected the binding interactions between heparin and murine and human IL-7 through surface resonance spectroscopy (149). The results showed that heparin had a greater affinity with human IL-7 when compared with murine IL-7. They believed that the degree of sulfation plays a key role in the interaction between IL-7 and heparin. As shown by the Borghesi group, heparan sulfate is required for the binding and bioactivity of IL-7 in pro-B cells (150). Other experiments in this study suggested that heparan sulfate proteoglycan expressed on stromal cell surfaces control the interaction of IL-7 to B-cell precursors. Therefore, they proposed that heparin and heparan sulfate proteoglycans may serve as a co-receptor of IL-7.

1.6.3. Interleukin 10 (IL-10)

IL-10 is a cytokine produced by many cell types, including macrophages, activated T and B cells, B-cell lymphomas, keratinocytes, and mast cells. IL-10 is a pleiotropic cytokine that exhibits suppressive and stimulatory effects on the immune system (151). For instance, IL-10 inhibits the expression of pro-inflammatory cytokines, including IL-12, secreted by macrophages and dendritic cells as well as antigen presentation. However, IL-10 enhances the proliferation and differentiation of B cells, murine thymocytes, mast cells, and megakaryocyte progenitor cells. The analyses of amino acid sequence have revealed that the C-terminus is rich in the basic amino acids arginine and lysine that serves as a binding site for GAGs (152). The expression of CD16 and CD64 stimulated by IL-10 on monocytes/macrophages could be inhibited by GAGs, such as soluble heparin, heparan sulfate, chondroitin sulfate, and dermatan sulfate in a concentration-dependent manner. Heparin and heparan sulfate were most effective with the half maximal inhibitory concentration (IC_{50}) values of 100 to 500 mg/mL. Considerably higher concentrations of dermatan sulfate and chondroitin 4-sulfate were required with an IC_{50} of 2000 to 5000 mg/mL, whereas chondroitin 6-sulfate was essentially inactive (152).

1.7. The binding of heparin-interleukin enhances the bioactivity of interleukins

1.7.1. Interleukin 3 (IL-3)

IL-3 was first discovered as a cytokine produced by concanavalin A-stimulated lymphocytes. IL-3 has multiple effects on proliferation and differentiation of many leukocytes (153, 154). Heparan sulfate, which is expressed on mouse bone marrow stroma, was found to adsorb and retain the biological activity of IL-3 (155). This discovery defined an important role for sulfated GAGs in the association of cytokines and hematopoietic stroma. The ability to bind and modulate IL-3 bioactivity of sulfated GAGs were investigated in another study that showed low doses of heparin enhance the bioactivity of IL-3 while high doses of heparin inhibit its bioactivity (156). This study also demonstrated that only heparin and heparan sulfate, not other GAGs, can modulate IL-3 activity.

1.7.2. Interleukin 5 (IL-5)

IL-5 plays an important role in eosinopoiesis and diseases associated with increased eosinophils (157, 158). IL-5 is secreted by T_H2 cells and mast cells. Lipscombe and colleagues showed that IL-5 can bind to heparin and this interaction enhances the proliferation of an IL-5 dependent cell line (159). In detail, the heparin-IL-5 interaction was detected using an ELISA-based binding assay that showed human IL-5 has a stronger affinity to heparin when compared with murine IL-5. Furthermore, the bioactivity of IL-5, which was measured by the proliferation rate of the Baf-IL-5 cell line, was found to be increased by the addition of heparan sulfate. The interaction between IL-5 and GAGs including heparin, heparan sulfate and dermatan sulfate was explained not only by electrostatic interaction but also by the presence of L-iduronic acid (159). Additionally, it was found that ethylenediaminetetraacetate (EDTA) can inhibit the interaction between IL-5 and heparin; this inhibition is enhanced by insufficient concentrations of zinc ions.

1.7.3. Interleukin 8 (IL-8)

IL-8 is a neutrophil chemotactic factor that is produced by multiple cell populations including monocytes, dermal fibroblasts, keratinocytes, endothelial cells, and hepatocytes (160, 161). To study the interaction between heparin and IL-8, Möbius and colleagues conducted multi-disciplinary approaches involving site-directed mutagenesis, mass spectrometry, fluorescence and solution NMR spectroscopy as well as computer modeling (162). The results indicated that the interaction between heparin and IL-8 was mainly due to the amine groups of lysine and the guanidinium group of arginine side chains. Specifically, they identified Lys25, Lys69 and Lys72 were the most relevant binding sites of IL-8 with heparin.

In another study, Spillmann and colleagues analyzed binding sequence for interaction between IL-8 and heparin/heparin sulfate (163). They found that the interaction of a monomer IL-8 and heparin/heparan sulfate is not strong enough to favor an interaction, while the dimeric form of IL-8 facilitates binding to sulfated domains of heparin/heparan sulfate. They suggested that the binding motif of IL-8 and heparan sulfate occurs in a horseshoe area over two antiparallel-oriented helical regions on the dimeric IL-8.

Webb and colleagues showed the interaction of IL-8 with heparin would be affected when IL-8 structure was truncated (164). Removal of the N-terminal region prior the first cysteine, which was the IL-8 receptor-binding site, did not impact the affinity to heparin. Affinity was decreased with truncation at the C terminus, and no binding was observed when the C-terminal alpha-helix was eliminated. When they induced neutrophils with IL-8 and heparan sulfate, neutrophil chemotaxis *in vitro* was enhanced up to 4-fold, whereas IL-8 alone did not enhance the chemotaxis of neutrophils. Therefore, these data emphasized that heparan sulfate

plays important functions in enhancing IL-8 dependent migration of neutrophils, as well as preventing IL-8 from lytic enzyme released from the migrating cells (164).

1.7.4. Interleukin 11 (IL-11)

IL-11, a member of the gp130 receptor family of cytokines, plays essential functions in T-cell-dependent development of immunoglobulin-producing B cells and synergizes with IL-3 in supporting murine megakaryocyte colony formation (165). Walton and colleagues investigated the cooperative activity between IL-11 and heparin to induce STAT3 activation (166). Their results revealed that heparin enhances both IL-11–induced STAT3-DNA complex formation and transactivation with unchanged level of STAT3 tyrosine or serine phosphorylation. Furthermore, heparin was also found to enhance IL-11's ability to induce the expression of both receptor activator of nuclear factor–B ligand (RANKL) and glycoprotein (gp) 130.

Rajgopal and colleagues examined the effect of serine kinase inhibitors on the co-operative activity between heparin and IL-11 (167). They found that heparin synergistically enhanced IL-11 signaling through up-regulation of the mitogen-activated protein kinase (MAPK) pathway. Heparin was found to increase IL-11-induced Erk1/2 activation in a time-and dose-dependent manner. These findings suggested that heparin enhanced IL-11-induced STAT3 activation and involved up-regulation of the MAPK pathway.

1.7.5. Interleukin 12 (IL-12)

IL-12 was shown to strongly bind to immobilized heparin-BSA complex (168). This binding affinity was determined greater than interactions between heparin and two well-known heparin-binding proteins, anti-thrombin III and FGF (168). Furthermore, key residues of the interaction between heparin and IL-12 were identified as N-sulfated glucoamine-2-O-sulfated iduronate disaccharides (168). These results showed for the first time that IL-12 is a heparin-

binding cytokine. A follow up study from the same group used truncated IL-12 molecules to narrow down the heparin binding domain to the D3 region on p40 (169).

The biological consequences of heparin-IL-12 binding was investigated in several studies by our group. (169-171). Jayanthi and colleagues developed a novel method to purify recombinant IL-12 protein (170). They showed a robust heparin-affinity based purification of recombinant IL-12 from the supernatants collected from hIL-12 transduced HEK293 cells. Putative heparin binding sites on hIL-12 were predicted on p40 subunit by using an *in silico* analysis. In a follow up study, it was shown that that heparin binds to IL-12 with low micromolar affinity and enhances the biological activity of IL-12 by up to 6-fold (171). Heparin potentially induced dimerization of hIL-12 and modestly protected hIL-12 from proteolytic degradation. Using a flow cytometry-based binding assay, the amount of hIL-12 bound to cell surfaces was increased in the presence of heparin. Recently, Garnier and colleagues characterized the interaction between heparin and IL-12 using several types of chemically modified heparins (169). Using endoprotease LysC as a proteolytic enzyme, they showed that heparin only protected the p40 subunit from proteolytic degradation in comparison with p35 subunit. This further suggests that the p40 subunit is the location of the heparin binding site. The endoprotease LysC was employed in this study because it cleaves adjacent to lysine residues, which due to their strongly basic side chains and are along with arginine, key residues in heparin binding sites (169).

1.8. Significance of the dissertation

IL-12 serves as a key link between innate and adaptive immunity based on its production by antigen presenting cells and its ability to activate natural killer (NK) cells and T lymphocytes (172). IL-12 is a potent cytokine that significantly enhances cell-mediated immune responses.

Due to this potent activity, IL-12 has been used in the clinic for the treatment of intracellular pathogens (173), and HIV infection (174). Our group and others are exploring the use of IL-12 for cancer immunotherapy (55, 60, 61, 69, 116).

Heparin, a negative charge glycosaminoglycan (GAG), is known to modulate the function of numerous cytokines, generally having a neutral or inhibitory effect (136, 142, 146, 152). Using *in silico* analysis, we found heparin-binding domains located on the p40 subunit of IL-12. These sites were exploited to purify recombinant IL-12 in a single-step purification procedure (170).

Prior to this dissertation research, the effect of heparin on the bioactivity of IL-12 had not been studied. After demonstrating, for the first time, that heparin binds to IL-12 with low micromolar affinity and increases IL-12 bioactivity by more than 6-fold (Chapter 2) (171), our research focused on understanding the mechanisms by which heparin influences IL-12 bioactivity. In Chapter 3, we demonstrated the characteristics of heparin that were necessary for enhanced IL-12 activity. Based on these required characteristics, we developed the first working model of stabilization which hypothesized that heparin molecules of sufficient length are able to span heparin binding domains on different subunits of IL-12 and its receptor. Binding to multiple subunits would serve to enhance or stabilize the IL-12/IL-12R complex leading to enhanced signaling. Additional research, found in Appendix 1, demonstrated for the first time, the ability of heparin to recover IL-12 signaling in cells deficient in the IL-12Rβ1 receptor subunit. Although the mechanism of IL-12 recovery could not be determined.

Taken together, the findings presented in this dissertation reveal a novel immunomodulatory function of heparin on one of the most important cytokines in human immunity. Completed studies describe the unique structure-function relationship of heparin and

IL-12 and improve our understanding of IL-12 immunobiology. In addition to these contributions to basic immunology, in the future, data in this dissertation may be exploited in the development of novel heparin-based delivery systems or IL-12-based immunotherapies. Furthermore, this research has significant implications in other IL-12 family cytokines which share similar subunits and subunit receptors.

1.9. Hypothesis and Specific Aims

Given that heparin modulates the activities of numerous cytokines, we hypothesized that the interaction of heparin and IL-12 plays a role in modulating biological functions of IL-12. To address this hypothesis as well as to study the mechanisms of heparin-induced IL-12 modulation, we proposed three specific aims: [1] assess heparin-induced modulation of IL-12 bioactivity, [2] explore the molecular mechanism(s) underlying heparin-induced modulation of IL-12 bioactivity, and [3] investigate the effect of heparin on IL-12 bioactivity in IL-12Rβ1 deficient cells.

In the first specific aim, we quantified the affinity of the heparin-IL-12 interaction and its biological effects in multiple cell types. Heparin was compared to other glycosaminoglycans to determine if binding as well as any immunomodulatory effects on IL-12 were specific to heparin. We also investigated biophysical and biochemical parameters to determine if heparin altered IL-12 conformation or susceptibility to proteolytic digestion.

In the second aim, we extended our study to examine characteristics of heparin that play essential roles in modulating hIL-12 bioactivity. Ultimately, we sought to develop a working model that describes how heparin interacts with IL-12 and its receptor subunit to enhance signaling.

In the third aim, because preliminary data demonstrated that heparin was able to recover the bioactivity of IL-12 in cells expressing non-functional IL-12 receptors, we sought to elucidate the mechanisms underlying this recovery. Experiments were performed in 2 cell types that lacked normal IL-12Rβ1 expression including IL-12Rβ1 deficient PBMCs from MSMD patients and IL-12Rβ1 mutant NK-92MI cells.

REFERENCES

1. Kobayashi M, Fitz L, Ryan M, Hewick RM, Clark SC, Chan S, Loudon R, Sherman F, Perussia B, Trinchieri G. 1989. Identification and purification of natural killer cell stimulatory factor (NKSF), a cytokine with multiple biologic effects on human lymphocytes. *J Exp Med* 170: 827-45

2. Gubler U, Chua AO, Schoenhaut DS, Dwyer CM, McComas W, Motyka R, Nabavi N, Wolitzky AG, Quinn PM, Familletti PC, et al. 1991. Coexpression of two distinct genes is required to generate secreted bioactive cytotoxic lymphocyte maturation factor. *Proc Natl Acad Sci U S A* 88: 4143-7

3. Wolf SF, Temple PA, Kobayashi M, Young D, Dicig M, Lowe L, Dzialo R, Fitz L, Ferenz C, Hewick RM, et al. 1991. Cloning of cDNA for natural killer cell stimulatory factor, a heterodimeric cytokine with multiple biologic effects on T and natural killer cells. *J Immunol* 146: 3074-81

4. Schoenhaut DS, Chua AO, Wolitzky AG, Quinn PM, Dwyer CM, McComas W, Familletti PC, Gately MK, Gubler U. 1992. Cloning and expression of murine IL-12. *J Immunol* 148: 3433-40

5. Merberg DM, Wolf SF, Clark SC. 1992. Sequence similarity between NKSF and the IL-6/G-CSF family. *Immunol Today* 13: 77-8

6. Trinchieri G, Pflanz S, Kastelein RA. 2003. The IL-12 family of heterodimeric cytokines: new players in the regulation of T cell responses. *Immunity* 19: 641-4

7. Jalah R, Rosati M, Ganneru B, Pilkington GR, Valentin A, Kulkarni V, Bergamaschi C, Chowdhury B, Zhang GM, Beach RK, Alicea C, Broderick KE, Sardesai NY, Pavlakis GN, Felber BK. 2013. The p40 subunit of interleukin (IL)-12 promotes stabilization and export of the p35 subunit: implications for improved IL-12 cytokine production. *J Biol Chem* 288: 6763-76

8. Gillessen S, Carvajal D, Ling P, Podlaski FJ, Stremlo DL, Familletti PC, Gubler U, Presky DH, Stern AS, Gately MK. 1995. Mouse interleukin-12 (IL-12) p40 homodimer: a potent IL-12 antagonist. *Eur J Immunol* 25: 200-6

9. Mattner F, Fischer S, Guckes S, Jin S, Kaulen H, Schmitt E, Rude E, Germann T. 1993. The interleukin-12 subunit p40 specifically inhibits effects of the interleukin-12 heterodimer. *Eur J Immunol* 23: 2202-8

10. Mazzeo D, Vigano P, Di Blasio AM, Sinigaglia F, Vignali M, Panina-Bordignon P. 1998. Interleukin-12 and its free p40 subunit regulate immune recognition of endometrial cells: potential role in endometriosis. *J Clin Endocrinol Metab* 83: 911-6

11. Heinzel FP, Hujer AM, Ahmed FN, Rerko RM. 1997. In vivo production and function of IL-12 p40 homodimers. *J Immunol* 158: 4381-8

12. Ling P, Gately MK, Gubler U, Stern AS, Lin P, Hollfelder K, Su C, Pan YC, Hakimi J. 1995. Human IL-12 p40 homodimer binds to the IL-12 receptor but does not mediate biologic activity. *J Immunol* 154: 116-27

13. Carra G, Gerosa F, Trinchieri G. 2000. Biosynthesis and posttranslational regulation of human IL-12. *J Immunol* 164: 4752-61

14. Zheng H, Ban Y, Wei F, Ma X. 2016. Regulation of interleukin-12 production in antigen-presenting cells. *Adv Exp Med Biol* 941: 117-38

15. Reis e Sousa C, Hieny S, Scharton-Kersten T, Jankovic D, Charest H, Germain RN, Sher A. 1997. In vivo microbial stimulation induces rapid CD40 ligand-independent production of interleukin 12 by dendritic cells and their redistribution to T cell areas. *J Exp Med* 186: 1819-29

16. Mashayekhi M, Sandau MM, Dunay IR, Frickel EM, Khan A, Goldszmid RS, Sher A, Ploegh HL, Murphy TL, Sibley LD, Murphy KM. 2011. CD8alpha(+) dendritic cells are the critical source of interleukin-12 that controls acute infection by Toxoplasma gondii tachyzoites. *Immunity* 35: 249-59

17. Hochrein H, Shortman K, Vremec D, Scott B, Hertzog P, O'Keeffe M. 2001. Differential production of IL-12, IFN-alpha, and IFN-gamma by mouse dendritic cell subsets. *J Immunol* 166: 5448-55

18. Henry CJ, Ornelles DA, Mitchell LM, Brzoza-Lewis KL, Hiltbold EM. 2008. IL-12 produced by dendritic cells augments CD8+ T cell activation through the production of the chemokines CCL1 and CCL17. *J Immunol* 181: 8576-84

19. Campos PC, Gomes MT, Guimaraes ES, Guimaraes G, Oliveira SC. 2017. TLR7 and TLR3 sense Brucella abortus RNA to induce proinflammatory cytokine production but they are dispensable for host control of infection. *Front Immunol* 8: 28

20. Swiecki M, Colonna M. 2010. Unraveling the functions of plasmacytoid dendritic cells during viral infections, autoimmunity, and tolerance. *Immunol Rev* 234: 142-62

21. Lawrence C, Nauciel C. 1998. Production of interleukin-12 by murine macrophages in response to bacterial peptidoglycan. *Infect Immun* 66: 4947-9

22. Trinchieri G. 1997. Cytokines acting on or secreted by macrophages during intracellular infection (IL-10, IL-12, IFN-gamma). *Curr Opin Immunol* 9: 17-23

23. Jarrossay D, Napolitani G, Colonna M, Sallusto F, Lanzavecchia A. 2001. Specialization and complementarity in microbial molecule recognition by human myeloid and plasmacytoid dendritic cells. *Eur J Immunol* 31: 3388-93

24. Kadowaki N, Ho S, Antonenko S, Malefyt RW, Kastelein RA, Bazan F, Liu YJ. 2001. Subsets of human dendritic cell precursors express different toll-like receptors and respond to different microbial antigens. *J Exp Med* 194: 863-9

25. Hayes MP, Murphy FJ, Burd PR. 1998. Interferon-gamma-dependent inducible expression of the human interleukin-12 p35 gene in monocytes initiates from a TATA-containing promoter distinct from the CpG-rich promoter active in Epstein-Barr virus-transformed lymphoblastoid cells. *Blood* 91: 4645-51

26. Ma X, Chow JM, Gri G, Carra G, Gerosa F, Wolf SF, Dzialo R, Trinchieri G. 1996. The interleukin 12 p40 gene promoter is primed by interferon gamma in monocytic cells. *J Exp Med* 183: 147-57

27. Ma X, Yan W, Zheng H, Du Q, Zhang L, Ban Y, Li N, Wei F. 2015. Regulation of IL-10 and IL-12 production and function in macrophages and dendritic cells. *F1000Res* 4

28. Naeger LK, McKinney J, Salvekar A, Hoey T. 1999. Identification of a STAT4 binding site in the interleukin-12 receptor required for signaling. *J Biol Chem* 274: 1875-8

29. Presky DH, Yang H, Minetti LJ, Chua AO, Nabavi N, Wu CY, Gately MK, Gubler U. 1996. A functional interleukin 12 receptor complex is composed of two beta-type cytokine receptor subunits. *Proc Natl Acad Sci U S A* 93: 14002-7

30. Wu C, Wang X, Gadina M, O'Shea JJ, Presky DH, Magram J. 2000. IL-12 receptor beta 2 (IL-12R beta 2)-deficient mice are defective in IL-12-mediated signaling despite the presence of high affinity IL-12 binding sites. *J Immunol* 165: 6221-8

31. Wu CY, Gadina M, Wang K, O'Shea J, Seder RA. 2000. Cytokine regulation of IL-12 receptor beta2 expression: differential effects on human T and NK cells. *Eur J Immunol* 30: 1364-74

32. van de Vosse E, Haverkamp MH, Ramirez-Alejo N, Martinez-Gallo M, Blancas-Galicia L, Metin A, Garty BZ, Sun-Tan C, Broides A, de Paus RA, Keskin O, Cagdas D, Tezcan I, Lopez-Ruzafa E, Arostegui JI, Levy J, Espinosa-Rosales FJ, Sanal O, Santos-Argumedo L, Casanova JL, Boisson-Dupuis S, van Dissel JT, Bustamante J. 2013. IL-12Rbeta1 deficiency: mutation update and description of the IL12RB1 variation database. *Hum Mutat* 34: 1329-39

33. Bacon CM, Petricoin EF, 3rd, Ortaldo JR, Rees RC, Larner AC, Johnston JA, O'Shea JJ. 1995. Interleukin 12 induces tyrosine phosphorylation and activation of STAT4 in human lymphocytes. *Proc Natl Acad Sci U S A* 92: 7307-11

34. Cho SS, Bacon CM, Sudarshan C, Rees RC, Finbloom D, Pine R, O'Shea JJ. 1996. Activation of STAT4 by IL-12 and IFN-alpha: evidence for the involvement of ligand-induced tyrosine and serine phosphorylation. *J Immunol* 157: 4781-9

35. Morinobu A, Gadina M, Strober W, Visconti R, Fornace A, Montagna C, Feldman GM, Nishikomori R, O'Shea JJ. 2002. STAT4 serine phosphorylation is critical for IL-12-induced IFN-gamma production but not for cell proliferation. *Proc Natl Acad Sci U S A* 99: 12281-6

36. Lund RJ, Chen Z, Scheinin J, Lahesmaa R. 2004. Early target genes of IL-12 and STAT4 signaling in th cells. *J Immunol* 172: 6775-82

37. Coccia EM, Passini N, Battistini A, Pini C, Sinigaglia F, Rogge L. 1999. Interleukin-12 induces expression of interferon regulatory factor-1 via signal transducer and activator of transcription-4 in human T helper type 1 cells. *J Biol Chem* 274: 6698-703

38. Fieschi C, Bosticardo M, de Beaucoudrey L, Boisson-Dupuis S, Feinberg J, Santos OF, Bustamante J, Levy J, Candotti F, Casanova JL. 2004. A novel form of complete IL-12/IL-23 receptor beta1 deficiency with cell surface-expressed nonfunctional receptors. *Blood* 104: 2095-101

39. Ozbek N, Fieschi C, Yilmaz BT, de Beaucoudrey L, Demirhan B, Feinberg J, Bikmaz YE, Casanova JL. 2005. Interleukin-12 receptor beta 1 chain deficiency in a child with disseminated tuberculosis. *Clin Infect Dis* 40: e55-8

40. Perussia B, Chan SH, D'Andrea A, Tsuji K, Santoli D, Pospisil M, Young D, Wolf SF, Trinchieri G. 1992. Natural killer (NK) cell stimulatory factor or IL-12 has differential effects

on the proliferation of TCR-alpha beta+, TCR-gamma delta+ T lymphocytes, and NK cells. *J Immunol* 149: 3495-502

41. Wilson DC, Matthews S, Yap GS. 2008. IL-12 signaling drives CD8+ T cell IFN-gamma production and differentiation of KLRG1+ effector subpopulations during Toxoplasma gondii Infection. *J Immunol* 180: 5935-45

42. Hsieh CS, Macatonia SE, Tripp CS, Wolf SF, O'Garra A, Murphy KM. 1993. Development of TH1 CD4+ T cells through IL-12 produced by Listeria-induced macrophages. *Science* 260: 547-9

43. Seder RA, Gazzinelli R, Sher A, Paul WE. 1993. Interleukin 12 acts directly on CD4+ T cells to enhance priming for interferon gamma production and diminishes interleukin 4 inhibition of such priming. *Proc Natl Acad Sci U S A* 90: 10188-92

44. Tominaga K, Yoshimoto T, Torigoe K, Kurimoto M, Matsui K, Hada T, Okamura H, Nakanishi K. 2000. IL-12 synergizes with IL-18 or IL-1beta for IFN-gamma production from human T cells. *Int Immunol* 12: 151-60

45. Robertson MJ, Soiffer RJ, Wolf SF, Manley TJ, Donahue C, Young D, Herrmann SH, Ritz J. 1992. Response of human natural killer (NK) cells to NK cell stimulatory factor (NKSF): cytolytic activity and proliferation of NK cells are differentially regulated by NKSF. *J Exp Med* 175: 779-88

46. Allavena P, Paganin C, Zhou D, Bianchi G, Sozzani S, Mantovani A. 1994. Interleukin-12 is chemotactic for natural killer cells and stimulates their interaction with vascular endothelium. *Blood* 84: 2261-8

47. Jelinek DF, Braaten JK. 1995. Role of IL-12 in human B lymphocyte proliferation and differentiation. *J Immunol* 154: 1606-13

48. Vogel LA, Lester TL, Van Cleave VH, Metzger DW. 1996. Inhibition of murine B1 lymphocytes by interleukin-12. *Eur J Immunol* 26: 219-23

49. Yoshimoto T, Okamura H, Tagawa YI, Iwakura Y, Nakanishi K. 1997. Interleukin 18 together with interleukin 12 inhibits IgE production by induction of interferon-gamma production from activated B cells. *Proc Natl Acad Sci U S A* 94: 3948-53

50. Bromberg JF, Horvath CM, Wen Z, Schreiber RD, Darnell JE, Jr. 1996. Transcriptionally active Stat1 is required for the antiproliferative effects of both interferon alpha and interferon gamma. *Proc Natl Acad Sci U S A* 93: 7673-8

51. Hollenbaugh JA, Dutton RW. 2006. IFN-gamma regulates donor CD8 T cell expansion, migration, and leads to apoptosis of cells of a solid tumor. *J Immunol* 177: 3004-11

52. Martini M, Testi MG, Pasetto M, Picchio MC, Innamorati G, Mazzocco M, Ugel S, Cingarlini S, Bronte V, Zanovello P, Krampera M, Mosna F, Cestari T, Riviera AP, Brutti N, Barbieri O, Matera L, Tridente G, Colombatti M, Sartoris S. 2010. IFN-gamma-mediated upmodulation of MHC class I expression activates tumor-specific immune response in a mouse model of prostate cancer. *Vaccine* 28: 3548-57

53. Hayakawa Y, Takeda K, Yagita H, Smyth MJ, Van Kaer L, Okumura K, Saiki I. 2002. IFN-gamma-mediated inhibition of tumor angiogenesis by natural killer T-cell ligand, alpha-galactosylceramide. *Blood* 100: 1728-33

54. Colombo MP, Trinchieri G. 2002. Interleukin-12 in anti-tumor immunity and immunotherapy. *Cytokine Growth Factor Rev* 13: 155-68

55. Zaharoff DA, Hance KW, Rogers CJ, Schlom J, Greiner JW. 2010. Intratumoral immunotherapy of established solid tumors with chitosan/IL-12. *J Immunother* 33: 697-705

56. Noguchi Y, Jungbluth A, Richards EC, Old LJ. 1996. Effect of interleukin 12 on tumor induction by 3-methylcholanthrene. *Proc Natl Acad Sci U S A* 93: 11798-801

57. Vizler C, Rosato A, Calderazzo F, Quintieri L, Fruscella P, Wainstok de Calmanovici R, Mantovani A, Vecchi A, Zanovello P, Collavo D. 1998. Therapeutic effect of interleukin 12 on mouse haemangiosarcomas is not associated with an increased anti-tumour cytotoxic T-lymphocyte activity. *Br J Cancer* 77: 656-62

58. Smyth MJ, Taniguchi M, Street SE. 2000. The anti-tumor activity of IL-12: mechanisms of innate immunity that are model and dose dependent. *J Immunol* 165: 2665-70

59. Brunda MJ, Luistro L, Warrier RR, Wright RB, Hubbard BR, Murphy M, Wolf SF, Gately MK. 1993. Antitumor and antimetastatic activity of interleukin 12 against murine tumors. *J Exp Med* 178: 1223-30

60. Atkins MB, Robertson MJ, Gordon M, Lotze MT, DeCoste M, DuBois JS, Ritz J, Sandler AB, Edington HD, Garzone PD, Mier JW, Canning CM, Battiato L, Tahara H, Sherman ML. 1997. Phase I evaluation of intravenous recombinant human interleukin 12 in patients with advanced malignancies. *Clin Cancer Res* 3: 409-17

61. Bajetta E, Del Vecchio M, Mortarini R, Nadeau R, Rakhit A, Rimassa L, Fowst C, Borri A, Anichini A, Parmiani G. 1998. Pilot study of subcutaneous recombinant human interleukin 12 in metastatic melanoma. *Clin Cancer Res* 4: 75-85

62. Motzer RJ, Rakhit A, Schwartz LH, Olencki T, Malone TM, Sandstrom K, Nadeau R, Parmar H, Bukowski R. 1998. Phase I trial of subcutaneous recombinant human interleukin-12 in patients with advanced renal cell carcinoma. *Clin Cancer Res* 4: 1183-91

63. Rook AH, Wood GS, Yoo EK, Elenitsas R, Kao DM, Sherman ML, Witmer WK, Rockwell KA, Shane RB, Lessin SR, Vonderheid EC. 1999. Interleukin-12 therapy of cutaneous T-cell lymphoma induces lesion regression and cytotoxic T-cell responses. *Blood* 94: 902-8

64. Lenzi R, Rosenblum M, Verschraegen C, Kudelka AP, Kavanagh JJ, Hicks ME, Lang EA, Nash MA, Levy LB, Garcia ME, Platsoucas CD, Abbruzzese JL, Freedman RS. 2002. Phase I study of intraperitoneal recombinant human interleukin 12 in patients with Mullerian carcinoma, gastrointestinal primary malignancies, and mesothelioma. *Clin Cancer Res* 8: 3686-95

65. Weiss GR, O'Donnell MA, Loughlin K, Zonno K, Laliberte RJ, Sherman ML. 2003. Phase 1 study of the intravesical administration of recombinant human interleukin-12 in patients with recurrent superficial transitional cell carcinoma of the bladder. *J Immunother* 26: 343-8

66. Wadler S, Levy D, Frederickson HL, Falkson CI, Wang Y, Weller E, Burk R, Ho G, Kadish AS, Eastern Cooperative Oncology G. 2004. A phase II trial of interleukin-12 in patients with advanced cervical cancer: clinical and immunologic correlates. Eastern Cooperative Oncology Group study E1E96. *Gynecol Oncol* 92: 957-64

67. Xu D, Gu P, Pan PY, Li Q, Sato AI, Chen SH. 2004. NK and CD8+ T cell-mediated eradication of poorly immunogenic B16-F10 melanoma by the combined action of IL-12 gene therapy and 4-1BB costimulation. *Int J Cancer* 109: 499-506

68. van Herpen CM, van der Laak JA, de Vries IJ, van Krieken JH, de Wilde PC, Balvers MG, Adema GJ, De Mulder PH. 2005. Intratumoral recombinant human interleukin-12 administration in head and neck squamous cell carcinoma patients modifies locoregional lymph node architecture and induces natural killer cell infiltration in the primary tumor. *Clin Cancer Res* 11: 1899-909

69. Little RF, Pluda JM, Wyvill KM, Rodriguez-Chavez IR, Tosato G, Catanzaro AT, Steinberg SM, Yarchoan R. 2006. Activity of subcutaneous interleukin-12 in AIDS-related Kaposi sarcoma. *Blood* 107: 4650-7

70. Younes A, Pro B, Robertson MJ, Flinn IW, Romaguera JE, Hagemeister F, Dang NH, Fiumara P, Loyer EM, Cabanillas FF, McLaughlin PW, Rodriguez MA, Samaniego F. 2004. Phase II clinical trial of interleukin-12 in patients with relapsed and refractory non-Hodgkin's lymphoma and Hodgkin's disease. *Clin Cancer Res* 10: 5432-8

71. Mortarini R, Borri A, Tragni G, Bersani I, Vegetti C, Bajetta E, Pilotti S, Cerundolo V, Anichini A. 2000. Peripheral burst of tumor-specific cytotoxic T lymphocytes and infiltration of metastatic lesions by memory CD8+ T cells in melanoma patients receiving interleukin 12. *Cancer Res* 60: 3559-68

72. Jenks S. 1996. After initial setback, IL-12 regaining popularity. *J Natl Cancer Inst* 88: 576-7

73. Lasek W, Zagozdzon R, Jakobisiak M. 2014. Interleukin 12: still a promising candidate for tumor immunotherapy? *Cancer Immunol Immunother* 63: 419-35

74. Heinzerling L, Dummer R, Pavlovic J, Schultz J, Burg G, Moelling K. 2002. Tumor regression of human and murine melanoma after intratumoral injection of IL-12-encoding plasmid DNA in mice. *Exp Dermatol* 11: 232-40

75. Yockman JW, Maheshwari A, Han SO, Kim SW. 2003. Tumor regression by repeated intratumoral delivery of water soluble lipopolymers/p2CMVmIL-12 complexes. *J Control Release* 87: 177-86

76. Shi F, Rakhmilevich AL, Heise CP, Oshikawa K, Sondel PM, Yang NS, Mahvi DM. 2002. Intratumoral injection of interleukin-12 plasmid DNA, either naked or in complex with cationic lipid, results in similar tumor regression in a murine model. *Mol Cancer Ther* 1: 949-57

77. Maheshwari A, Han S, Mahato RI, Kim SW. 2002. Biodegradable polymer-based interleukin-12 gene delivery: role of induced cytokines, tumor infiltrating cells and nitric oxide in anti-tumor activity. *Gene Ther* 9: 1075-84

78. Mahato RI, Lee M, Han S, Maheshwari A, Kim SW. 2001. Intratumoral delivery of p2CMVmIL-12 using water-soluble lipopolymers. *Mol Ther* 4: 130-8

79. Mahvi DM, Henry MB, Albertini MR, Weber S, Meredith K, Schalch H, Rakhmilevich A, Hank J, Sondel P. 2007. Intratumoral injection of IL-12 plasmid DNA--results of a phase I/IB clinical trial. *Cancer Gene Ther* 14: 717-23

80. Heinzerling L, Burg G, Dummer R, Maier T, Oberholzer PA, Schultz J, Elzaouk L, Pavlovic J, Moelling K. 2005. Intratumoral injection of DNA encoding human interleukin 12 into patients with metastatic melanoma: clinical efficacy. *Hum Gene Ther* 16: 35-48

81. Lohr F, Lo DY, Zaharoff DA, Hu K, Zhang X, Li Y, Zhao Y, Dewhirst MW, Yuan F, Li CY. 2001. Effective tumor therapy with plasmid-encoded cytokines combined with in vivo electroporation. *Cancer Res* 61: 3281-4

82. Heller LC, Heller R. 2006. In vivo electroporation for gene therapy. *Hum Gene Ther* 17: 890-7

83. Lucas ML, Heller L, Coppola D, Heller R. 2002. IL-12 plasmid delivery by in vivo electroporation for the successful treatment of established subcutaneous B16.F10 melanoma. *Mol Ther* 5: 668-75

84. Lucas ML, Heller R. 2003. IL-12 gene therapy using an electrically mediated nonviral approach reduces metastatic growth of melanoma. *DNA Cell Biol* 22: 755-63

85. Li S, Zhang X, Xia X. 2002. Regression of tumor growth and induction of long-term antitumor memory by interleukin 12 electro-gene therapy. *J Natl Cancer Inst* 94: 762-8

86. Tamura T, Nishi T, Goto T, Takeshima H, Dev SB, Ushio Y, Sakata T. 2001. Intratumoral delivery of interleukin 12 expression plasmids with in vivo electroporation is effective for colon and renal cancer. *Hum Gene Ther* 12: 1265-76

87. Sedlar A, Kranjc S, Dolinsek T, Cemazar M, Coer A, Sersa G. 2013. Radiosensitizing effect of intratumoral interleukin-12 gene electrotransfer in murine sarcoma. *BMC Cancer* 13: 38

88. Li S, Zhang L, Torrero M, Cannon M, Barret R. 2005. Administration route- and immune cell activation-dependent tumor eradication by IL12 electrotransfer. *Mol Ther* 12: 942-9

89. Pavlin D, Cemazar M, Kamensek U, Tozon N, Pogacnik A, Sersa G. 2009. Local and systemic antitumor effect of intratumoral and peritumoral IL-12 electrogene therapy on murine sarcoma. *Cancer Biol Ther* 8: 2114-22

90. Pavlin D, Cemazar M, Cor A, Sersa G, Pogacnik A, Tozon N. 2011. Electrogene therapy with interleukin-12 in canine mast cell tumors. *Radiol Oncol* 45: 31-9

91. Chuang TF, Lee SC, Liao KW, Hsiao YW, Lo CH, Chiang BL, Lin XZ, Tao MH, Chu RM. 2009. Electroporation-mediated IL-12 gene therapy in a transplantable canine cancer model. *Int J Cancer* 125: 698-707

92. Kishida T, Asada H, Satoh E, Tanaka S, Shinya M, Hirai H, Iwai M, Tahara H, Imanishi J, Mazda O. 2001. In vivo electroporation-mediated transfer of interleukin-12 and interleukin-18 genes induces significant antitumor effects against melanoma in mice. *Gene Ther* 8: 1234-40

93. Yamashita YI, Shimada M, Hasegawa H, Minagawa R, Rikimaru T, Hamatsu T, Tanaka S, Shirabe K, Miyazaki JI, Sugimachi K. 2001. Electroporation-mediated interleukin-12 gene therapy for hepatocellular carcinoma in the mice model. *Cancer Res* 61: 1005-12

94. Shibata MA, Ito Y, Morimoto J, Kusakabe K, Yoshinaka R, Otsuki Y. 2006. In vivo electrogene transfer of interleukin-12 inhibits tumor growth and lymph node and lung metastases in mouse mammary carcinomas. *J Gene Med* 8: 335-52

95. Heller L, Merkler K, Westover J, Cruz Y, Coppola D, Benson K, Daud A, Heller R. 2006. Evaluation of toxicity following electrically mediated interleukin-12 gene delivery in a B16 mouse melanoma model. *Clin Cancer Res* 12: 3177-83

96. Daud AI, DeConti RC, Andrews S, Urbas P, Riker AI, Sondak VK, Munster PN, Sullivan DM, Ugen KE, Messina JL, Heller R. 2008. Phase I trial of interleukin-12 plasmid electroporation in patients with metastatic melanoma. *J Clin Oncol* 26: 5896-903

97. Mendiratta SK, Quezada A, Matar M, Wang J, Hebel HL, Long S, Nordstrom JL, Pericle F. 1999. Intratumoral delivery of IL-12 gene by polyvinyl polymeric vector system to murine renal and colon carcinoma results in potent antitumor immunity. *Gene Ther* 6: 833-9

98. Mendiratta SK, Quezada A, Matar M, Thull NM, Bishop JS, Nordstrom JL, Pericle F. 2000. Combination of interleukin 12 and interferon alpha gene therapy induces a synergistic antitumor response against colon and renal cell carcinoma. *Hum Gene Ther* 11: 1851-62

99. Maheshwari A, Mahato RI, McGregor J, Han S, Samlowski WE, Park JS, Kim SW. 2000. Soluble biodegradable polymer-based cytokine gene delivery for cancer treatment. *Mol Ther* 2: 121-30

100. Kelly E, Russell SJ. 2007. History of oncolytic viruses: genesis to genetic engineering. *Mol Ther* 15: 651-9

101. Nguyen K, Nguyen D, Nguyen L. 2015. Oncolytic virus–an effective targeting therapy for cancer treatment. *Vietnam J Sci* 2: 25-30

102. Patel DM, Foreman PM, Nabors LB, Riley KO, Gillespie GY, Markert JM. 2016. Design of a Phase I Clinical Trial to Evaluate M032, a Genetically Engineered HSV-1 Expressing IL-12, in Patients with Recurrent/Progressive Glioblastoma Multiforme, Anaplastic Astrocytoma, or Gliosarcoma. *Hum Gene Ther Clin Dev* 27: 69-78

103. Wang P, Li X, Wang J, Gao D, Li Y, Li H, Chu Y, Zhang Z, Liu H, Jiang G, Cheng Z, Wang S, Dong J, Feng B, Chard LS, Lemoine NR, Wang Y. 2017. Re-designing Interleukin-12 to enhance its safety and potential as an anti-tumor immunotherapeutic agent. *Nat Commun* 8: 1395

104. Ortiz-Sanchez E, Helguera G, Daniels TR, Penichet ML. 2008. Antibody-cytokine fusion proteins: applications in cancer therapy. *Expert Opin Biol Ther* 8: 609-32

105. Lo KM, Lan Y, Lauder S, Zhang J, Brunkhorst B, Qin G, Verma R, Courtenay-Luck N, Gillies SD. 2007. huBC1-IL12, an immunocytokine which targets EDB-containing oncofetal fibronectin in tumors and tumor vasculature, shows potent anti-tumor activity in human tumor models. *Cancer Immunol Immunother* 56: 447-57

106. Fallon J, Tighe R, Kradjian G, Guzman W, Bernhardt A, Neuteboom B, Lan Y, Sabzevari H, Schlom J, Greiner JW. 2014. The immunocytokine NHS-IL12 as a potential cancer therapeutic. *Oncotarget* 5: 1869-84

107. Pasche N, Wulhfard S, Pretto F, Carugati E, Neri D. 2012. The antibody-based delivery of interleukin-12 to the tumor neovasculature eradicates murine models of cancer in combination with paclitaxel. *Clin Cancer Res* 18: 4092-103

108. Sharifi J, Khawli LA, Hu P, King S, Epstein AL. 2001. Characterization of a phage display-derived human monoclonal antibody (NHS76) counterpart to chimeric TNT-1 directed against necrotic regions of solid tumors. *Hybrid Hybridomics* 20: 305-12

109. Zaharoff DA, Rogers CJ, Hance KW, Schlom J, Greiner JW. 2007. Chitosan solution enhances the immunoadjuvant properties of GM-CSF. *Vaccine* 25: 8673-86

110. Portielje JE, Kruit WH, Schuler M, Beck J, Lamers CH, Stoter G, Huber C, de Boer-Dennert M, Rakhit A, Bolhuis RL, Aulitzky WE. 1999. Phase I study of subcutaneously administered recombinant human interleukin 12 in patients with advanced renal cell cancer. *Clin Cancer Res* 5: 3983-9

111. Egilmez NK, Jong YS, Sabel MS, Jacob JS, Mathiowitz E, Bankert RB. 2000. In situ tumor vaccination with interleukin-12-encapsulated biodegradable microspheres: induction of tumor regression and potent antitumor immunity. *Cancer Res* 60: 3832-7

112. Egilmez NK, Jong YS, Hess SD, Jacob JS, Mathiowitz E, Bankert RB. 2000. Cytokines delivered by biodegradable microspheres promote effective suppression of human tumors by human peripheral blood lymphocytes in the SCID-Winn model. *J Immunother* 23: 190-5

113. Kuriakose MA, Chen FA, Egilmez NK, Jong YS, Mathiowitz E, DeLacure MD, Hicks WL, Jr., Loree TL, Bankert RB. 2000. Interleukin-12 delivered by biodegradable microspheres promotes the antitumor activity of human peripheral blood lymphocytes in a human head and neck tumor xenograft/SCID mouse model. *Head Neck* 22: 57-63

114. Arora A, Su G, Mathiowitz E, Reineke J, Chang AE, Sabel MS. 2006. Neoadjuvant intratumoral cytokine-loaded microspheres are superior to postoperative autologous cellular vaccines in generating systemic anti-tumor immunity. *J Surg Oncol* 94: 403-12

115. Sabel MS, Skitzki J, Stoolman L, Egilmez NK, Mathiowitz E, Bailey N, Chang WJ, Chang AE. 2004. Intratumoral IL-12 and TNF-alpha-loaded microspheres lead to regression of breast cancer and systemic antitumor immunity. *Ann Surg Oncol* 11: 147-56

116. Smith SG, Baltz JL, Koppolu BP, Ravindranathan S, Nguyen K, Zaharoff DA. 2017. Immunological mechanisms of intravesical chitosan/interleukin-12 immunotherapy against murine bladder cancer. *Oncoimmunology* 6: e1259050

117. Vo JL, Yang L, Kurtz SL, Smith SG, Koppolu BP, Ravindranathan S, Zaharoff DA. 2014. Neoadjuvant immunotherapy with chitosan and interleukin-12 to control breast cancer metastasis. *Oncoimmunology* 3: e968001

118. Smith SG, Koppolu BP, Ravindranathan S, Kurtz SL, Yang L, Katz MD, Zaharoff DA. 2015. Intravesical chitosan/interleukin-12 immunotherapy induces tumor-specific systemic immunity against murine bladder cancer. *Cancer Immunol Immunother* 64: 689-96

119. Lim GB. 2017. Milestone 1: Discovery and purification of heparin. *Nat Rev Cardiol*

120. Rabenstein DL. 2002. Heparin and heparan sulfate: structure and function. *Nat Prod Rep* 19: 312-31

121. Sasisekharan R, Raman R, Prabhakar V. 2006. Glycomics approach to structure-function relationships of glycosaminoglycans. *Annu Rev Biomed Eng* 8: 181-231

122. Nelson DL, Cox MM. 2004. *Lehninger Principles of Biochemistry, Fourth Edition*

123. Folkman J, Langer R, Linhardt RJ, Haudenschild C, Taylor S. 1983. Angiogenesis inhibition and tumor regression caused by heparin or a heparin fragment in the presence of cortisone. *Science* 221: 719-25

124. Crum R, Szabo S, Folkman J. 1985. A new class of steroids inhibits angiogenesis in the presence of heparin or a heparin fragment. *Science* 230: 1375-8

125. Holodniy M, Kim S, Katzenstein D, Konrad M, Groves E, Merigan TC. 1991. Inhibition of human immunodeficiency virus gene amplification by heparin. *J Clin Microbiol* 29: 676-9

126. Herold BC, Gerber SI, Polonsky T, Belval BJ, Shaklee PN, Holme K. 1995. Identification of structural features of heparin required for inhibition of herpes simplex virus type 1 binding. *Virology* 206: 1108-16

127. Baba M, Pauwels R, Balzarini J, Arnout J, Desmyter J, De Clercq E. 1988. Mechanism of inhibitory effect of dextran sulfate and heparin on replication of human immunodeficiency virus in vitro. *Proc Natl Acad Sci U S A* 85: 6132-6

128. Rider CC, Coombe DR, Harrop HA, Hounsell EF, Bauer C, Feeney J, Mulloy B, Mahmood N, Hay A, Parish CR. 1994. Anti-HIV-1 activity of chemically modified heparins: correlation between binding to the V3 loop of gp120 and inhibition of cellular HIV-1 infection in vitro. *Biochemistry* 33: 6974-80

129. Howell AL, Taylor TH, Miller JD, Groveman DS, Eccles EH, Zacharski LR. 1996. Inhibition of HIV-1 infectivity by low molecular weight heparin. Results of in vitro studies and a pilot clinical trial in patients with advanced AIDS. *Int J Clin Lab Res* 26: 124-31

130. Harrop HA, Rider CC. 1998. Heparin and its derivatives bind to HIV-1 recombinant envelope glycoproteins, rather than to recombinant HIV-1 receptor, CD4. *Glycobiology* 8: 131-7

131. Kazatchkine MD, Fearon DT, Metcalfe DD, Rosenberg RD, Austen KF. 1981. Structural determinants of the capacity of heparin to inhibit the formation of the human amplification C3 convertase. *J Clin Invest* 67: 223-8

132. Sharath MD, Merchant ZM, Kim YS, Rice KG, Linhardt RJ, Weiler JM. 1985. Small heparin fragments regulate the amplification pathway of complement. *Immunopharmacology* 9: 73-80

133. Peysselon F, Ricard-Blum S. 2014. Heparin-protein interactions: from affinity and kinetics to biological roles. Application to an interaction network regulating angiogenesis. *Matrix Biol* 35: 73-81

134. Yokota T, Arai N, Lee F, Rennick D, Mosmann T, Arai K. 1985. Use of a cDNA expression vector for isolation of mouse interleukin 2 cDNA clones: expression of T-cell growth-factor activity after transfection of monkey cells. *Proc Natl Acad Sci U S A* 82: 68-72

135. Cerretti DP, McKereghan K, Larsen A, Cantrell MA, Anderson D, Gillis S, Cosman D, Baker PE. 1986. Cloning, sequence, and expression of bovine interleukin 2. *Proc Natl Acad Sci U S A* 83: 3223-7

136. Najjam S, Gibbs RV, Gordon MY, Rider CC. 1997. Characterization of human recombinant interleukin 2 binding to heparin and heparan sulfate using an ELISA approach. *Cytokine* 9: 1013-22

137. Najjam S, Mulloy B, Theze J, Gordon M, Gibbs R, Rider CC. 1998. Further characterization of the binding of human recombinant interleukin 2 to heparin and identification of putative binding sites. *Glycobiology* 8: 509-16

138. Hirano T, Yasukawa K, Harada H, Taga T, Watanabe Y, Matsuda T, Kashiwamura S, Nakajima K, Koyama K, Iwamatsu A, et al. 1986. Complementary DNA for a novel human interleukin (BSF-2) that induces B lymphocytes to produce immunoglobulin. *Nature* 324: 73-6

139. Schafer ZT, Brugge JS. 2007. IL-6 involvement in epithelial cancers. *J Clin Invest* 117: 3660-3

140. Fisher DT, Appenheimer MM, Evans SS. 2014. The two faces of IL-6 in the tumor microenvironment. *Semin Immunol* 26: 38-47

141. Kumari N, Dwarakanath BS, Das A, Bhatt AN. 2016. Role of interleukin-6 in cancer progression and therapeutic resistance. *Tumour Biol* 37: 11553-72

142. Mummery RS, Rider CC. 2000. Characterization of the heparin-binding properties of IL-6. *J Immunol* 165: 5671-9

143. Howard M, Farrar J, Hilfiker M, Johnson B, Takatsu K, Hamaoka T, Paul WE. 1982. Identification of a T cell-derived b cell growth factor distinct from interleukin 2. *J Exp Med* 155: 914-23

144. Walter MR, Cook WJ, Zhao BG, Cameron RP, Jr., Ealick SE, Walter RL, Jr., Reichert P, Nagabhushan TL, Trotta PP, Bugg CE. 1992. Crystal structure of recombinant human interleukin-4. *J Biol Chem* 267: 20371-6

145. Lortat-Jacob H, Garrone P, Banchereau J, Grimaud JA. 1997. Human interleukin 4 is a glycosaminoglycan-binding protein. *Cytokine* 9: 101-5

146. Jones CA, Williams KA, Finlay-Jones JJ, Hart PH. 1995. Interleukin 4 production by human amnion epithelial cells and regulation of its activity by glycosaminoglycan binding. *Biol Reprod* 52: 839-47

147. Goodwin RG, Lupton S, Schmierer A, Hjerrild KJ, Jerzy R, Clevenger W, Gillis S, Cosman D, Namen AE. 1989. Human interleukin 7: molecular cloning and growth factor activity on human and murine B-lineage cells. *Proc Natl Acad Sci U S A* 86: 302-6

148. Clarke D, Katoh O, Gibbs RV, Griffiths SD, Gordon MY. 1995. Interaction of interleukin 7 (IL-7) with glycosaminoglycans and its biological relevance. *Cytokine* 7: 325-30

149. Zhang F, Liang X, Pu D, George KI, Holland PJ, Walsh ST, Linhardt RJ. 2012. Biophysical characterization of glycosaminoglycan-IL-7 interactions using SPR. *Biochimie* 94: 242-9

150. Borghesi LA, Yamashita Y, Kincade PW. 1999. Heparan sulfate proteoglycans mediate interleukin-7-dependent B lymphopoiesis. *Blood* 93: 140-8

151. Ng TH, Britton GJ, Hill EV, Verhagen J, Burton BR, Wraith DC. 2013. Regulation of adaptive immunity; the role of interleukin-10. *Front Immunol* 4: 129

152. Salek-Ardakani S, Arrand JR, Shaw D, Mackett M. 2000. Heparin and heparan sulfate bind interleukin-10 and modulate its activity. *Blood* 96: 1879-88

153. Ihle JN, Pepersack L, Rebar L. 1981. Regulation of T cell differentiation: in vitro induction of 20 alpha-hydroxysteroid dehydrogenase in splenic lymphocytes from athymic mice by a unique lymphokine. *J Immunol* 126: 2184-9

154. Yang YC, Ciarletta AB, Temple PA, Chung MP, Kovacic S, Witek-Giannotti JS, Leary AC, Kriz R, Donahue RE, Wong GG, et al. 1986. Human IL-3 (multi-CSF): identification by expression cloning of a novel hematopoietic growth factor related to murine IL-3. *Cell* 47: 3-10

155. Roberts R, Gallagher J, Spooncer E, Allen TD, Bloomfield F, Dexter TM. 1988. Heparan sulphate bound growth factors: a mechanism for stromal cell mediated haemopoiesis. *Nature* 332: 376-8

156. Alvarez-Silva M, Borojevic R. 1996. GM-CSF and IL-3 activities in schistosomal liver granulomas are controlled by stroma-associated heparan sulfate proteoglycans. *J Leukoc Biol* 59: 435-41

157. Campbell HD, Tucker WQ, Hort Y, Martinson ME, Mayo G, Clutterbuck EJ, Sanderson CJ, Young IG. 1987. Molecular cloning, nucleotide sequence, and expression of the gene encoding human eosinophil differentiation factor (interleukin 5). *Proc Natl Acad Sci U S A* 84: 6629-33

158. Milburn MV, Hassell AM, Lambert MH, Jordan SR, Proudfoot AE, Graber P, Wells TN. 1993. A novel dimer configuration revealed by the crystal structure at 2.4 A resolution of human interleukin-5. *Nature* 363: 172-6

159. Lipscombe RJ, Nakhoul AM, Sanderson CJ, Coombe DR. 1998. Interleukin-5 binds to heparin/heparan sulfate. A model for an interaction with extracellular matrix. *J Leukoc Biol* 63: 342-50

160. Yoshimura T, Matsushima K, Tanaka S, Robinson EA, Appella E, Oppenheim JJ, Leonard EJ. 1987. Purification of a human monocyte-derived neutrophil chemotactic factor that has peptide sequence similarity to other host defense cytokines. *Proc Natl Acad Sci U S A* 84: 9233-7

161. Takashiba S, Takigawa M, Takahashi K, Myokai F, Nishimura F, Chihara T, Kurihara H, Nomura Y, Murayama Y. 1992. Interleukin-8 is a major neutrophil chemotactic factor

derived from cultured human gingival fibroblasts stimulated with interleukin-1 beta or tumor necrosis factor alpha. *Infect Immun* 60: 5253-8

162. Mobius K, Nordsieck K, Pichert A, Samsonov SA, Thomas L, Schiller J, Kalkhof S, Teresa Pisabarro M, Beck-Sickinger AG, Huster D. 2013. Investigation of lysine side chain interactions of interleukin-8 with heparin and other glycosaminoglycans studied by a methylation-NMR approach. *Glycobiology* 23: 1260-9

163. Spillmann D, Witt D, Lindahl U. 1998. Defining the interleukin-8-binding domain of heparan sulfate. *J Biol Chem* 273: 15487-93

164. Webb LM, Ehrengruber MU, Clark-Lewis I, Baggiolini M, Rot A. 1993. Binding to heparan sulfate or heparin enhances neutrophil responses to interleukin 8. *Proc Natl Acad Sci U S A* 90: 7158-62

165. Paul SR, Bennett F, Calvetti JA, Kelleher K, Wood CR, O'Hara RM, Jr., Leary AC, Sibley B, Clark SC, Williams DA, et al. 1990. Molecular cloning of a cDNA encoding interleukin 11, a stromal cell-derived lymphopoietic and hematopoietic cytokine. *Proc Natl Acad Sci U S A* 87: 7512-6

166. Walton KJ, Duncan JM, Deschamps P, Shaughnessy SG. 2002. Heparin acts synergistically with interleukin-11 to induce STAT3 activation and in vitro osteoclast formation. *Blood* 100: 2530-6

167. Rajgopal R, Butcher M, Weitz JI, Shaughnessy SG. 2006. Heparin synergistically enhances interleukin-11 signaling through up-regulation of the MAPK pathway. *J Biol Chem* 281: 20780-7

168. Hasan M, Najjam S, Gordon MY, Gibbs RV, Rider CC. 1999. IL-12 is a heparin-binding cytokine. *J Immunol* 162: 1064-70

169. Garnier P, Mummery R, Forster MJ, Mulloy B, Gibbs RV, Rider CC. 2018. The localisation of the heparin binding sites of human and murine interleukin-12 within the carboxyterminal domain of the P40 subunit. *Cytokine* 110: 159-68

170. Jayanthi S, Koppolu B, Smith SG, Jalah R, Bear J, Rosati M, Pavlakis GN, Felber BK, Zaharoff DA, Kumar TK. 2014. Efficient production and purification of recombinant human interleukin-12 (IL-12) overexpressed in mammalian cells without affinity tag. *Protein Expr Purif* 102: 76-84

171. Jayanthi S, Koppolu BP, Nguyen KG, Smith SG, Felber BK, Kumar TKS, Zaharoff DA. 2017. Modulation of Interleukin-12 activity in the presence of heparin. *Sci Rep* 7: 5360

172. Trinchieri G. 1994. Interleukin-12: a cytokine produced by antigen-presenting cells with immunoregulatory functions in the generation of T-helper cells type 1 and cytotoxic lymphocytes. *Blood* 84: 4008-27

173. Trinchieri G. 2003. Interleukin-12 and the regulation of innate resistance and adaptive immunity. *Nat Rev Immunol* 3: 133-46

174. Jacobson MA, Hardy D, Connick E, Watson J, DeBruin M. 2000. Phase 1 trial of a single dose of recombinant human interleukin-12 in human immunodeficiency virus-infected patients with 100-500 CD4 cells/microL. *J Infect Dis* 182: 1070-6

175. Maciel TT, Moura IC, Hermine O. 2015. The role of mast cells in cancers. *F1000Prime Rep* 7: 09

176. Theoharides TC, Alysandratos KD, Angelidou A, Delivanis DA, Sismanopoulos N, Zhang B, Asadi S, Vasiadi M, Weng Z, Miniati A, Kalogeromitros D. 2012. Mast cells and inflammation. *Biochim Biophys Acta* 1822: 21-33

177. Urb M, Sheppard DC. 2012. The role of mast cells in the defence against pathogens. *PLoS Pathog* 8: e1002619

CHAPTER 2: MODULATION OF INTERLEUKIN-12 ACTIVITY IN THE PRESENCE OF HEPARIN *

2.1. Introduction

Polyanionic glycosaminoglycans (GAGs) have been shown to bind numerous growth factors and cytokines (1-5). The physiological significance of this binding is two-fold. First, GAGs can serve as co-receptors on cell surfaces to maintain high, local concentrations of cytokines (6-10). Second, GAGs can regulate bioactivities of growth factors and cytokines through multiple mechanisms including dimerization and protection from proteolytic degradation (11-14). The two most heavily N-sulfated GAGs, heparin and heparan sulfate (HS), are known to interact with more than 400 proteins involved in various biological processes (10). In its most obvious role, heparin binds to antithrombin and increases its anticoagulant activity. Heparin binding is also an essential prerequisite for basic fibroblast growth factor (bFGF) dimerization and engagement with its high affinity receptor for angiogenesis, wound healing, stem cell differentiation, etc.

Beyond antithrombin and bFGF, the binding of sulfated GAGs plays a significant role in the biology of numerous other pleiotropic cytokines and growth factors (15-18). For example, binding of GM-CSF to sulfated GAGs in the extracellular matrix produced by stromal cells is

Contributions of Khue G Nguyen (KGN):
• <u>Experiments</u>: KGN performed IL-12 bioactivity assays, proteolytic digestion assays, heparin binding and IL-12 bioactivity on IL12R mutant and wild-type cells, and statistical analyses.
• <u>Writing</u>: KGN wrote Introduction, Material & Methods, Results, and Discussion of this paper.

critical for maintaining high local concentrations in the bone marrow microenvironment (19) and increasing GM-CSF-induced myeloid cell proliferation (20). Additionally, heparin binding decreases IFN-γ clearance (21), interferes with cellular binding (22) and inhibits IFN-γ-induced upregulation of class II MHC and adhesion molecules on the surfaces of vascular endothelial cells (15, 23).

GAG-interleukin interactions have been explored, albeit to a significantly lesser extent. Interleukins mediate signaling primarily between leukocytes. Given that leukocytes are highly mobile populations of cells, the need for compartmentalization of interleukins through GAG binding is not as obvious. Nevertheless, heparin and HS have been shown to bind to many interleukins with mixed effects on their bioactivities.

Heparin binds to human but not murine IL-2 (24, 25), however, heparin binding has no effect on hIL-2 bioactivity as measured by proliferation of CTLL-2 cells (25). The effect of heparin/HS binding on IL-3 bioactivity is concentration-dependent with IL-3-induced proliferation of myeloid cells increasing at low heparin concentrations and decreasing at high heparin concentrations (20). HS binds to and inhibits IL-4-based suppression of lipopolysaccharide-stimulated monocytes (26). Yet, HS enhances the proliferative activity of IL-5 in specialized Baf-IL-5 cells (27). Heparin/HS has no impact on IL-6-stimulated proliferation of Ba/F3 cells (28). Heparin complexation protects IL-7 from proteolytic degradation, however, heparin binding inhibits the growth of IL-7 dependent pre-B cells (29). HS augments IL-8-induced neutrophil chemotaxis and Ca^{2+} responses (30) while heparin facilitates similar IL-8-induced Ca^{2+} responses but either inhibited, or had no impact on, neutrophil chemotaxis (30, 31). Lastly, heparin and HS both inhibit IL-10-induced upregulation of CD16 and CD64 on monocytes/macrophages (13). In general, while the effects of heparin/HS on interleukin

bioactivity are mixed, interleukin binding to highly sulfated GAGs appears to be more inhibitory than augmentative.

IL-12 has been shown previously to be a heparin-binding protein (32, 33). Our recent in silico analysis found two heparin-binding domains located on the p40 subunit of IL-12 (33). These sites were exploited in the single-step purification of tagless IL-12, while the affinity of heparin for IL-12 was well characterized via isothermal calorimetry (ITC) (33).

In this study, the ability of heparin/HS to modulate IL-12 bioactivity is described for the first time. In an effort to determine the mechanism(s) by which heparin influences IL-12 bioactivity, comprehensive biophysical and cell-based studies were performed. Specifically, we assessed the ability of heparin to: [1] stabilize IL-12 conformation; [2] protect IL-12 from proteolytic degradation; [3] induce oligomerization of IL-12; and [4] enhance IL-12 binding to cell surfaces and IL-12 receptors. Results of this study are important in that they contribute significantly to our understanding of the immunobiology of IL-12 and potentially other IL-12 family cytokines which have been recently suggested as having more influence on shaping immunity than any other cytokine family (34).

2.2. Materials and Methods

2.2.1. IL-12 bioactivity assays

Recombinant hIL-12 was purified from hIL-12-expressing HEK-293 cells as described previously (33). Low molecular weight heparin, HS, hyaluronic acid, chondroitin sulfate and dextran were purchased from Sigma-Aldrich.

The IL-2-independent, IL-12-responsive human natural killer cell line, NK-92MI (CRL-2408TM; ATCC), was cultured in complete media consisting of Alpha MEM supplemented with 12% fetal bovine serum, 12% horse serum, 1% penicillin/streptomycin, 0.2 mM inositol, 0.02

mM folic acid, and 0.1 mM 2-mercaptoethanol. Cell density was maintained between $1x10^5$ and $1x10^6$ viable cells/mL using a 1:3 split ratio. Peripheral blood mononuclear cells (PBMCs) were isolated from whole blood on a density gradient (Lympholyte H; Cedarlane Labs). Whole blood was either collected from healthy donors, under informed consent, as approved by the Institutional Review Board at the University of Arkansas, or purchased, de-identified, from the New York Blood Center. All experiments were performed in accordance with relevant guidelines and regulations at the University of Arkansas, the University of North Carolina and North Carolina State University.

IFN-γ secretion from NK-92MI cells and PBMCs was used as an indicator of hIL-12 bioactivity. NK-92MI cells and PBMCs were seeded in a 96-well plate at 20,000 and 100,000 cells/well, respectively. hIL-12 was added to achieve final concentrations from 0.04 to 5 ng/ml. Heparin, HS, hyaluronic acid, chondroitin sulfate or dextran was added to a final concentration of 10 µg/ml. Cells in hIL-12 alone or culture media alone served as controls. After 24-48 hours, hIL-12-dependent secretion of IFN-γ into the supernatant of the culture was quantified via enzyme-linked immunosorbent assay (ELISA) (88-7317; eBiosciences). For PBMC subset analysis, stimulated cells were analyzed for intracellular IFN-γ expression on a BD Celesta flow cytometer (BD Biosciences).

HEK-Blue™ IL-12 cells (Invivogen) express a STAT4-inducible secreted embryonic alkaline phosphatase (SEAP) reporter gene that is triggered upon binding of IL-12 to IL-12R. HEK-Blue™ IL-12 cells were seeded onto a 96 well plate at 50,000 cells/well and exposed to media containing 0.04 to 20 ng/ml hIL-12 with or without 10 µg/ml heparin. After 12 hours, SEAP concentrations in supernatants were detected through the addition of Quanti-Blue™ (Invivogen) and quantified via absorbance readings at 650 nm.

2.2.2. IL-12-GAG binding studies

Binding affinities between hIL-12 and various GAGs were quantified by isothermal titration calorimetry on an iTC200 (MicroCal Inc.). Both hIL-12 and GAGs were prepared in 10 mM sodium phosphate buffer with 100 mM sodium chloride at pH 7.2. All samples were subjected to high speed centrifugation to remove any suspended particulate material and degassed to remove dissolved air before titration. GAGs (2 mM) were titrated into hIL-12 (200 µM) for a total of 30 injections. Titrations were performed at physiological temperature (37°C). Titration curves were fit to the one-set of sites binding model using Origin^{TM} v7.0 software to derive binding constants.

2.2.3. Proteolytic digestion assays

To evaluate hIL-12 degradation in spent media, NK-92MI cells were cultured in media without serum for 3 days at a starting cell density of 1×10^6 cells/ml. Spent media were collected, centrifuged, 0.2 µm-filtered and co-incubated with 500 pg/ml hIL-12 ± 10 µg/ml heparin. Fresh cell culture media with 50 µg/ml bovine serum albumin as a stabilizing protein was used as a negative control. Fresh cell culture media with 0.125% trypsin was used as a positive control. Samples from each treatment were collected at 0, 24, 48 and 72 hours. Full length hIL-12p70 concentrations were quantified via ELISA (88-7126; eBiosciences).

To evaluate hIL-12 degradation by known proteases, trypsin, chymotrypsin, thermolysin, thrombin and protease inhibitor cocktail tablets were purchased from Sigma-Aldrich. A protease cocktail was prepared by mixing trypsin, chymotrypsin, thrombin and thermolysin in PBS. hIL-12 (1 µg/ml) ± heparin (10 µg/ml) was added to the cocktail at protein to protease molar ratio of 10:1. PBS with 0.1% w/v bovine serum albumin as a stabilizing protein was used as a negative control. The mixture was incubated at room temperature and samples were collected at 0, 1, 2, 5,

10, 15, 20 and 30 min. Full length hIL-12p70 concentrations were quantified via ELISA (88-7126; eBiosciences).

2.2.4. Size exclusion chromatography

Oligomerization of hIL-12 in the presence of heparin was observed on a Sephacryl S-200 size exclusion chromatography column connected to an AKTA fast protein liquid chromatography system. All samples were resolved at room temperature at a flow rate of 1 mL/min in 10 mM sodium phosphate buffer (pH 7.2) containing 100 mM NaCl. The apparent molecular mass of the hIL-12 samples was determined against a standard curve constructed under similar conditions using common protein standards – β-amylase (200 kDa), alcohol dehyrogenase (150 kDa), conalbumin (75 kDa), ovalbumin (45 kDa), carbonic anhydrase (29 kDa) and RNaseA (13.7 kDa).

2.2.5. Circular Dichroism

The secondary structure of hIL-12, in the presence and absence of heparin, was monitored by far-UV circular dichroism (CD) using a Jasco-710 spectropolarimeter. Samples contained 100 µM hIL-12 in 10 mM sodium phosphate buffer (pH 7.2) with 100 mM sodium chloride. A total of 15 scans were acquired at 25°C with a scan speed of 50 nm/minute. Data for hIL-12 with heparin at a 1:5 molar ratio were collected under the same conditions. Appropriate blank titrations were performed to eliminate background noise. Processed data was expressed in molar ellipticity (deg. cm^2. dmol^{-1}).

2.2.6. Differential Scanning Calorimetry

Thermal denaturation of hIL-12 (100 µM), in the absence and presence of heparin, was performed on a NANO DSC III differential scanning calorimeter (TA Instruments) with a ramping temperature of 1°C/min spanning from 10°C to 90°C in 10 mM sodium phosphate buffer

(pH 7.2) containing 100 mM sodium chloride. Thermodynamic values were calculated using Origin™ v7.0 software

2.2.7. Equilibrium unfolding and ANS binding

Guanidine hydrochloride-induced unfolding was performed on 10 µM hIL-12 in the presence and absence of heparin. The equilibrium unfolding data was plotted to derive the melting concentration (C_m) and ΔG (H_2O). The surface accessible non-polar surfaces in hIL-12, in the presence and absence of heparin, was monitored by 8-anilinonaphthalene-1-sulfonic acid (ANS) fluorescence. All fluorescence experiments were performed at 25°C on a Hitachi F2500 spectrofluorimeter. The excitation wavelength was set to 280 nm and bandwidths for excitation and emission were set to 2.5 and 10 nm, respectively. A stock solution of 20 mM ANS solution was used for titration into 10 µM hIL12 in 10 mM sodium phosphate buffer (pH 7.2) containing 100 mM sodium chloride. Samples were excited at 380 nm and emission spectra were monitored between 450 to 600 nm with a peak observed at 500 nm. Data from the ANS binding assay were overlaid to identify differences in surface hydrophobicity.

2.2.8. Small-angle X-ray Scattering (SAXS) Analysis

SAXS data of hIL-12, in the absence and presence of heparin, was acquired at the Cornell High Energy Synchrotron Source (CHESS) beamline G1 source. Inline size exclusion chromatography (SEC) was used to minimize polydispersity. hIL-12 (150 µM), with and without low molecular weight heparin (in ten-fold excess) was loaded onto a Sephacryl-S 300 column attached to AKTA explorer (GE Healthcare). Eluted protein sample entered the flow cell of the BioSAXS at CHESS and was subjected to X-ray beam exposure. Beamline characteristics used for acquiring the data were as follows: energy = 9.968 keV (1.257 A); beam diameter = 250 µm x 250 µm; photon flux = 1.6×10^{11} photons/sec. The detector used for this

experiment is a dual Pilatus 100K-S with a q-space range between 0.006 to 0.8 Å. Data acquired was processed using BioXTAS RAW software for performing the buffer subtraction. Buffer subtracted plots were analyzed using the ATSAS program (35) with a sequence of steps to obtain an average low resolution structure.

2.2.9. Heparin binding and IL-12 bioactivity on IL-12R mutant and wild-type cells

Both IL-12 receptor subunits, IL-12Rβ1 and IL-12Rβ2, were functionally deleted from NK-92MI cells via CRISPR/Cas9 genome editing (see 2.2.10 for details). The resulting mutants are denoted as IL12Rβ1^{mut}/IL12Rβ2^{mut} NK-92MI cells. For analysis of cell surface binding, wild-type NK-92MI cells, IL12Rβ1^{mut}/IL12Rβ2^{mut} NK-92MI cells, PBMCs and HEK-293 cells (CRL-1573; ATCC) were incubated at 4°C, to inhibit cellular uptake, with Alexa Fluor 647 (ThermoScientific)-labeled hIL-12 (AF647-IL12) (10 ng/ml), in the presence and absence of 10 μg/ml heparin. Cells in culture media alone served as controls. After one hour, cells were analyzed on a BD FACSCantoII or a BD Celesta (BD Biosciences).

To assess the effect of IL12R deletion on heparin binding, parental NK-92MI and IL12Rβ1^{mut} /IL12Rβ2^{mut} cells were exposed to 10 μg/ml heparin, labeled with Cyanine5 (heparin-Cy5) (Nanocs), for 1 hour at 4 °C. Cells in culture media alone served as controls. After one hour, cells were washed once with cold PBS and analyzed on a BD FACSCantoII.

To assess the effect of heparin on hIL-12 bioactivity in IL12R mutant cells, parental NK-92MI and IL12Rβ1^{mut}/IL12Rβ2^{mut} cells were cultured with 200 pg/ml hIL-12 ± 10 μg/ml heparin for 24 hours. IFN-γ production was quantified by ELISA as described above.

2.2.10. CRISPR/Cas9-mediated deletion of IL12Rβ1 and IL12Rβ2

Two 20-bp guide sequences, (5'-GGAGCACTCGTAACGATCAC-3') and (5'-CAGGATTAACTTGTTACGTC-3'), targeting DNA within exon $305-419$ of IL12Rβ1 and exon

49

717 – 1004 of IL12Rβ2, respectively, were selected from "the CRISPR design tool" provided by the Zhang lab at MIT (http://crispr.mit.edu/). Guide sequences were cloned into separate pCas-GuideEF1a-GFP plasmids provided by Origene. Plasmids were amplified by *E. coli* and then purified using QIAGEN Plasmid Maxi Kit.

NK-92MI cells ($2x10^6$ cells) were re-suspended in 100 μl of the electroporation buffer (Harvard Apparatus, Holliston, MA) and added to an electroporation cuvette. Plasmid (10 μg) was added to the electroporation cuvette and mixed well by pipetting. The cell suspension was electroporated with 250 volts, 25 ohms, and 750 μF in a 2 mm cuvette using the electroporation system ECM630 (Harvard Apparatus, Holliston, MA). Electroporated cells were then transferred to pre-warmed 1 ml culture media in a well of 6-well plate. These cells were cultured at 37°C for 72 hours.

NK-92MI transfected cells were harvested by centrifugation and diluted to a concentration of $2x10^6$ cells/ml in PBS. Then, the cells were filtered through a 50 μm filter into a FACS tube. The transfected cells were sorted using FACS Aria III system (BD Biosciences). Only the top 5% of GFP-positive cells were collected to ensure high transfection levels of CRISPR/Cas9 complexes.

To create a double mutant IL12Rβ1^{mut}/IL12Rβ2^{mut} NK-92MI cell line, IL12Rβ2 was first functionally deleted. An IL-12Rβ2^{mut} clone was selected and propagated for one month to allow transient GFP expression to subside. IL12Rβ1 was subsequently functionally deleted using the transfection method described above. Cells were once again sorted and cloned. Functional deletion of IL12Rβ1 and IL12Rβ2 was verified by loss of IL-12 responsiveness (Fig. 2.5).

2.2.11. Analysis of Intracellular IFN-γ expression in PBMC subsets

One million freshly isolated human PBMCs were stimulated with IL-12 alone (200 pg/ml) or IL-12 plus heparin (10 µg/ml) for 12 hours in a 96 well plate. Monensin (554724; BD Biosciences) was added for the last 10 hours of stimulation to block intracellular transport. After 12 hours of stimulation, cells were rinsed and stained with viability markers (Fixable Viability Stain 510; BD Biosciences) followed by blocking Fcγ receptors (564220; BD Biosciences) and staining for the following cell surface markers: CD3 (clone: UCHT1), CD19 (clone: SJ25C1), CD4 (clone: RPA-T4), CD8 (clone: RPA-T8), CD56 (clone: B159) and CD45 (clone: HI30). After surface staining, cells were fixed and permeabilized (554715; BD Biosciences) prior to staining for IFN-γ (clone: B27). Twenty thousand live PBMCs were acquired on a BD FACSCelesta (BD Biosciences) and analyzed using FlowJo v10 software (FlowJo LLC, Ashland, OR).

2.2.12. IL12R expression in mutant NK-92MI via flow cytometry and western blot.

For analysis of IL12R expression via flow cytometry, IL12Rβ1^{mut}/IL12Rβ2^{mut} and wildtype NK-92MI cells were stained with 1 µg/10^6 cells of APC-conjugated anti-IL12Rβ1 (FAB839A; R&D Systems), APC-conjugated anti-IL12Rβ2 (FAB1959A; R&D Systems) or APC-conjugated mouse IgG1, k isotype control (550854; BD Biosciences). Cells were rinsed twice in cold PBS and read on a BD FACSCelesta. Data were analyzed using FlowJo v10 software (FlowJo LLC, Ashland, OR). For qualitative assessment of IL12R expression via western blot, IL12Rβ1^{mut}/IL12Rβ2^{mut} and wild-type NK-92MI cells as well as HEK-293 cells (negative control) were lysed using RIPA lysis buffer with a protease and phosphatase inhibitor cocktail (78440; ThermoFisher). Homogenates were incubated for 5 minutes and then centrifuged at 13,000 × g for 10 minutes at 4 °C. Cell lysates were collected by withdrawing the

supernatant without disturbing the pellet. Protein concentration was estimated via bicinchoninic acid assay (BCA) (23250; Pierce). 50 µg/lane of protein was separated on 12% SDS-PAGE under reduced condition. The proteins were transferred onto a polyvinylidene difluoride (PVDF) membrane and blocked with Odyssey Blocking Buffer (927-50000; LI-COR Biosciences) at room temperature for 2 h. The membranes were then probed overnight with rabbit anti-IL12Rβ1 antibody (ab96517; Abcam), mouse anti-IL12Rβ2 (MAB19591; R&D Systems) and mouse anti-beta-actin (ab8226; Abcam) in Odyssey Blocking Buffer. Beta-actin was used as the gel loading control. Primary antibodies were used at a dilution of 1:5000. Secondary antibodies, goat anti-rabbit IgG H&L-alkaline phosphatase (ab97048; Abcam) and goat anti-mouse IgG H&L -alkaline phosphatase (ab97020; Abcam) were used at a dilution of 1:5000. After blotting, protein bands were developed with NBT/BCIP substrate solution (34042; ThermoFisher). Qualitative images of blots were taken with an 8.0-megapixel digital camera.

2.2.13. Statistical analysis

All experiments were carried out in triplicate or quadruplicate. Where appropriate, data are presented as mean ± standard deviation. Where indicated, analysis of variance (ANOVA) or Student's t-test were performed using Prism 7 software (GraphPad Software, Inc, La Jolla, CA). Statistical significance was accepted at the $p \leq 0.05$ level.

2.2.14. Data availability statement

All data and relevant materials are available from the corresponding author upon reasonable request.

2.3. Results

2.3.1. Effect of heparin and other GAGs on hIL-12 bioactivity

IFN-γ production from NK-92MI cells exposed to hIL-12 in the presence and absence of heparin was used as a measure of hIL-12 bioactivity. NK-92MI cells produced low levels of IFN-γ (47.3±7.0 pg/ml) in the absence of hIL-12 (Fig. 2.1A). Upon exposure to 0.04 to 5 ng/ml hIL-12, IFN-γ concentrations increased steadily from 48±7 to 1523±178 pg/ml. Overall, the addition of heparin significantly augmented hIL-12-induced IFN-γ production by 55 to 661% ($p<0.05$ vs. hIL-12 alone via ANOVA). Treatment of cells with heparin alone (0 pg/ml hIL-12) had no effect on IFN-γ production ($p>0.05$ vs. untreated controls via t-test).

To determine if the order of heparin addition influenced hIL-12 bioactivity, heparin was added to culture medium 30 minutes before hIL-12, at the same time as hIL-12 or 30 minutes after hIL-12. The order of heparin addition was found to have no effect ($p>0.05$ for all comparisons within each hIL-12 concentration via two-way ANOVA) (Fig. 2.1B).

The effect(s) of other common GAGs, including HS, hyaluronic acid, and chondroitin sulfate, on hIL-12 bioactivity were also examined. Similar to heparin, HS enhanced hIL-12-mediated production of IFN-γ by about 2.5 times (Fig. 2.1C). Conversely, chondroitin sulfate, hyaluronic acid and dextran, as a non-GAG control polysaccharide, had no discernable effect on hIL-12 bioactivity.

To determine if the heparin-induced increase in hIL-12 bioactivity was a widespread phenomenon, similar experiments were performed in human PBMCs and HEK-Blue™ IL-12 sensing cells. Indeed, heparin significantly enhanced IL-12 bioactivity on both human PBMCs (Fig. 2.1D) and HEK-Blue™ IL-12 cells (Fig. 2.1E). In PBMCs, the effect was most pronounced at 200 ng/ml hIL-12 where IFN-γ production was increased by more than 3-fold in the presence

of heparin. The enhancing properties of heparin decreased at higher hIL-12 concentrations. An analysis of intracellular IFN-γ expression by PBMC subsets via flow cytometry revealed that NK cells, and not CD4$^+$ or CD8$^+$ T cells, were primarily responsible for the observed increases in IFN-γ production (Supplementary Fig. S.2.1).

2.3.2. Effect of heparin and other GAGs on hIL-12 binding

ITC experiments were performed to compare the binding affinities between several GAGs and hIL-12. The affinity of hIL-12 to heparin was found to be in the low micromolar range with an apparent K_d value of ~23 μM (Table 2.1). HS also bound to hIL-12 in the low micromolar range (K_d ~9 μM). However, no binding was observed between hIL-12 and the other GAGs or dextran examined. Representative isothermograms are shown in Supplementary Fig. S.2.2.

The stoichiometry of binding, obtained from the fitting ITC data to a one-set of sites binding model, was approximately 1 for both HS/IL12 and heparin/IL-12 complexes (Table 2.1). This indicates a single binding site for heparin/HS on hIL-12. Heparin/HS binding was accompanied by a large decrease in enthalpy (ΔH) and an increase in entropy (ΔS). These changes indicate that the IL-12/heparin binding is facilitated by both hydrophobic and electrostatic interactions.

2.3.3. Effect of heparin in preventing proteolytic degradation of hIL-12

To determine if the heparin-dependent increase in hIL-12 bioactivity could be attributed to protection from proteolytic enzymes in cell culture media, the time-dependent degradation of hIL-12 in fresh and spent media, with and without heparin, was quantified. Spent media were obtained from NK-92MI cells cultured at high density for 24 hours without serum supplementation. After up to 72 hours of incubation, there was no appreciable degradation of

54

hIL-12 in spent media regardless of heparin addition (Fig. 2.2A). In fact, concentrations of hIL-12 in spent media or fresh media were indistinguishable. The addition of strong proteolytic enzyme, trypsin, completely degraded hIL-12, apparently irrespective of heparin addition, within 24 hours. In a follow up experiment, hIL-12 alone or hIL-12 with heparin, was cultured with a protease cocktail for up to 30 minutes (Fig. 2.2B). At this shorter time scale, it became apparent that heparin partially protects hIL-12 from strong proteolytic enzymes.

2.3.4. Analysis of heparin-hIL-12 interactions

Following up on the ITC binding studies, the nature of the interactions between heparin and hIL-12 was characterized by SEC and SAXS. SEC revealed that hIL-12 migrated with an apparent molecular mass of 103.6 kDa (Table 2.2). The difference between this apparent molecular mass from SEC and the experimental molecular mass of hIL-12 (65 kDa) obtained from our previous electrospray ionization-mass spectrometry analysis (33), could be attributed to the extensive glycosylation pattern that is found in this class of cytokines (36-40) and the extended, non-globular structure of hIL-12 (33, 41). In the presence of heparin, hIL-12 showed an apparent molecular mass of ~172.9 kDa suggesting that binding of heparin likely induces dimerization of the protein. The marginal difference between the expected molecular mass and the observed molecular mass, calculated from the SEC experiment, can be attributed to the non-globular nature of the IL12-heparin complex and also the minor uncertainties introduced due to data extrapolation on the standard molecular mass curve which did not include proteins of molecular mass greater than 180 kDa.

SAXS analysis indicated that the average molecular mass of hIL-12, calculated from the radius of gyration, was approximately 70 kDa (Table 2.2). This is in good agreement with the

55

predicted molecular mass of hIL-12 including glycosylation. For heparin-hIL-12 complexes, the average molecular mass was approximately ~200 kDa which corroborates the SEC data.

2.3.5. Effect of heparin on hIL-12 conformation and stability

Far-UV CD measurements were performed to determine if heparin influenced the secondary structure of hIL-12. In the absence of heparin, hIL-12 showed a strong negative ellipticity band at around 210 nm (Fig. 2.3A) and a shoulder around 222 nm indicating the presence of alpha-helix and beta-sheet secondary structures. Incubating hIL-12 with heparin revealed only minor changes in the shape of the spectrum. These results suggest that heparin does not induce discernable backbone conformational changes in IL-12.

Intrinsic tryptophan fluorescence is a sensitive technique to monitor subtle tertiary structural changes induced by ligand binding. An overlay of intrinsic fluorescence emission spectra in the absence and presence of heparin for hIL12 showed an identical emission maxima at 341 nm (Fig. 2.3B) suggesting there was no significant change in the microenvironment of tryptophan upon binding to heparin. A marginal increase in the relative fluorescence intensity in the presence of heparin could be attributed to an increased rigidity in the tertiary structure of the protein with an enhanced hydrophobic content around the sites of tryptophan.

Similar to thermal unfolding, proteins undergo denaturation in the presence of strong chaotropes such as, guanidinium salts or urea. In this study, hIL-12 was subjected to guanidinium chloride-based equilibrium unfolding. It was observed that hIL-12 is moderately stabilized in the presence of heparin as evidenced by an increase in the C_m value [concentration of the denaturant at which 50% of the protein population is in the denatured state(s)] from 2.0 M to 2.5 M (Fig. 2.3C-E).

ANS binding assay was used to monitor surface hydrophobicity and solvent accessibility of surface residues in hIL-12 in the absence and presence of heparin. ANS is a hydrophobic fluorescent dye which binds to solvent-exposed non-polar surface of proteins. Emission spectrum of ANS upon binding to IL-12 shows an emission maximum at 500 nm. The ANS concentration-dependent binding curve (Fig. 2.3F) shows a steady increase in the emission intensity at 500 nm (Fig. 2.3F) in the range of $0 - 200$ μM and plateaus at higher concentrations. The ANS concentration-dependent binding curve in the presence of heparin shows a similar trend. However, the 500 nm emission intensity, in the presence of heparin, is marginally lower in the ANS concentration of 75 μM $-$ 200 μM suggesting that the binding of heparin only causes a subtle conformational change in IL-12.

To understand the effect of heparin on the thermal stability of hIL-12, protein unfolding was monitored using differential scanning calorimetry. hIL-12 in the absence of heparin, showed a melting temperature (T_m) of ~ 65°C (Fig. 2.3G). The unfolding process was irreversible as the cooling cycle did not show a sharp peak as observed during the heating cycle. In the presence of heparin, T_m increased marginally by only 1.2°C.

2.3.6. Effect of heparin on cell surface binding of hIL-12

Binding of AF647-hIL12 to NK-92MI cells, PBMCs and HEK cells in the presence and absence of heparin was assessed via flow cytometry. The addition of AF647-hIL12 alone to NK-92MI cells resulted in a significant shift in cell surface fluorescence compared to unstained controls (Fig. 2.4A). When exogenous heparin was included, the mean fluorescence intensity due to AF647-hIL12 binding increased from 2,200 to 12,561.

Recognizing that heparin could be facilitating non-specific binding to the cell surface, i.e. binding to moieties other than the IL-12 receptors, the experiment was repeated in NK-92MI

cells in which both IL-12 receptor subunits, IL12Rβ1 and IL12Rβ2, were functionally deleted via CRISPR-Cas9 gene editing. Indeed, disrupting the heterodimeric IL-12 receptor had no effect on the increase in AF647-hIL12 binding to the cell surface in the presence of heparin (Fig. 2.4B). Additionally, heparin binding, as visualized by heparin-Cy5, was not influenced by the IL12R deletion (Fig. 2.4C).

Follow up western blot and flow cytometry assays, revealed that the IL12Rβ1^{mut}/IL12Rβ2^{mut} NK-92MI cells still expressed some portion of the IL12R subunits (Supplementary Fig. S.2.3). Therefore, an additional experiment was performed to measure hIL-12 binding to HEK-293 cells which do not express IL12R and PBMCs which mostly do not express IL12R. Fig. 2.4D and 2.4E demonstrated that heparin modestly increases IL-12 binding to the surfaces of HEK-293 cells and PBMCs.

Perhaps most interestingly, even though hIL-12 alone poorly bound in IL12Rβ1^{mut}/IL12Rβ2^{mut} NK-92MI cells, the addition of heparin almost completely restored hIL-12 bioactivity ($p < 0.0001$ hIL-12 alone vs. hIL-12 plus heparin in mutant cells via two-tailed t test) (Fig. 2.5). In fact, IFN-γ production by the IL-12R mutant cells treated with hIL-12 and heparin was greater than 90% of the IFN-γ production by wild-type NK-92MI cells treated with hIL-12 plus heparin ($p > 0.05$ hIL-12 plus heparin in mutant cells vs. hIL-12 plus heparin in wild-type cells via two-tailed t test).

2.4. Discussion

Our previous study demonstrated that hIL-12 binds to heparin specifically and that heparin binding sites are primarily located on the p40 subunit of hIL-12 (33). This study is the first to unambiguously demonstrate that heparin positively modulates the activity of hIL-12 (Fig. 2.1). Initial bioactivity studies were performed on a human NK cell line and subsequently

confirmed using human PBMCs and an IL-12-sensing HEK cell line. Thus, the heparin-induced increase in hIL-12 activity appears to be widespread. A PBMC subset analysis revealed that NK cells, and not CD4^{+} nor CD8^{+} T cells, were responsible for the increase in IFN-γ production in response to stimulation with hIL-12 and heparin (Supplementary Fig. S.2.1).

Binding and modulation of hIL-12 activity was restricted to heparin and HS, the two most N-sulfated GAGs. Chondroitin sulfate and hyaluronic acid did not bind to hIL-12 nor did they have an effect on hIL-12 bioactivity. The fact that dextran, chondroitin sulfate and hyaluronic acid did not influence hIL-12 bioactivity indicates that a high density of sulfation is critical for binding and modulating hIL-12.

ITC binding analyses demonstrated that hIL-12 contains a distinct, accessible heparin binding pocket. The low micromolar binding affinities for heparin and HS, together with moderate increases in entropy and decreases in enthalpy are indicative of a robust, specific electrostatic and non-polar interaction.

SEC and SAXS data demonstrated that hIL-12 predominantly forms dimeric structures (Table 2.2). This dimerization/oligomerization could help stabilize the IL-12/receptor complex. Similar observations have been made with other interleukins. The extracellular domain of IL-5R binds to a homodimeric form of IL-5 attaining a critical "wrench-like" structural conformation (42). Likewise, IL-22 was shown to form dimers and tetramers in solution and organize into a V-shaped dimeric conformation binding to IL-22R1 receptor (43). The effect of heparin on stabilizing the IL-12/receptor complex is the subject of ongoing studies.

With respect to other mechanism(s) by which heparin modulates hIL-12 activity, we explored a number of possibilities based on the heparin literature. Heparin has been shown to protect proteins, such as bFGF, from the hydrolytic action of plasmin and other proteases present

in the extracellular milieu (44). However, our data showed that hIL-12 was not significantly

degraded by proteases or any other molecules that may be present in spent media (Fig. 2.2A). As

expected, trypsin, used as a positive control, quickly and completely degraded hIL-12 equally in

the presence and absence of heparin. Because trypsin digested all of the hIL-12 within the first

time point, i.e. 24 hours, a subsequent experiment with a defined protease cocktail was

performed over a shorter time frame. Within 30 minutes, heparin was found to reduce protease-

driven hIL-12 degradation by up to 14% (Fig. 2.2B). However, it should be noted that all hIL-12,

regardless of heparin inclusion, is expected to be inactivated by the protease cocktail within a

few hours. Thus, although heparin can somewhat protect hIL-12 from strong proteolytic

degradation, this is not a plausible mechanism for the increased hIL-12 activity in vitro that we

observed.

Conformational analysis of hIL-12 in the presence and absence of heparin was performed

as other heparin-binding proteins have been shown to be stabilized with heparin. Biophysical

characterization of heparin-hIL-12 binding via far-UV CD measurements, folding studies, ANS

binding and thermal stability assays demonstrate that heparin causes a slight change in hIL-12

conformation but no gross secondary or tertiary structural changes (Fig. 2.3). There is also a

minor increase in thermal stability. Taken together, conformational and stability changes are not

so significant to suggest that they would lead to a major shift in hIL-12 bioactivity.

The strongest evidence for the mechanism by which heparin enhances hIL-12 bioactivity

points to heparin serving as a co-receptor for hIL-12. Heparin clearly increases the concentration

of hIL-12 at cell surfaces (Fig. 2.4). The effect was more pronounced in cells expressing IL-

12R, e.g. mutant and wild-type NK-92MI. Nevertheless, a small increase in hIL-12 on the cell

surface could also be found in cells expressing relatively little (PBMCs) or no IL-12R (HEK-

293). That heparin binds to cell surfaces at high levels suggest that exogenous heparin is capable of maintaining a reservoir of IL-12 at the cell surface. Heparin may also control the kinetics of association and dissociation of IL-12 to IL-12Rβ1 and IL-12Rβ2. Ibrahami et al (45), studying the kinetics of the FGF signaling complex assembly, suggested that heparin regulates the cell proliferation activity due to FGF by switching FGFR between high and low affinity states. While heparin may bind to specifically IL-12R just as it does to FGFR, follow up studies showed that heparin binds equally to wild type and IL12Rβ1^{mut}/IL12Rβ2^{mut} cells (Fig. 2.4C). Thus, it appears that heparin is binding at high levels to numerous proteins on the cell surface.

Most surprisingly, heparin was shown to facilitate hIL-12 signaling in NK-92MI cells in which both IL-12Rβ1 and IL-12Rβ2 had been functionally deleted (Fig. 2.5). A follow up analysis of IL12R expression via flow cytometry and western blot indicate that forms of both IL-12Rβ1 and IL-12Rβ2, although non-functional, were still expressed by the CRISPR/Cas9-modified NK-92MI cells (Supplementary Fig. S.2.3). Thus, it is likely that during the Cas9 dsDNA break, random insertion/deletion of nucleotides resulted in nonsynonomous mutations which allowed for expression of mutant IL12R subunits. Experiments to sequence the mutant IL12R subunits are planned.

In the absence of heparin, hIL-12 likely has poor affinity to mutated IL-12R and thus loses its ability to signal. In the presence of heparin, the interaction of hIL-12 with IL12Rβ1^{mut} and IL12Rβ2^{mut} appears to be stabilized enough to recover hIL-12 signaling. Using a string tool algorithm developed by our group (46), we searched the amino acid sequences of IL12Rβ1 and IL12Rβ2 for putative heparin binding segments, e.g. XBXXBX, XBBXBX, BXBBXB, etc. where B is a basic residue and X is a non-basic residue. Results from this search indicated that the extracellular domain (ECD) of IL-12Rβ1 contains 2 very prominent heparin binding

segments located at amino acids 293-298 and 454-459. The ECD of IL-12Rβ2 contains 3 potential heparin binding segments, amino acids 53-58, 273-278 and 353-358. Thus, heparin may simultaneously bind to and stabilize hIL-12 with one or both IL-12R subunits. Quantitation of heparin's influence on the affinities of hIL-12 for wild-type and mutated IL-12R ECDs is the subject of ongoing research.

Data from these studies clearly demonstrate a physiological role for heparin in IL-12 immunobiology. The observed increase in hIL-12 activity in the presence of heparin is rare among interleukins, for which heparin-binding is typically more inhibitory than augmentative. A potential evolutionary explanation for heparin binding is to compartmentalize IL-12 at specific sites. IL-12, when administered systemically, is known to induce life-threatening adverse events (47). Thus, heparin's ability to localize IL-12, for example at a site of infection, while increasing its activity may provide a way to limit the systemic toxicity of this potent cytokine. A similar compartmentalization phenomenon has been observed with other cytokines whose systemic dissemination is detrimental (48). Furthermore, the finding that heparin can recover IL-12 signaling in cells with mutated IL-12R has significant implications for patients with atopic diseases driven by IL-12 family receptor point mutations (49, 50). These patients are susceptible to mycobacterial infections due to defects in the IL-12/IFN-γ axis. Strategies to use heparin to co-deliver IL-12 are now being developed by our group.

Given the similarities among cytokines in the IL-12 family, our data also imply a role for heparin in modulating the activities of IL-23, IL-27 and IL-35. IL-23, like IL-12, contains the heparin-binding p40 subunit, while IL-27 and IL-35 contain the Epstein-Barr virus induced gene 3 (EBI3) subunit which is homologous to p40 (34, 51). Because the IL-12 family is central to

human immunoregulation (34), the above studies should motivate further study of heparin as a

surprisingly important immunomodulatory agent.

Table 2.1: Binding parameters of various GAGs interacting with IL-12 derived from ITC analysis

	K_d (µM)	Stoichiometry/ number of binding sites (n)	ΔH [cal/mol]	TΔS [cal/mol/°K]	ΔG [cal/mol/°K]
Heparin	23 ± 3.1	0.98 ± 0.02	-2526.2	4350.8	-1824.6
Heparan sulfate (HS)	9 ± 1.2	1.01 ± 0.02	-1920.2	4350.8	-2430.6
Chondroitin sulfate (CS)	NB	NB	NB	NB	NB
Hyaluronic Acid (HA)	NB	NB	NB	NB	NB
Dextran	NB	NB	NB	NB	NB

*NB – no binding observed

Table 2.2: Comparison of MW$_{app}$ of hIL-12 in the absence and presence of heparin using different methods

	ESI-MS	GPC Sephacryl-S200	SEC-SAXS
- Heparin	65 kDa (33)	~100 kDa	~70 kDa
+ Heparin	Not performed	~170 kDa	~200 kDa
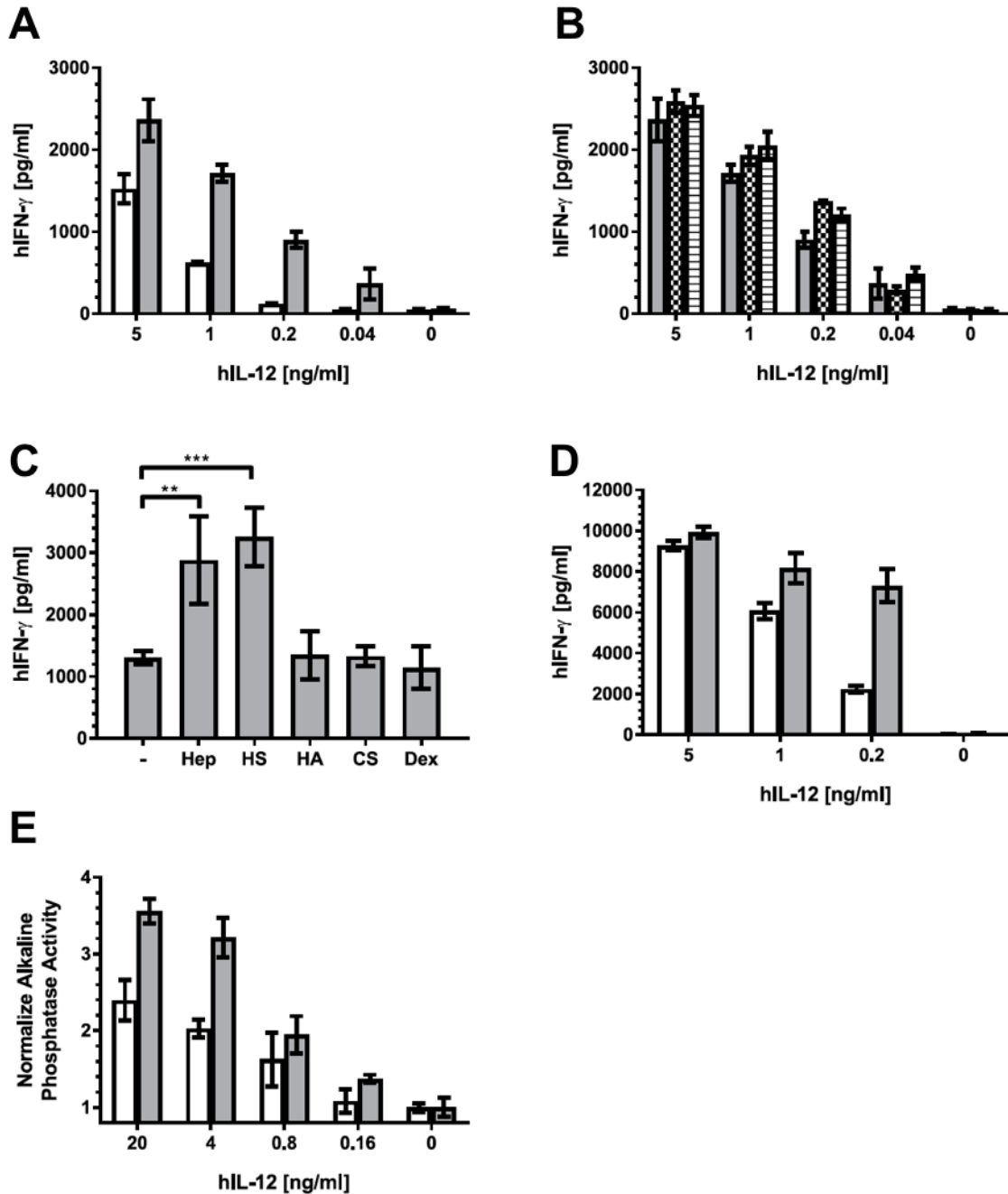
Figure 2.1. Effect of heparin and other GAGs on hIL-12 bioactivity. (A) hIFN-γ production by NK-92MI cells when incubated with media containing hIL-12 alone (white bars) or with 10 µg/ml heparin (gray bars) was quantified using ELISA. Heparin significantly enhanced hIL-12 bioactivity (p<0.0001 vs. hIL-12 alone via two-way ANOVA) (B) hIFN-γ production by NK-92MI cells when heparin (10 µg/ml) was added to NK-92MI cells at the same time as hIL-12

(gray bars), 30 mins prior to hIL-12 (checkered bars) or 30 mins after hIL-12 (horizontal). The order of heparin addition had no significant effect on hIL-12 activity (p>0.05 for all comparisons within each hIL-12 concentration via two-way ANOVA). (C) hIFN-γ production by NK-92MI cells cultured in media containing 200 ng/ml hIL-12 alone (-) or with heparin (Hep), heparin sulfate (HS), hyaluronic acid (HA), chondroitin sulfate (CS), or dextran (Dex) at 10 µg/ml was quantified using ELISA. Asterisks indicate a significant difference between indicated groups (*=p<0.01 and ***=p<0.001 via one-way ANOVA with Dunnett's post hoc correction). (D) hIFN-γ production by PBMCs when incubated with media containing hIL-12 alone (white bars) or with 10 µg/ml heparin (gray bars) was quantified using ELISA. Heparin significantly enhanced hIL-12 bioactivity (p<0.0001 vs. hIL-12 alone via two-way ANOVA). (E) Alkaline phosphate activity by HEK-Blue™ IL-12 cells in response to incubation with media containing hIL-12 alone (white bars) or with 10 µg/ml heparin (gray bars) was determined in accordance with manufacturer's instructions. Heparin significantly enhanced hIL-12 bioactivity (p<0.0001 vs. hIL-12 alone via two-way ANOVA). All data are represented as mean ± standard deviation from triplicate samples. Experiments were performed in triplicate and repeated three times with similar results.
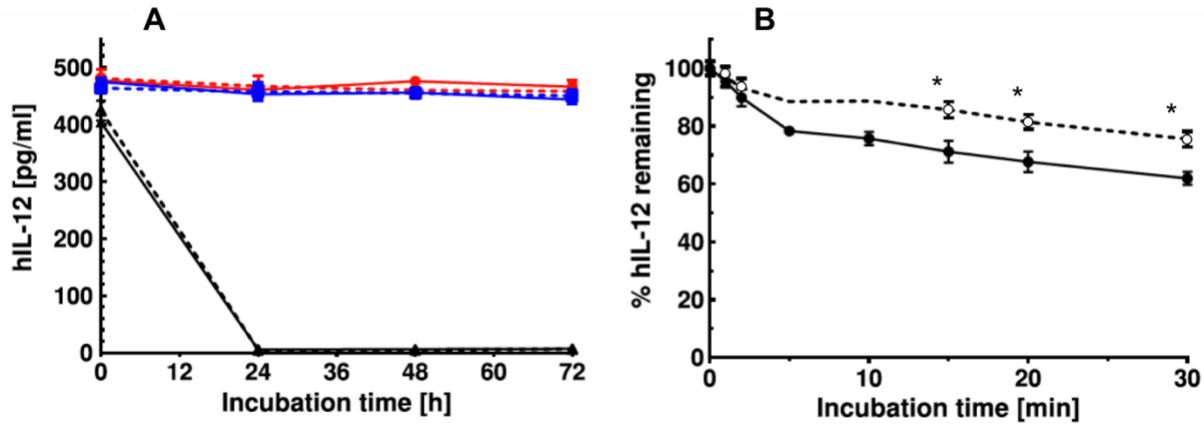
Figure 2.2. Effect of heparin on proteolytic degradation of hIL-12. (A) hIL-12 degradation when incubated with heparin (dashed lines) and without heparin (solid lines) in spent media (blue squares), fresh AMEM containing BSA (red circles) or fresh AMEM containing 0.125% trypsin (black triangles). Samples were collected at intervals of 0, 24, 48 and 72 hours and hIL-12 concentrations were quantified via ELISA. Heparin did not affect hIL-12 degradation ($p>0.05$ vs. hIL-12 alone via two-way ANOVA). (B) hIL-12 degradation when incubated with heparin (empty circles) and without heparin (filled circles) in protease cocktail containing trypsin, chymotrypsin, thrombin and thermolysin. Proteases were added to hIL-12 solution at a protein to protease molar ratio of 10:1. Samples were collected and neutralized with protease inhibitor cocktail at intervals of 0, 1, 2, 5, 10, 15, 20 and 30 min and hIL-12 concentrations were quantified via ELISA. Heparin significantly inhibited hIL-12 degradation by protease cocktails. Asterisks indicate a significant difference between groups at a particular time point (*=$p<0.05$ vs. hIL-12 alone via two-tailed t-test). All data are represented as mean ± standard deviation from triplicate samples. Experiments were performed in triplicate and repeated three times with similar results.
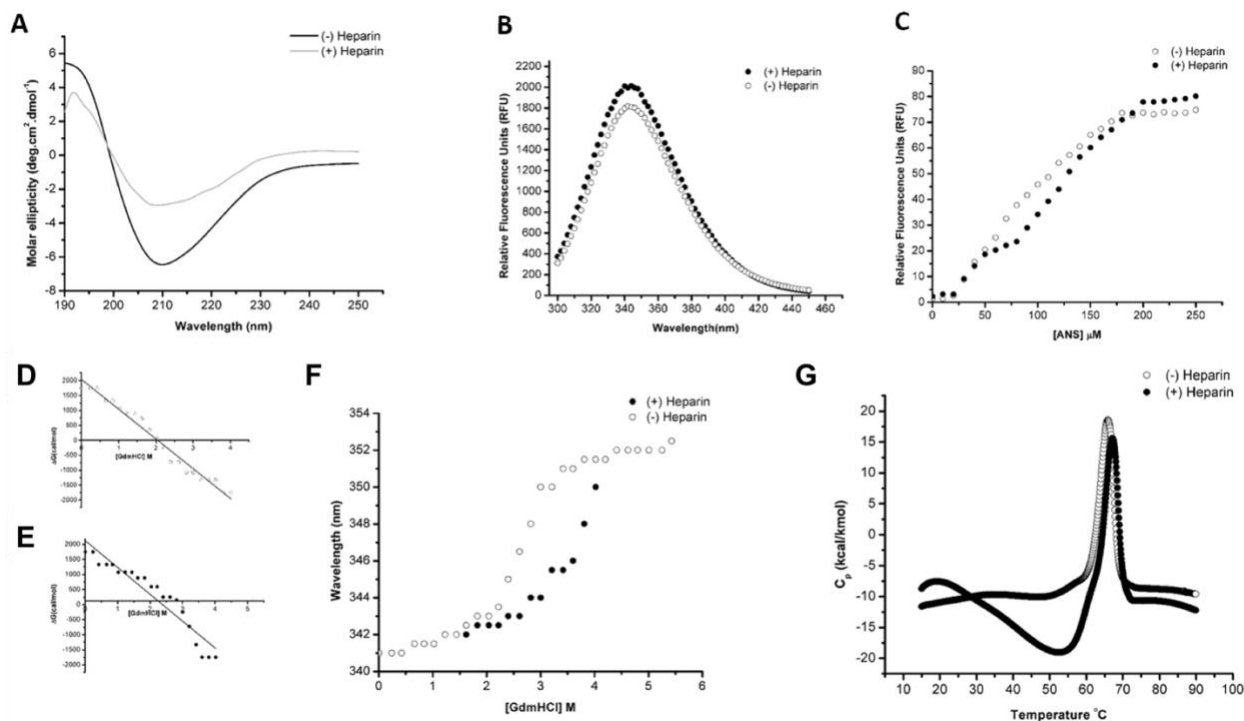
Figure 2.3. Effect of heparin on the conformation and stability of hIL12. (A) Overlay of the far-UV CD spectra (190 nm-250 nm) of hIL-12, in the absence (solid black) and presence (solid gray) of heparin. (B) Overlay of the steady-state fluorescence emission spectra on hIL-12 in the absence (empty circle) and presence (filled circle) of heparin. (C) Overlay of the equilibrium unfolding curves of IL-12, in the presence (filled circle) and absence (empty circle) of heparin. (D, E). A plot of the concentration of GdmHCl [M] versus ΔG (cal/mol) to determine the concentration (C_m) of the denaturant required for denaturation of 50% of the protein population, present in the native conformation. (F) Overlay of the ANS binding curves of hIL-12 in the absence (empty circle) and presence (filled circle) of heparin. (G) Overlay of the thermal denaturation curves of hIL12 in the absence (empty circle) and presence (filled circle) of heparin. Thermal denaturation was carried out by ramping the temperature at a rate of 1°C/min. Data obtained was plotted as heat capacity at constant pressure (Cp) versus temperature (°C) to obtain the T_m of hIL12.
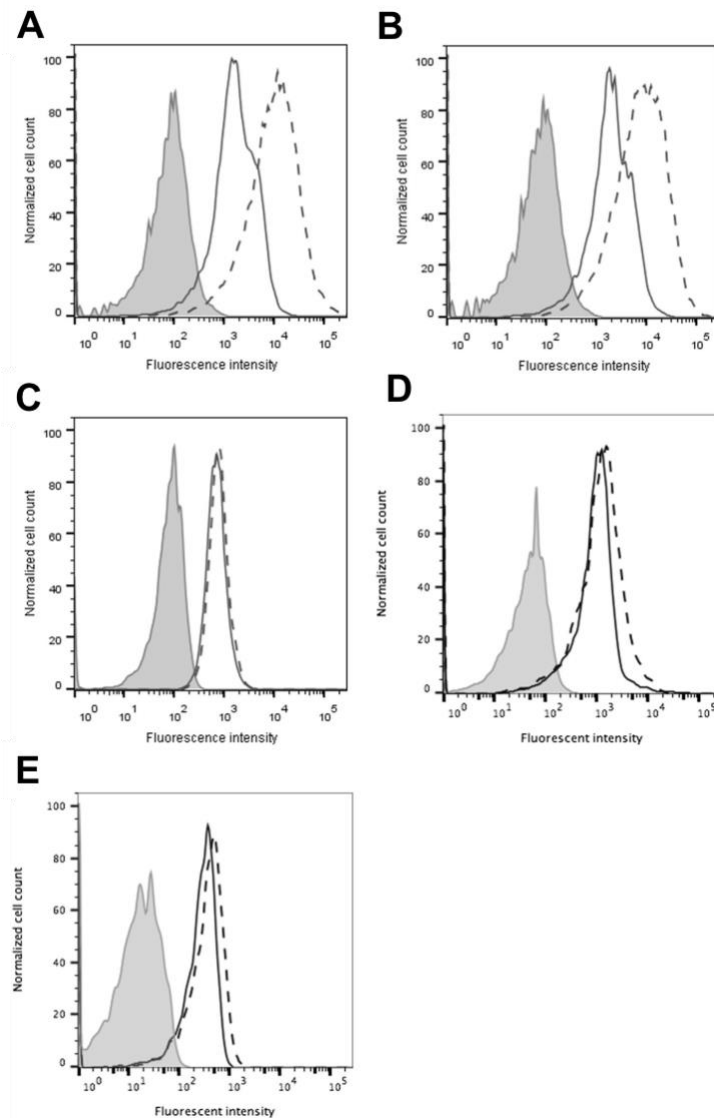
Figure 2.4. Effect of heparin on hIL12 binding to cell surfaces. (A) NK-92MI cells, (B) IL-12Rβ1^{mut}/IL-12Rβ2^{mut} NK-92MI cells, (D) HEK-293 cells or (E) PBMCs cultured with AF647-IL12 alone (solid line) or AF647-IL12 plus 10 μg/ml heparin (dashed line). Untreated cells (filled histogram) served as a negative control. (C) NK-92MI cells (solid line) and IL-12Rβ1^{mut}/IL-12Rβ2^{mut} NK-92MI cells (dashed line) were cultured for at 4°C with heparin-Cy5. Untreated NK-92MI cells (filled histogram) served as a negative control. Each panel shows the relative amounts of AF647-IL12 or heparin-Cy5 binding to cells as assessed via flow cytometry.
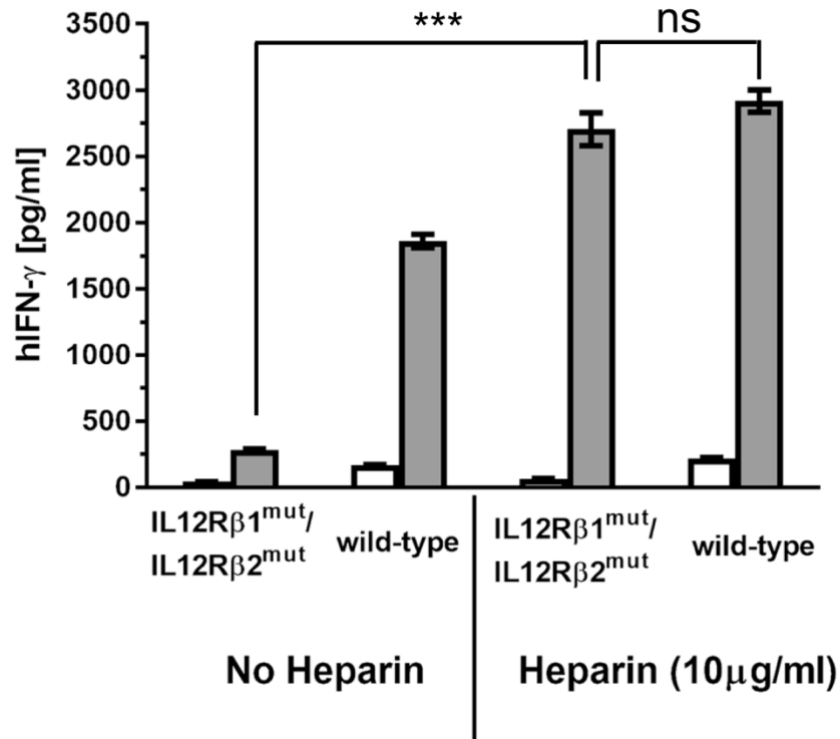
Figure 2.5. Heparin-induced recovery of hIL-12 activity. hIFN-γ production by parental NK-92MI cells and IL-12Rβ1^{mut}/IL-12Rβ2^{mut} NK-92MI cells treated with 0 ng/ml hIL-12 (white bars) or 200 ng/ml hIL-12 (gray bars) in the presence and absence of 10 μg/ml heparin was quantified via ELISA. The addition of heparin almost completely restored hIL-12 bioactivity in mutant cells (***p< 0.0001 hIL-12 alone vs. hIL-12 plus heparin in mutant cells via two-tailed t test) (p>0.05 hIL-12 plus heparin in mutant cells vs. hIL-12 plus heparin in wild-type cells via two-tailed t test), ns: not significant. All data are represented as mean ± standard deviation from triplicate samples.
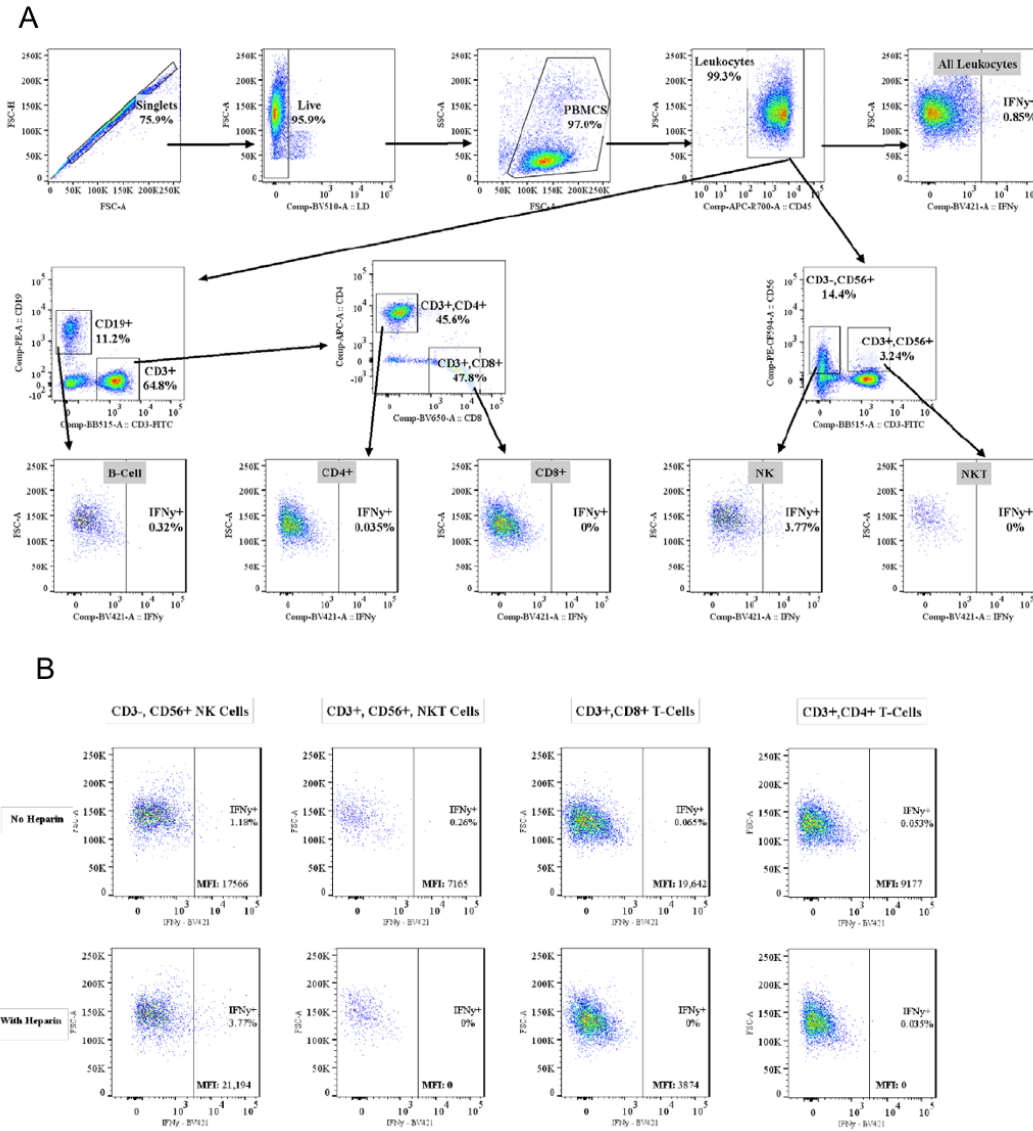
Supplementary Figure S.2.1. Intracellular IFN-γ expression among PBMC subsets. Freshly

isolated human PBMCs were stimulated with hIL-12 ± heparin and analyzed by flow cytometry.

(A) Gating strategy for analysis of intracellular IFN-γ expression. IFN-γ positive populations

were determined based on background production in cells that were not stimulated with IL-12.

(B) PBMC subset analysis revealed that natural killer cells are the primary responders to hIL-

12+heparin stimulation. NK: natural killer cells; NKT: natural killer T-cells; PBMCs: peripheral

blood mononuclear cells; IL-12: Interleukin-12; IFN-γ: Interferon-gamma.
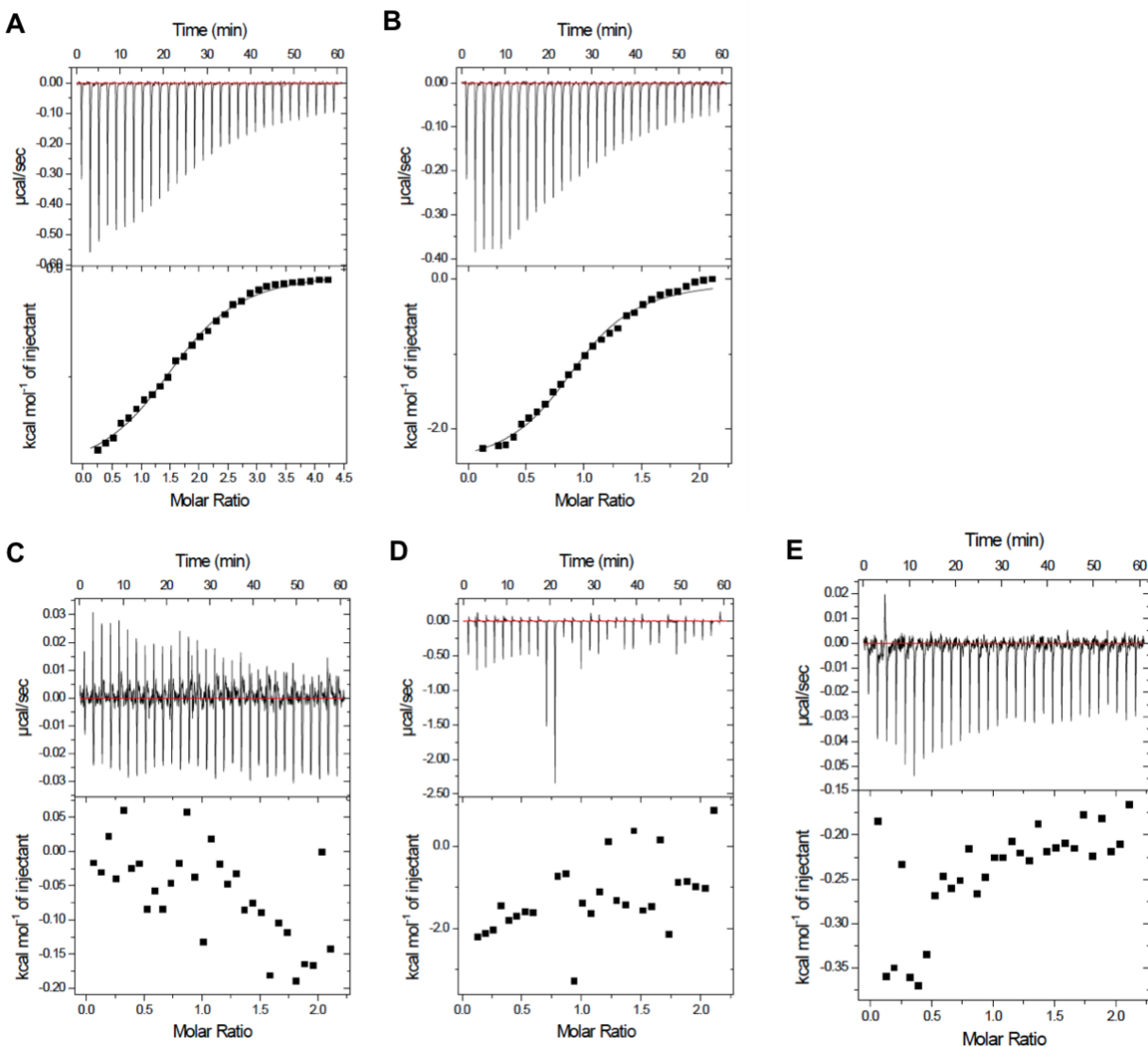
Supplementary Figure S.2.2. Isothermograms for hIL-12 interactions with various GAGs.
Isothermograms describe binding interactions between hIL-12 and (A) heparin, (B) heparin sulfate, (C) chondroitin sulfate, (D) hyaluronic acid, or (E) dextran. The upper panel of each isothermogram shows the raw data obtained for each of the 30 injections. The lower panels display the best fit data to one-set of sites binding model using Origin^{TM} v7.0 software.
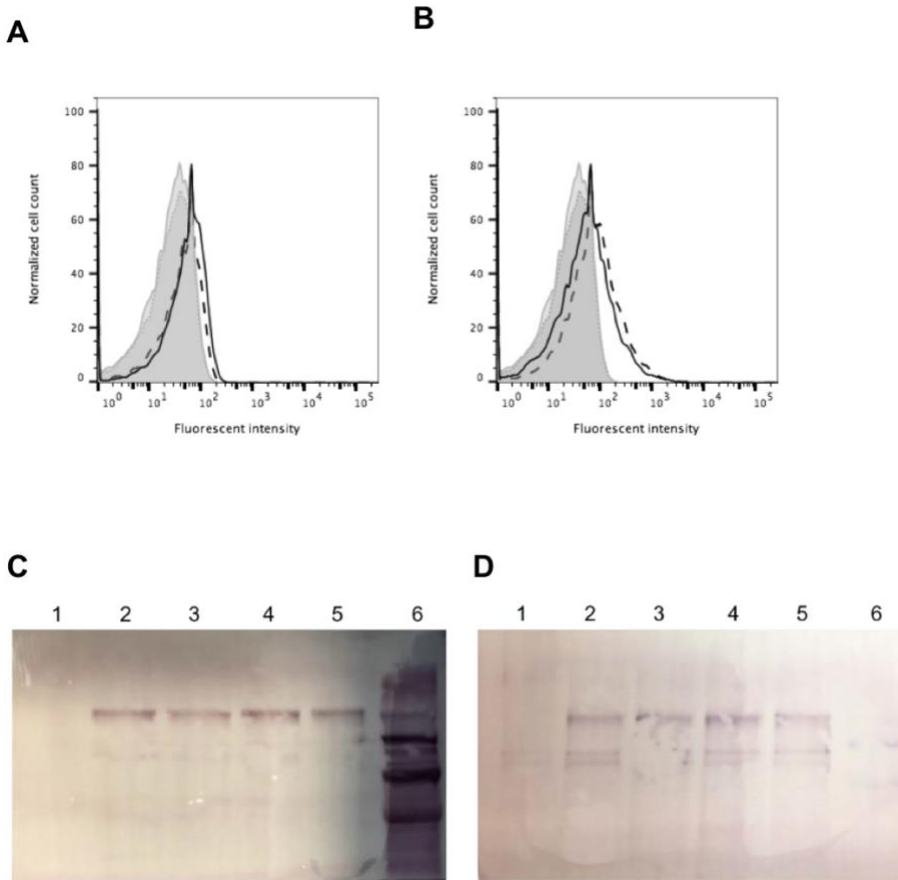
Supplementary Figure S.2.3. Analysis of IL12R expression in mutant and wild-type NK92MI cells. IL12Rβ1^{mut}/IL12Rβ2^{mut} and wild-type NK-91MI were stained with antibodies raised against IL-12Rβ1 and IL-12Rβ2 and analyzed via flow cytometry. (A) IL12Rβ1 expression in wild-type NK-91MI cells (solid line) and IL12Rβ1^{mut}/IL12Rβ2^{mut} NK-92MI cells (dashed line). (B) IL12Rβ2 expression in wild-type NK-91MI cells (solid line) and IL12Rβ1^{mut}/IL12Rβ2^{mut} NK-92MI cells (dashed line). Isotype controls for wild-type NK-92MI cells (dark filled histogram) and IL12Rβ1^{mut}/IL12Rβ2^{mut} NK-92MI cells (light filled histogram) are displayed in each panel. Data are representative of three independent experiments. Expression of IL12Rβ1 (C) and IL12Rβ2 (D) was investigated by Western blotting. *Lane 1*: HEK-293 cells; *Lanes 2-4*: IL12Rβ1^{mut}/IL12Rβ2^{mut} NK-92MI cells; *Lane 5*: wild-type NK-92MI; *Lane 6*: protein ladder.

REFERENCES

1. Fang J, Dong Y, Salamat-Miller N, Middaugh CR. 2008. DB-PABP: a database of polyanion-binding proteins. *Nucleic Acids Res* 36: D303-6

2. Salamat-Miller N, Fang J, Seidel CW, Assenov Y, Albrecht M, Middaugh CR. 2007. A network-based analysis of polyanion-binding proteins utilizing human protein arrays. *J Biol Chem* 282: 10153-63

3. Shute J. 2012. Glycosaminoglycan and chemokine/growth factor interactions. *Handb Exp Pharmacol*: 307-24

4. Gandhi NS, Mancera RL. 2008. The structure of glycosaminoglycans and their interactions with proteins. *Chem Biol Drug Des* 72: 455-82

5. Taipale J, Keski-Oja J. 1997. Growth factors in the extracellular matrix. *FASEB J* 11: 51-9

6. Elass E, Masson M, Mazurier J, Legrand D. 2002. Lactoferrin inhibits the lipopolysaccharide-induced expression and proteoglycan-binding ability of interleukin-8 in human endothelial cells. *Infect Immun* 70: 1860-6

7. Frevert CW, Kinsella MG, Vathanaprida C, Goodman RB, Baskin DG, Proudfoot A, Wells TN, Wight TN, Martin TR. 2003. Binding of interleukin-8 to heparan sulfate and chondroitin sulfate in lung tissue. *Am J Respir Cell Mol Biol* 28: 464-72

8. Kuschert GS, Hoogewerf AJ, Proudfoot AE, Chung CW, Cooke RM, Hubbard RE, Wells TN, Sanderson PN. 1998. Identification of a glycosaminoglycan binding surface on human interleukin-8. *Biochemistry* 37: 11193-201

9. Murdoch C, Finn A. 2000. Chemokine receptors and their role in inflammation and infectious diseases. *Blood* 95: 3032-43

10. Peysselon F, Ricard-Blum S. 2014. Heparin-protein interactions: from affinity and kinetics to biological roles. Application to an interaction network regulating angiogenesis. *Matrix Biol* 35: 73-81

11. Mobius K, Nordsieck K, Pichert A, Samsonov SA, Thomas L, Schiller J, Kalkhof S, Teresa Pisabarro M, Beck-Sickinger AG, Huster D. 2013. Investigation of lysine side chain

interactions of interleukin-8 with heparin and other glycosaminoglycans studied by a methylation-NMR approach. *Glycobiology* 23: 1260-9

12. Poluri KM, Joseph PR, Sawant KV, Rajarathnam K. 2013. Molecular basis of glycosaminoglycan heparin binding to the chemokine CXCL1 dimer. *J Biol Chem* 288: 25143-53

13. Salek-Ardakani S, Arrand JR, Shaw D, Mackett M. 2000. Heparin and heparan sulfate bind interleukin-10 and modulate its activity. *Blood* 96: 1879-88

14. Spillmann D, Witt D, Lindahl U. 1998. Defining the interleukin-8-binding domain of heparan sulfate. *J Biol Chem* 273: 15487-93

15. Douglas MS, Rix DA, Dark JH, Talbot D, Kirby JA. 1997. Examination of the mechanism by which heparin antagonizes activation of a model endothelium by interferon-gamma (IFN-gamma). *Clin Exp Immunol* 107: 578-84

16. Fernandez-Botran R, Yan J, Justus DE. 1999. Binding of interferon gamma by glycosaminoglycans: a strategy for localization and/or inhibition of its activity. *Cytokine* 11: 313-25

17. Rider CC. 2006. Heparin/heparan sulphate binding in the TGF-beta cytokine superfamily. *Biochem Soc Trans* 34: 458-60

18. Lortat-Jacob H, Garrone P, Banchereau J, Grimaud JA. 1997. Human interleukin 4 is a glycosaminoglycan-binding protein. *Cytokine* 9: 101-5

19. Gordon MY, Riley GP, Watt SM, Greaves MF. 1987. Compartmentalization of a haematopoietic growth factor (GM-CSF) by glycosaminoglycans in the bone marrow microenvironment. *Nature* 326: 403-5

20. Alvarez-Silva M, Borojevic R. 1996. GM-CSF and IL-3 activities in schistosomal liver granulomas are controlled by stroma-associated heparan sulfate proteoglycans. *J Leukoc Biol* 59: 435-41

21. Lortat-Jacob H, Baltzer F, Grimaud JA. 1996. Heparin decreases the blood clearance of interferon-gamma and increases its activity by limiting the processing of its carboxyl-terminal sequence. *J Biol Chem* 271: 16139-43

22. Fluhr H, Spratte J, Heidrich S, Ehrhardt J, Steinmuller F, Zygmunt M. 2011. Heparin inhibits interferon-gamma signaling in human endometrial stromal cells by interference with the cellular binding of interferon-gamma. *Fertil Steril* 95: 1272-7

23. Fritchley SJ, Kirby JA, Ali S. 2000. The antagonism of interferon-gamma (IFN-gamma) by heparin: examination of the blockade of class II MHC antigen and heat shock protein-70 expression. *Clin Exp Immunol* 120: 247-52

24. Najjam S, Gibbs RV, Gordon MY, Rider CC. 1997. Characterization of human recombinant interleukin 2 binding to heparin and heparan sulfate using an ELISA approach. *Cytokine* 9: 1013-22

25. Najjam S, Mulloy B, Theze J, Gordon M, Gibbs R, Rider CC. 1998. Further characterization of the binding of human recombinant interleukin 2 to heparin and identification of putative binding sites. *Glycobiology* 8: 509-16

26. Jones CA, Williams KA, Finlay-Jones JJ, Hart PH. 1995. Interleukin 4 production by human amnion epithelial cells and regulation of its activity by glycosaminoglycan binding. *Biol Reprod* 52: 839-47

27. Lipscombe RJ, Nakhoul AM, Sanderson CJ, Coombe DR. 1998. Interleukin-5 binds to heparin/heparan sulfate. A model for an interaction with extracellular matrix. *J Leukoc Biol* 63: 342-50

28. Mummery RS, Rider CC. 2000. Characterization of the heparin-binding properties of IL-6. *J Immunol* 165: 5671-9

29. Clarke D, Katoh O, Gibbs RV, Griffiths SD, Gordon MY. 1995. Interaction of interleukin 7 (IL-7) with glycosaminoglycans and its biological relevance. *Cytokine* 7: 325-30

30. Webb LM, Ehrengruber MU, Clark-Lewis I, Baggiolini M, Rot A. 1993. Binding to heparan sulfate or heparin enhances neutrophil responses to interleukin 8. *Proc Natl Acad Sci U S A* 90: 7158-62

31. Ramdin L, Perks B, Sheron N, Shute JK. 1998. Regulation of interleukin-8 binding and function by heparin and alpha2-macroglobulin. *Clin Exp Allergy* 28: 616-24

32. Hasan M, Najjam S, Gordon MY, Gibbs RV, Rider CC. 1999. IL-12 is a heparin-binding cytokine. *J Immunol* 162: 1064-70

33. Jayanthi S, Koppolu B, Smith SG, Jalah R, Bear J, Rosati M, Pavlakis GN, Felber BK, Zaharoff DA, Kumar TK. 2014. Efficient production and purification of recombinant human interleukin-12 (IL-12) overexpressed in mammalian cells without affinity tag. *Protein Expr Purif* 102: 76-84

34. Vignali DA, Kuchroo VK. 2012. IL-12 family cytokines: immunological playmakers. *Nat Immunol* 13: 722-8

35. Petoukhov MV, Franke D, Shkumatov AV, Tria G, Kikhney AG, Gajda M, Gorba C, Mertens HDT, Konarev PV, Svergun DI. 2012. New developments in the ATSAS program package for small-angle scattering data analysis. *J Appl Crystallogr* 45: 342-50

36. Aghamohseni H, Ohadi K, Spearman M, Krahn N, Moo-Young M, Scharer JM, Butler M, Budman HM. 2014. Effects of nutrient levels and average culture pH on the glycosylation pattern of camelid-humanized monoclonal antibody. *J Biotechnol* 186: 98-109

37. Croset A, Delafosse L, Gaudry JP, Arod C, Glez L, Losberger C, Begue D, Krstanovic A, Robert F, Vilbois F, Chevalet L, Antonsson B. 2012. Differences in the glycosylation of recombinant proteins expressed in HEK and CHO cells. *J Biotechnol* 161: 336-48

38. Gross V, Andus T, Castell J, Vom Berg D, Heinrich PC, Gerok W. 1989. O- and N-glycosylation lead to different molecular mass forms of human monocyte interleukin-6. *FEBS Lett* 247: 323-6

39. Hossler P, Khattak SF, Li ZJ. 2009. Optimal and consistent protein glycosylation in mammalian cell culture. *Glycobiology* 19: 936-49

40. Nam JH, Zhang F, Ermonval M, Linhardt RJ, Sharfstein ST. 2008. The effects of culture conditions on the glycosylation of secreted human placental alkaline phosphatase produced in Chinese hamster ovary cells. *Biotechnol Bioeng* 100: 1178-92

41. Yoon C, Johnston SC, Tang J, Stahl M, Tobin JF, Somers WS. 2000. Charged residues dominate a unique interlocking topography in the heterodimeric cytokine interleukin-12. *EMBO J* 19: 3530-41

42. Kusano S, Kukimoto-Niino M, Hino N, Ohsawa N, Ikutani M, Takaki S, Sakamoto K, Hara-Yokoyama M, Shirouzu M, Takatsu K, Yokoyama S. 2012. Structural basis of interleukin-5 dimer recognition by its a receptor. *Protein Sci* 21: 850-64

43. de Oliveira Neto M, Ferreira JR, Jr., Colau D, Fischer H, Nascimento AS, Craievich AF, Dumoutier L, Renauld JC, Polikarpov I. 2008. Interleukin-22 forms dimers that are recognized by two interleukin-22R1 receptor chains. *Biophys J* 94: 1754-65

44. Saksela O, Moscatelli D, Sommer A, Rifkin DB. 1988. Endothelial cell-derived heparan sulfate binds basic fibroblast growth factor and protects it from proteolytic degradation. *J Cell Biol* 107: 743-51

45. Ibrahimi OA, Zhang F, Hrstka SC, Mohammadi M, Linhardt RJ. 2004. Kinetic model for FGF, FGFR, and proteoglycan signal transduction complex assembly. *Biochemistry* 43: 4724-30

46. Dempewolf C, Morris J, Chopra M, Jayanthi S, Kumar TKS, Li WN. 2013. *Identification of consensus glycosaminoglycan binding strings in proteins*. Presented at Proceedings of the 4th International Conference on Information Science & Applications

47. Leonard JP, Sherman ML, Fisher GL, Buchanan LJ, Larsen G, Atkins MB, Sosman JA, Dutcher JP, Vogelzang NJ, Ryan JL. 1997. Effects of single-dose interleukin-12 exposure on interleukin-12-associated toxicity and interferon-gamma production. *Blood* 90: 2541-8

48. Dexter TM, Spooncer E. 1987. Growth and differentiation in the hemopoietic system. *Annu Rev Cell Biol* 3: 423-41

49. Fieschi C, Bosticardo M, de Beaucoudrey L, Boisson-Dupuis S, Feinberg J, Santos OF, Bustamante J, Levy J, Candotti F, Casanova JL. 2004. A novel form of complete IL-12/IL-23 receptor beta1 deficiency with cell surface-expressed nonfunctional receptors. *Blood* 104: 2095-101

50. de Beaucoudrey L, Samarina A, Bustamante J, Cobat A, Boisson-Dupuis S, et al. 2010. Revisiting human IL-12Rbeta1 deficiency: a survey of 141 patients from 30 countries. *Medicine (Baltimore)* 89: 381-402

51. Song M, Ma X. 2016. The Immunobiology of Interleukin-35 and Its Regulation and Gene Expression. *Adv Exp Med Biol* 941: 213-25

CHAPTER 3: MOLECULAR MECHANISMS OF HEPARIN-INDUCED MODULATION OF HUMAN IL-12 BIOACTIVITY **

3.1. Introduction

Sulfated GAGs, such as heparin and heparan sulfate, interact with and modulate the activities of numerous proteins (1). Although it is well known that heparin and heparan sulfate enhance the activities of growth factors, such as basic fibroblast growth factor (bFGF) (2-4), their effects on cytokines, particularly, interleukins are highly variable and often inhibitory. For example, heparin was shown to bind strongly to human IL-2 but has no effect on its bioactivity (5). IL-3-induced proliferation of FDCP-1 cells is inhibited at high heparin concentrations (6). The complex of heparin and IL-7 protects this cytokine from proteolytic degradation, however, the growth of IL-7 dependent pre-B cells is suppressed by heparin (7). Also, heparin prevents IL-10-induced expression of CD16 and CD64 on monocytes/macrophages (8).

IL-12, a central regulator of human immunity, has been shown by our group and others to be a heparin-binding protein (9-11). Our previous work identified two potential heparin-binding domains located on the p40 subunit of hIL-12 (10). These sites were exploited in the single-step

---

Contributions of Khue G. Nguyen (KGN):
• <u>Experiments</u>: KGN performed all IL-12 bioactivity assays including the evaluation of heparin concentrations, heparin chain length, heparin sulfation level, half maximal effective dose, cytokine profiling and intracellular cytokine staining. KGN performed all statistical analyses.
• <u>Writing</u>: KGN wrote Introduction, Material & Methods, Results, and Discussion of this manuscript.

purification of tag-less hIL-12 (10). Recently, we demonstrated that heparin binds hIL-12 with low micromolar affinity and increases the activity of hIL-12 by several fold (12). Remarkably, heparin was found to recover hIL-12 signaling in a natural killer cell line, NK-92MI expressing mutant forms of IL-12Rβ1 and IL-12Rβ2 that were poorly active (12).

In circulation, IL-12 induces profound systemic inflammation (13). It has been posited, therefore, that binding to sulfated GAGs present in extracellular matrix keeps IL-12 localized to a site of injury or infection and prevents its systemic dissemination. In addition to this localization effect, our recent studies indicated that sulfated GAGs, including heparin, increased IL-12 binding to cell surfaces (12). While this is one possible mechanism to increase IL-12 signaling, a more complete picture of how heparin influences IL-12 function is needed.

In the current study, because heparin is a polydisperse, heterogeneous polysaccharide, we began by exploring the effects of heparin's biophysical characteristics on hIL-12 function in order to make inferences about heparin's mechanisms of action. Specifically, because chain length, sulfation level and concentration have been shown to influence heparin's ability to modulate growth factor activity (8, 14-17), we investigated the effects of these characteristics on hIL-12 binding and bioactivity. For robustness, bioactivity studies were performed in 4 different cell types: an NK cell line (NK-92MI), an IL-12 indicator cell line (HEK-Blue™ IL-12) as well as PBMCs and T cells from healthy donors. Additional bioactivity experiments were performed in a murine system to elucidate species-dependent differences. An analysis of cytokine production was performed to determine if heparin facilitates non-canonical hIL-12 signaling. Finally, data gathered were used to develop a proposed model for heparin-induced stabilization of hIL-12/hIL-12R which was visualized with molecular graphics software.

3.2. Materials and Methods

3.2.1. Mice

Eight to ten week-old female C57BL/6J mice were purchased from The Jackson Laboratory (Bar Harbor, ME). Animal use was in compliance with the Public Health Service (PHS) Policy on Humane Care and Use of Laboratory Animals. All experiments involving laboratory animals were approved by the Institutional Animal Care and Use Committee at North Carolina State University.

3.2.2. Recombinant proteins and heparin compounds

Recombinant hIL-12 was purified from hIL-12-expressing HEK293 cells as described previously (10). Recombinant mIL-12 was overexpressed by HEK293 cells stably transfected with optimized mIL-12p70 plasmid (AG250) (18). mIL-12-producing HEK293 cells were grown in serum-free media in a fiber cell bioreactor (FiberCell Systems, C2008). Recombinant mIL-12 was purified via heparin sepharose chromatography as described previously (10). mIL-12 cytokine production was quantified via ELISA (Thermo Fisher, BMS6004). Low molecular weight heparin (LMWH) and heparin oligosaccharides were purchased from Sigma-Aldrich and Iduron (Manchester, UK), respectively. Structurally homogeneous heparan sulfate (HS)-derived oligosaccharides were synthesized using a chemo-enzymatic approach. The purity analysis and structural characterization of the oligosaccharides were described previously (19, 20).

3.2.3. Cell culture and isolation of human peripheral blood mononuclear cells (PBMCs) and T cells

The IL-2-independent, IL-12-responsive human natural killer cell line, NK-92MI (ATCC; CRL-2408TM), was cultured in complete media consisting of Alpha MEM supplemented with 12% FBS, 12% horse serum, 100 U/mL penicillin/streptomycin, 0.2 mM inositol, 0.02 mM folic acid, and 0.1 mM 2-mercaptoethanol. The mIL-12 responsive T cell line,

2D6, was cultured in RPMI 1640 supplemented with 10% FBS, 100 U/mL penicillin/streptomycin, 2 mM L-glutamine and 250 pg/ml mIL-12. HEK-Blue™ IL-12 cells (Invivogen, San Diego, CA) were maintained in DMEM supplemented with 2 mM L-glutamine, 10% FBS, 100 U/mL penicillin/streptomycin and 100 μg/mL normocin.

Human PBMCs were isolated from leukopaks on a density gradient using Lympholyte H (Cedarlane Labs, CL5016). De-identified leukopaks from healthy donors were purchased from the New York Blood Center (New York City, NY). Human T cells were isolated from PBMCs by negative selection with magnetic beads (ThermoFisher, 11344D). PBMCs and T cells were cultured in RPMI 1640 medium supplemented with 10% FBS, 1 mM sodium pyruvate, 2 mM L-glutamine, 10 mM HEPES, 100 U/mL penicillin/streptomycin. All experiments were performed in accordance with relevant guidelines and regulations at the University of North Carolina at Chapel Hill and North Carolina State University.

3.2.4. IL-12 bioactivity assay and cytokine measurement

IFN-γ secretion from NK-92MI cells, PBMCs and activated T cells was used as an indicator of hIL-12 bioactivity. T cells were activated by incubating 10^6 cells/ml with anti-CD3/CD28 coated superparamagnetic beads (Thermo Fisher, 111.31D) in cultured media at a bead:cell ratio of 1:1 for 3 days.

As described previously, cells were seeded in a 96-well plate at 20,000 cells/well (NK-92MI) or 500,000 cells/well (PBMCs and T cells) (12). hIL-12 was added to achieve final concentrations from 0 to 1000 pg/ml. Heparin was added to a final concentration ranging from 0 to 500 μg/ml. Cells in hIL-12 alone or culture media alone served as controls. After 24 h, hIL-12-dependent secretion of IFN-γ into the supernatant of the culture was quantified via ELISA (Thermo Fisher, 88-7316-86). In other experiments, levels of human Th1/Th2/Th17 cytokines,

including IL-2, IL-4, IL-6, IL-10, TNFα, IFN-γ, and IL-17A, in culture supernatants were determined via BD Cytometric Bead Array (CBA) (BD Biosciences, 560484) and analyzed using FACSDiva™ Software (BD Biosciences).

In the murine system, 2D6 cells were starved of mIL-12 overnight before culturing (20,000 cells/well) with increasing doses of heparin (0 μg/mL to 500 μg/mL) and either mIL-12 (200 pg/mL) or hIL-12 (200 pg/mL) in a 96-well plate. After 24 h, IL-12-induced proliferation was examined via CellTiter-Glo® 3D Cell Viability Assay (Promega, G9682).

HEK-Blue™ IL-12 cells (Invivogen, San Diego, CA) express a STAT4-inducible secreted embryonic alkaline phosphatase (SEAP) reporter gene that is triggered upon binding of IL-12 to IL-12R. HEK-Blue™ IL-12 cells were seeded in a 96-well plate at 50,000 cells/well and cultured with 0 to 5 ng/ml hIL-12 and 0 to 500 μg/ml heparin. After 24 h, SEAP concentrations in supernatants were developed with Quanti-Blue™ (Invivogen, San Diego, CA) and quantified via absorbance readings at 650 nm on a Cytation5 microplate reader (Biotek, Winooski, VT).

3.2.5. Intracellular flow cytometry

The following antibodies used for staining cell surface markers were obtained from BD Biosciences (San Diego, CA): anti-human CD3 FITC (clone: UCHT1), anti-human CD4 PerCP-Cy5.5 (clone: RPA-T4), anti-human CD8 APC-R700 (clone: RPA-T8), anti-human CD56 PE-CF594 or PerCP-Cy5.5 (clone: B159). Blocking of non-specific Fc receptor was performed by incubating cells with 25 μg/mL human Fc block (BD Bioscience, 564220) in staining buffer (PBS supplemented with 0.2% BSA and 0.09% sodium azide). For intracellular staining of IFN-γ, a protein transport inhibitor containing monensin (BD Biosciences, 554724) was added to the cells during induction. Cells were fixed in Fixation/Permeabilization Solutions (BD Biosciences,

554715) using the manufacturer's recommended protocols. Anti-human IFN-γ BV421 (clone: B27) was used for intracellular IFN-γ staining. Data were acquired using a BD FACSCelesta flow cytometer (BD Biosciences) and analyzed using FlowJo software (Flow Jo LLC, Ashland, OR). IFN-γ^+ cells were quantified in the gated $CD3^+CD4^+$ T cells, $CD3^+CD8^+$ T cells, and $CD3^-$ $CD56^+$ NK cells as illustrated in the gating strategies (Supplementary Figs. S.3.1 and S.3.2).

3.2.6. Isothermal calorimetry

Isothermal Titration Calorimetry (ITC) experiments were performed on a iTC-200 (Malvern Inc., UK) at 25° C. Both recombinant hIL-12 or mIL-12 (200 µM) and heparin oligosaccharides (2 mM) were dissolved in 10 mM phosphate buffer (pH 7.2) containing 150 mM NaCl. The molar ratios of hIL-12 or mIL-12 to heparin oligosaccharides were maintained at 1:10. All solutions were degassed prior to titration. Isothermal titrations were performed by injecting individual heparin oligosaccharides into hIL-12 or mIL-12 solutions in the reaction vessel. Isothermograms were obtained using 30 injections and were best-fit to a one-site/multiple-site binding model using the Origin™ v7.0 software supplied by Microcal. Necessary blank corrections were performed to eliminate contributions originating from heats of dilution. To account for inaccuracy associated with fitting of non-ideal/non-sigmoidal binding isotherms, the K_d values are reported as $K_{d(apparent)}$.

3.2.7. Microarray of HS-derived compounds

A custom HS-microarray was fabricated as described previously (21). To prepare the array chip, 50 µM HS oligosaccharides were dissolved in sodium phosphate buffer (pH 8.5, 50 mM). The solution was spatially arrayed onto NHS-activated slides (Nexterion® Slide H; SCHOTT, Jena, Germany) under ~50% relative humidity at 20ºC. The robotic arrayer S11 (Scienion, Berlin, Germany) delivered 426 pL of HS oligosaccharide solution to 16 spots arranged in a 4 x 4 grid.

The array spots had an average diameter of about 80 μm with a distance of 400 μm between the centers of adjacent spots. The slides were incubated overnight in a saturated $(NH_4)_2SO_4$ chamber (81% relative humidity). The slides were then washed with water to remove the unreacted oligosaccharides from the surface. The remaining *N*-hydroxysuccinimidyl groups were blocked by placing slides in a solution that contained 50 mM ethanolamine in PBST (137 mM NaCl, 13.2 mM Na_2HPO_4, 1.56 mM NaH_2PO_4, 2.68 mM KCl, 0.01% Tween 20) at 50°C for at least 1.5 h. Slides were rinsed several times with deionized water, and the residual liquid was dried by centrifugation.

The hybridization solution contained fluorescent-tagged hIL-12 (10 μg/mL) and PBST (137mM NaCl, 2.7 mM KCl, 4.3 mM Na_2HPO_4, 1.4 mM KH_2PO_4, 0.05% Tween 20), 20 mM Tris (pH 7.5) and 10% bovine serum albumin (BSA). The solution was placed between the array slide and cover slip and incubated for 1 h at room temperature in a saturated $(NH_4)_2SO_4$ chamber (81% relative humidity). The slide was then washed with 45 mL of PBST solution containing BSA (1%) and Tris (20 mM) for 5 min in a clean 50 mL conical tube. The wash process was repeated twice before analyzing the slide with an array scanner as described below.

The array slides were scanned by a GenePix 4300 scanner (Molecular Dynamics). Scanning wavelength was 488 nm. Resolution was set at 10 μm. The array images were analyzed by GenePix Pro 7.2.29.002 software. Mean fluorescence intensities of array spots were calculated by Array Quality Control software. Some thresholds were listed as follows: median signal-to-background, >10; mean of median background, < 500; median signal-to-noise, > 10; feature variation, 0.5; background variation, 0.5; features with saturated pixels, 0.1 %; not found features, 7 %; bad features, < 7 %.

3.2.8. hIL-12/hIL-12R complex modeling

Molecular modeling was performed using PyMOL molecular visualization software (Schrödinger, LLC) in conjunction with ClusPro protein-protein docking software and the Phyre2 web portal (22-27). The intensive modeling mode of the Phyre2 web portal was used to predict the structure of each IL-12 receptor subunit extracellular domain (ECD) based on primary structure and homogeneity to known protein structures. Next, hIL-12 protein (PDB: 1F45) was used as an input into the ClusPro software together with each receptor subunit individually to calculate their likely placement (23, 24). From the top clusters predicted by the software, files with correct subunit interactions, i.e. hIL12Rβ1 with p40 and hIL12Rβ2 with p35, and orientation were chosen (28, 29). These two criteria alone eliminated all but two models per receptor subunit for a total of four clusters. The final two clusters were eliminated based on the non-phsyiological overlap of the receptor subunits when they were superimposed based on the hIL-12 protein in PyMOL.

Heparin binding sites on each receptor subunit were predicted using ClusPro as well, using the heparin docking function. The top scoring segments for each of the subunits were selected and highlighted in the protein structure models. After each set of predictions was made, the location of each receptor in relation to the other was modeled by superimposing the hIL-12 molecules onto each other using the 'cealign' command of the Alignment/Superposition plugin in the PyMOL software. After the alignment of each individual interaction based on the hIL-12 molecule, no further modifications to the model were performed.

Distances between heparin binding sites within the hIL-12/hIL-12R complex were determined using PyMol's Measurement tool. For each measurement, residues within the heparin

binding segments of interest that were closest to each other were used as endpoints. Within these residues, the carbon atom was chosen to approximate the distance between heparin binding sites.

3.2.9. Statistical analysis

All experiments were performed multiple times to ensure reproducibility. Two-tailed t test was used to compare the positive percentages of intracellular IFN-γ in response to hIL-12 alone and hIL-12 plus heparin. An extra sum-of-squares F test was used to evaluate differences in the calculated EC_{50} value generated by hIL-12 alone and hIL-12 plus heparin. One-way ANOVA was used to discern differences in cytokine release from cells undergoing multiple treatments of a fixed concentration of hIL-12 and increasing concentrations of heparin (1 factor). Two-way ANOVA was used to distinguish differences of cytokine release from cells undergoing combination treatments of hIL-12 and heparin (2 factors). Tukey's posttest was used after the ANOVA to compare individual treatment groups. Dunnett's posttest was used after ANOVA to compare individual treatment groups (hIL-12 plus range concentrations of heparin) with a control group (hIL-12 alone). Statistical significance was accepted at the $p \leq 0.05$ level. All analyses were conducted using GraphPad Prism 7 software (GraphPad Software, CA).

3.3. Results

3.3.1. Heparin modulates hIL-12 bioactivity in a dose-dependent manner.

The effect of heparin concentration on hIL-12 activity was quantified via IFN-γ production by NK-92MI cells, activated human T cells or by activation of signaling in HEK-Blue™ IL-12 cells. There was a significant increase of IFN-γ production or SEAP production in response to hIL-12 with increasing heparin concentrations in NK-92MI, T cells or HEK-Blue™ IL-12 cells (p<0.0001 via one-way ANOVA). In detail, IFN-γ production by NK-92MI cells in response to 200 pg/mL hIL-12 more than doubled from 4438 ± 479 to 7876 ± 395 pg/mL as

exogenous heparin concentration increased from 0 μg/mL to 25 μg/mL (Fig. 3.1A) (p<0.0001

via Tukey's posttest). Additional heparin, beyond 25 μg/mL, produced no further increase in

hIL-12 activity, indicating a potential plateau. HEK-Blue™ IL-12 cells and T cells responded

similarly with increasing levels of heparin inducing enhanced hIL-12 bioactivity (Fig. 3.1B,C).

At very high heparin concentrations (500 μg/mL vs. 25 μg/mL), there was a decrease in hIL-12

bioactivity in the HEK-Blue™ IL-12 cells indicating a possible inhibitory effect (p=0.0029 for

500 μg/mL vs. 25 μg/mL heparin via Tukey's posttest).

Unlike in the human system, heparin did not enhance the activity of mIL-12 on either

murine 2D6 cells (Fig. 3.1D) or splenocytes isolated from C57BL/6J mice (Fig. 3.1E).

Interestingly, heparin significantly enhanced the activity of mIL-12 on human NK-92MI cells

(Fig. 3.1F). Heparin facilitated a 1.55-fold increase in mIL-12 function on human NK cells

which was greater than the heparin-induced increase in hIL-12 function on human NK cells. hIL-

12 was not active in the murine 2D6 cell line with or without heparin (Fig. 3.1D-F).

3.3.2. Heparin does not facilitate non-canonical hIL-12 signaling

IFN-γ expression is a key indicator of hIL-12 bioactivity. However, it is possible that

heparin facilitated expression of other T helper cytokines via non-canonical signaling. Thus, we

investigated the production of prototype Th1, Th2 and Th17 cytokines by NK-92MI cells and

activated T cells exposed to hIL-12 with and without exogenous heparin. As expected, in

response to hIL-12 alone, NK-92MI cells secreted high levels of IFN-γ (663.5±4.9 pg/mL)

whereas heparin had no effect (Fig. 3.2A). Treatment with hIL-12 alone also increased the

production of IL-10 and IL-6 by NK-92MI cells, which was similarly reported by another group

(30). Upon addition of heparin, NK-92MI significantly increased production of IFN-γ, IL-10 and

IL-6 by 1.26, 1.47 and 1.92-fold (Fig. 3.2A), respectively. It should be noted that IL-2 was

detected in all treatment groups because the NK-92MI cell line is stably transfected with the IL-2 gene to maintain consistent cell proliferation (31). The amount of IL-2 did not change significantly with the addition of heparin. NK-92MI did not produce significant amounts of TNFα, IL-4 or IL-17A regardless of heparin treatment (Supplementary Fig. S.3.3A,C). These cytokines are not normally produced in response to IL-12. Any expression in the presence of heparin would have indicated non-canonical signaling. A similar analysis showed that, activated T cells produced 626.8$\pm$2.4 pg/mL of IFN-γ in response to hIL-12. This was increased to 1031.9$\pm$27.9 pg/mL when heparin was included (Fig. 3.2B). Like NK-92MI cells, no cytokine other than IFN-γ was secreted by activated T cells in response to heparin, hIL-12 or their combination (Supplementary Fig. S.3.3B,D).

To validate IFN-γ production measured by cytokine profiling analysis, we investigated the intracellular expression of IFN-γ by CD4$^+$ T cells, CD8$^+$ T cells, CD56$^+$ cells in PBMCs and NK92-MI cells in response to hIL-12 alone and hIL-12 plus heparin (Fig. 3.2C-E). The results showed that the combination of hIL-12 and heparin increased the percentages of cells producing IFN-γ over hIL-12 alone (CD4$^+$ T cells: from 2.633$\pm$0.291% to 4.207$\pm$0.522%; CD8$^+$ T cells: from 1.757$\pm$0.378% to 3.597$\pm$ 0.616%; CD56$^+$ NK cells: from 2.293$\pm$0.040% to 3.103 $\pm$ 0.496%; NK-92MI cells: from 1.473 $\pm$0.163% to 9.810$\pm$0.132%) (p<0.05 hIL-12 alone vs. hIL-12 plus heparin via two-tailed t test) (Fig. 3.2C-E).

3.3.3. Half-maximal effective concentration of IL-12 is reduced by heparin

The ability of heparin to reduce the half-maximal effective concentration (EC$_{50}$) of IL-12 was quantified in NK-92MI cells, T cells and PBMCs. Supernatants from cells treated with increasing concentrations of hIL-12, with or without heparin, showed a typical sigmoidal dose-response relationship (Fig. 3.3). For NK-92MI cells, the EC$_{50}$ values for IL-12 alone and IL-12

with heparin were 27.67 pg/mL and 2.34 pg/mL, respectively. Based on this result, heparin decreased the EC_{50} of IL-12 by 11.8-fold. Similar results were observed on T cells showed a reduction in EC_{50} value of hIL-12 from 61.71 pg/mL to 44.71 pg/mL, or 1.4-fold, and PBMCs showed a reduction in EC_{50} from 121.9 pg/mL to 13.76 pg/mL, or 8.9-fold, respectively.

3.3.4. Effect of heparin chain length on IL-12 binding

ITC measures the binding affinity and binding stoichiometry of protein-ligand interactions under well-defined conditions. The interactions of heparin with mIL-12 and hIL-12 are exothermic. Under the experimental conditions used, the binding isotherms are observed to be hyperbolic and heparin binds to both hIL-12 and mIL-12 nearly in a 1:1 stoichiometry. Analysis of ITC data indicate that the binding affinity ($K_{d(apparent)}$) of heparin − IL12 interaction is strongly influenced by the chain length of heparin (Supplementary Fig. S.3.4). Specifically, heparin oligosaccharides with lesser than six saccharide units, like heparin di-, tetra-, and hexasaccharide, do not bind measurably to either hIL-12 or mIL-12 (Table 3.1). Heparin octasaccharide shows reasonably strong binding ($K_{d(apparent)} = 39$ μM) to hIL-12 but not to mIL-12 (Table 3.1 and Supplementary Fig. S.3.4). The binding affinities of longer chain length heparin oligosaccharides, heparin decasaccharide and heparin dodesaccharide, to IL-12 are the strongest and range from 5.3 μM to 8.6 μM (Table 3.1). The binding affinities of hIL-12 and mIL-12 to LMWH, which is a polydisperse mixture of heparin with varying lengths of saccharide units, are ~10 μM and ~ 44 μM, respectively.

In summary, ITC data suggest that hIL-12, in general, exhibits slightly higher binding affinity to heparin than mIL-12. In addition, the binding affinity between hIL-12 and heparin is strongly dependent on heparin chain length and plateaus at 10 to 12 saccharide units.

3.3.5. Heparin-induced modulation of hIL-12 bioactivity is dependent on heparin's chain length

The effect of heparin's chain length on hIL-12 bioactivity was investigated in NK-92MI cells and HEK-Blue^{TM} IL-12 cells. IFN-γ production data from NK-92MI cells showed that tetrasaccharides did not enhance hIL-12 bioactivity while hexasaccharides generated a modest enhancing effect (Fig. 3.4B). Interestingly, octasaccharides, decasaccharides, and dodecasaccharides produced similar enhancements in hIL-12 bioactivity to LMWH, which is typically 15 to 25 saccharide units (average molecular weight: 4 - 6 kDa) (Fig. 3.4B). Similar effects were observed with HEK-Blue^{TM} IL-12 cells as only octasaccharides, decasaccharides and dodecasaccharides increased hIL-12 activity.

3.3.6. Effect of sulfation on hIL-12 binding

To determine how sulfation level affects heparin binding to hIL-12, a novel microarray approach was used. Fifty-two HS-derived compounds were synthesized with 1, 2 or 3 sulfate groups per disaccharide unit ranging in size from 5 to 18 saccharides (Fig. 3.5A). The compounds were arrayed on a slide and treated with fluorescence-labeled hIL-12. After rinsing, fluorescence analysis was performed to quantify levels of IL-12 binding to each of the HS-derived compounds. Our analysis revealed that the highest amounts of hIL-12 were bound to heparin-derived compounds 18 and 19, which are dodecasaccharides containing 3 sulfate groups per disaccharide unit (Fig. 3.5B). Other sulfated HS-derived compounds also bound and retained hIL-12, however at lower levels.

3.3.7. Sulfation is essential for HS-induced modulation of hIL-12 bioactivity

To determine the effect of sulfation level on the HS-induced modulation of hIL-12 bioactivity, selected heparan sulfate dodecasaccharides containing 1, 2 or 3 sulfate groups per disaccharide unit (Fig. 3.5A) were formulated with hIL-12 for treatment on NK-92MI and HEK-

Blue^{TM} IL-12 cells. Data from NK-92MI cells showed that compounds 21, 24 and 25, which contained less than 3 sulfate groups per disaccharide did not enhance hIL-12 bioactivity (Fig. 3.5C) (p>0.05 in comparison of IL-12 alone vs. IL-12 plus compounds 21, 24, and 25 via Tukey's posttest). On the other hand, compounds 18 and 19, which consisted of 3 sulfate groups per disaccharide unit, significantly enhanced hIL-12 bioactivity to levels similar to LMWH (p<0.0001 in comparison of IL-12 alone vs. IL-12 plus compounds 18, 19, and LMWH via Tukey's posttest). Data from HEK-Blue^{TM} IL-12 cells exhibited similar phenomena in that hIL-12 activity was only enhanced with compounds 18 and 19 (p<0.0001 in comparison of IL-12 alone vs. IL-12 plus compounds 18, 19, and LMWH via Tukey's posttest). It should be noted that compound 23 produced different effects on IL-12 bioactivity in NK-92MI cells (p<0.0001 via Tukey's posttest) and HEK blue^{TM} IL-12 cells (p<0.0001 via Tukey's posttest) indicating that certain HS enhancement phenomena may be cell dependent.

3.3.8. Proposed model of heparin-stabilized hIL-12/hIL-12R complex

The structure of hIL-12 was imported from the PDB archive (1F45) (Fig. 3.6A). The heparin docking function in ClusPro was used to identify two heparin-binding motifs on the p40 subunit of hIL-12 (^{117}LKDQKEPKNK^{126} and ^{276}QVQGKSKREKK^{286}) (Fig. 3.6A). These correlate with our previous *in silico* string analysis (10).

Models of each receptor subunit were based on the solved structure of interleukin-6 receptor subunit β with differences. hIL-12Rβ1 was also based on the structures of anosmin-1, leukemia inhibitory factor receptor, and insulin receptor. The structure of hIL-12Rβ2 was further detailed using homology to human receptor 2 protein tyrosine phosphatase sigma, chicken mdga1, and the ectodomain of the receptor protein tyrosine2 phosphatase mu. Each prediction showed high (>90%) confidence in the model. Heparin binding segments on receptor subunit

92

ECDs were predicted using ClusPro. The top scoring segment for each receptor subunit were identified and highlighted in the protein models (Fig. 3.6B,C).

To determine the spatial relationship of the heparin-binding segments and the potential role of heparin in stabilizing ligand-receptor interactions, we constructed a model of the hIL-12/hIL-12R complex using the available crystal structure of hIL-12 and its predicted binding to the ECDs (Fig. 3.6D,E). The predicted hIL-12/hIL-12R complex shows the heparin-binding motifs located on hIL-12 to be in close proximity to hIL-12Rβ1. Estimated distances from the heparin binding sites on hIL-12 to the putative heparin binding site on hIL-12Rβ1 were 14 and 18 Å (Fig. 3.6F). For the hIL-12Rβ2 ECD, the heparin-binding site is facing away from the p35 subunit of hIL-12. Consequently, the distances from the heparin binding sites on hIL-12 to the top scoring heparin binding site on hIL-12Rβ2 were longer at 43 and 75 Å. Based on the putative heparin binding sites, this model predicts that only heparin molecules of a certain size could simultaneously bind to both the IL-12 ligand and receptor. Using an average length of 4 Angstroms per disaccharide, it becomes clear that only heparin molecules with chain lengths of 4, 5 or 6 disaccharide units, i.e. 8, 10 or 12 saccharides, are able to bridge the heparin-binding domains. In addition, the increased binding and activities observed with higher sulfation levels indicate that the stabilization interaction is likely mediated by non-specific electrostatic interactions and not particular sulfation patterns.

3.4. Discussion

Our previous study was the first to demonstrate that sulfated GAGs, such as heparin and heparan sulfate, could enhance the bioactivity of hIL-12 (12). In this follow up study, we extended this research to identify the characteristics of heparin that were required to modulate

hIL-12 bioactivity. In doing so, we aimed to develop a working model capable of explaining the mechanism(s) of heparin-induced hIL-12 enhanced function.

Initial studies to determine the optimal concentration of heparin found that, for most cell types, a maximal or plateau effect was achieved between 10 μg/mL and 25 μg/ml heparin (Fig. 3.1). These concentrations are considered physiologically relevant as circulating levels of heparin in humans are 1 to 5 μg/ml (32). During inflammation, , systemic concentrations of heparin and heparan sulfate are significantly increased (33, 34). Although, not explored, we hypothesize that local sites of inflammation have similar increases in heparin and heparan sulfate.

Because our previous study demonstrated that heparin can recover IL-12 signaling in cells lacking functional IL-12 receptors (12), we hypothesized that IL-12 could be signaling through non-canonical pathways, perhaps via receptors associated with other IL-12 family members. However, our cytokine profiling analyses and intracellular cytokine staining showed that no other Th1, Th2 or Th17 cytokines were induced in the presence of heparin (Fig. 3.2). Heparin simply appears to make hIL-12 signaling more efficient by stabilizing the interaction of hIL-12 and hIL-12R. In particular, a greater percentage of lymphocytes respond to hIL-12 in the presence of heparin (Fig. 3.2C,D). Also, the EC_{50} data demonstrated that heparin can reduce the effective concentration of hIL-12 by 1.5 to 11.8-fold (Fig. 3.3).

In terms of heparin characteristics, both chain length and sulfation level exhibited a threshold-type effect on hIL-12. Specifically, heparin molecules less than a threshold of 6 saccharide units did not affect hIL-12 activity, while those above 8 saccharide units induced a bioactivity plateau that was similar to LMWH (Fig. 3.4). It should be noted that heparin hexasaccharides which only modestly enhanced hIL-12 activity, were not found bind strongly to

hIL-12 in ITC studies. This apparent discrepancy may be due to differences in sensitivity between the two approaches. ITC requires higher concentrations of heparin and hIL-12 while the limit of reliable detection of binding is on the order of a couple hundred μM. Hexasaccharides binding to hIL-12 may be too weak to be detected but still strong enough to provide partial enhancement of hIL-12 activity. Regarding sulfation level, HS with less than 3 sulfate groups per disaccharide did not significantly improve hIL-12 bioactivity. In contrast, both HS molecules containing 3 sulfate groups per disaccharide, compounds 18 and 19, showed improved hIL-12 binding and bioactivity (Fig. 3.5). HS-derived molecules with less than 3 sulfate groups per disaccharide have lower negative charge densities which likely results in weaker interactions with both hIL-12 and hIL-12R. These data imply that the heparin-IL-12 interaction is a non-specific electrostatic interaction as opposed to an interaction that depends on a particular sulfation pattern. The inability of poorly sulfated heparins to enhance hIL-12 bioactivity agreed with our previous data demonstrating that poorly or non-sulfated GAGs, e.g. chondroitin sulfate and hyaluronic acid, had no effect on hIL-12 bioactivity (12).

Using the chain length data in particular, we hypothesized that heparin could be stabilizing the hIL-12/hIL-12R complex by binding to heparin-binding domains on both ligand and receptor. We reasoned that only heparin molecules of a sufficient size would be able to bind simultaneously to heparin-binding sites on different subunits of the complex. Our *in silico* analysis identified two major heparin-binding domains on hIL-12 as well as the top scoring heparin binding segments on each hIL-12R subunit (Fig. 3.6). When hIL-12 is bound to hIL-12R, the distances between heparin-binding domains located on different proteins, i.e. hIL-12, hIL-12Rβ1 and hIL-12Rβ2, range from 14 to 75 Å. A tetrasaccharide, with a maximum distance

of approximately 16-17 Å between sulfate groups, would therefore have a lower probability of binding to and stabilizing the hIL-12/hIL-12R interactions than an octasaccharide or LMWH.

It should be noted that the tertiary complex and the identified heparin binding domains on hIL-12, hIL-12Rβ1 and hIL-12Rβ2 are merely predictions at this point. Although, Garnier et al. demonstrated that truncation of the carboxyterminal domain on the p40 subunit to exclude the putative heparin binding segment located within amino acids 279 to 287 significantly reduced the heparin-binding ability of hIL-12 (11). Where exactly heparin binds to IL-12, both human and mouse, as well as each IL-12R subunit is the subject of ongoing crystallography work. Once completed, we will have a definitive picture of the heparin/IL-12/IL-12R quaternary complex.

An observation that appears to agree with our stabilization hypothesis was that heparin did not improve mIL-12 bioactivity on mouse 2D6 cells, but significantly improved mIL-12 bioactivity on human NK-92MI cells (Fig. 3.1). We hypothesize that the binding of mIL-12 to mIL-12R is of sufficient affinity such that heparin is not needed to enhance binding and signaling. On the other hand, the affinity of mIL-12 for hIL-12R is expected to be much lower than the affinity of mIL-12 for mIL-12R or hIL-12 for hIL-12R. Therefore, the benefit of adding heparin to stabilize the potentially 'loose' mIL-12/hIL-12R complex results in a robust enhancement of mIL-12 activity. In fact, the activity of mIL-12 was increased 1.55-fold, which was greater than heparin-induced enhancements for hIL-12 (1.18-fold) (Fig. 3.1D).

Drawing from our previous work, heparin's ability to stabilize weak IL-12/IL-12R interactions may be a key mechanism by which hIL-12 signaling was recovered in cells lacking functional hIL-12R (12). In these previous studies, hIL-12Rβ1 and hIL-12Rβ2 were functionally deleted via CRISPR/Cas9 genome editing. However, the Cas9-induced cleavage of the hIL-12Rβ1 and hIL-12Rβ2 genes likely induced random mutations in the receptor subunits instead of

a complete knockout. The mutated hIL-12R did not bind hIL-12 sufficiently to allow signaling, however, the addition of heparin may have stabilized this 'loose' complex enough to recover hIL-12 bioactivity. Ongoing studies are aimed at understanding which portions of the hIL-12R subunits are critical for signaling in the presence and absence of heparin. We postulate that this research could lead to a new therapeutic option for patients with mutations in IL-12Rβ1 that lead to Mendelian susceptibility to mycobacterial diseases (35, 36) (Appendix 1).

Lastly, other heterodimeric cytokines of the IL-12 family have overlapping structural features (37), and therefore, could be modulated by heparin. In particular, IL-23 shares the p40 subunit along with its cognate receptor IL-12Rβ1 with IL-12. IL-35 shares p35 and IL-12Rβ2 with IL-12. Our preliminary data indicate that heparin's enhancement of hIL-23 bioactivity is even more robust than its effects on hIL-12 (Appendix 2). Furthermore, heparin was found to inhibit the antagonist activity of p40 monomer and dimer in preliminary experiments (Appendix 3). Given the diverse immunological functions of the IL-12 family, the impact of heparin as a regulator of immunity is of great interest.

Table 3.1. Binding affinities between hIL-12 or mIL-12 and heparin oligosaccharides or LMWH.

	Tetra-saccharide	Hexa-saccharide	Octa-saccharide	Deca-saccharide	Dodeca-saccharide	LMWH
hIL-12	NB	NB	39 μM	6.6 μM	5.3 μM	10 μM
mIL-12	NB	NB	NB	5.7 μM	8.6 μM	44 μM

NB: no binding observed
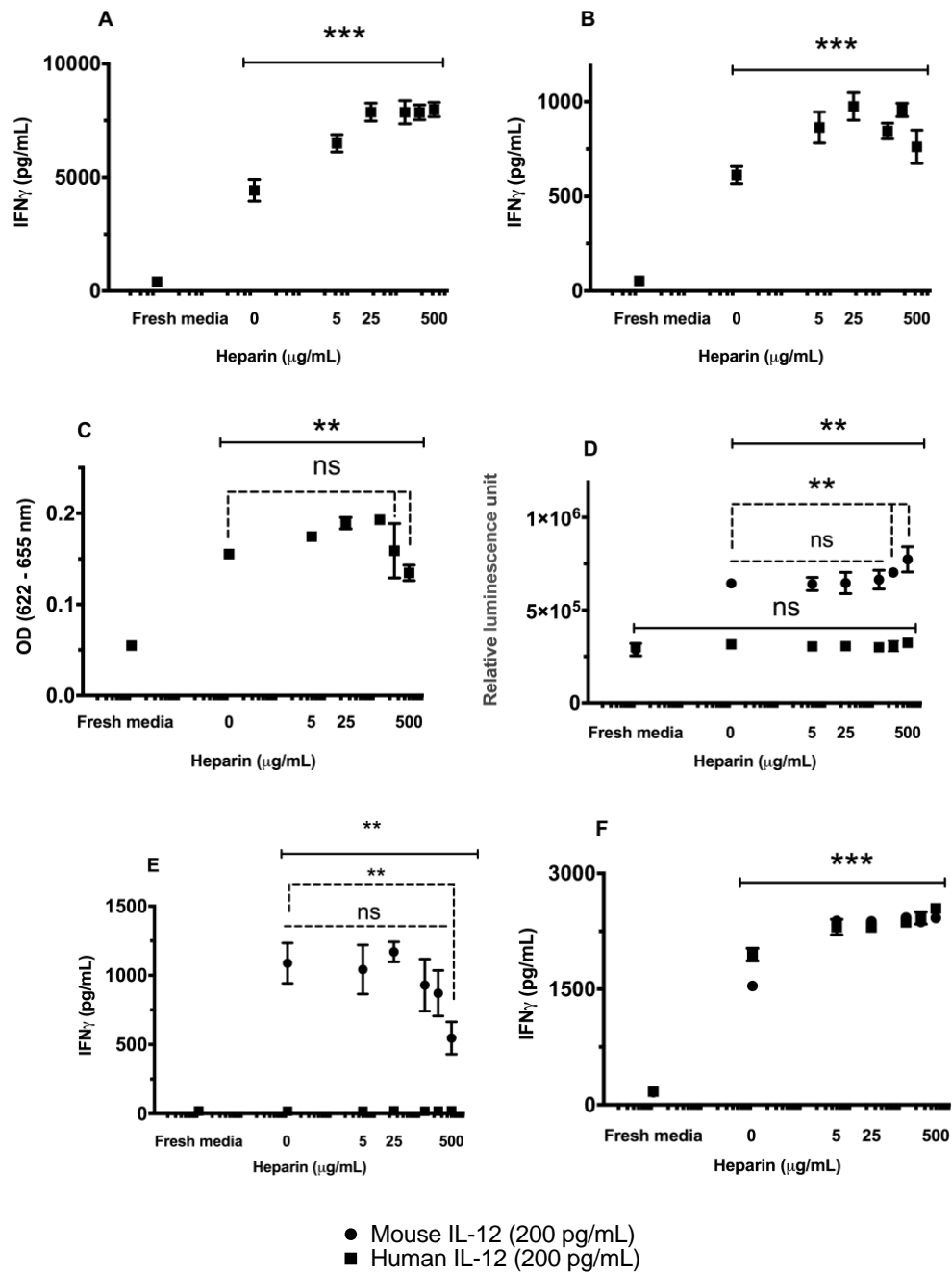
Figure 3.1. IL-12 bioactivity is modulated by heparin in a dose-dependent manner. The

production of IFN-γ by (A) NK-92MI cells or (B) Human T cells or (C) alkaline phosphatase by

HEK-Blue™ IL-12 cells was measured after exposure to a fixed concentration of hIL-12, 200

pg/ml for (A) and (B), or 1 ng/ml for (C), and increasing concentrations of heparin. (D) The

proliferation of mIL-12 sensitive 2D6 cells in response to mIL-12 and hIL-12 with increasing heparin concentrations was indirectly assessed via CellTiter-Glo® 3D Cell Viability Assay. IFN-γ production by (E) murine splenocytes isolated from C57BL/6J mouse, and (F) NK-92MI cells in response to mIL-12 and hIL-12 with increasing heparin concentrations was measure via ELISA. Asterisks indicate a significant difference between the treatments of IL-12 alone and IL-12 plus increasing heparin concentrations (**=$p<0.01$ and ***=$p<0.001$ via one-way ANOVA: solid lines), ns: not significant. The comparison of IL-12 bioactivity in response to hIL-12 alone and different heparin concentrations plus hIL-12 (200 pg/mL) was evaluated by Dunnett's posttest (dashed lines). Data points represent mean ± standard deviation of triplicate measurements. Experiments were performed in triplicate and repeated three times with similar results.

A
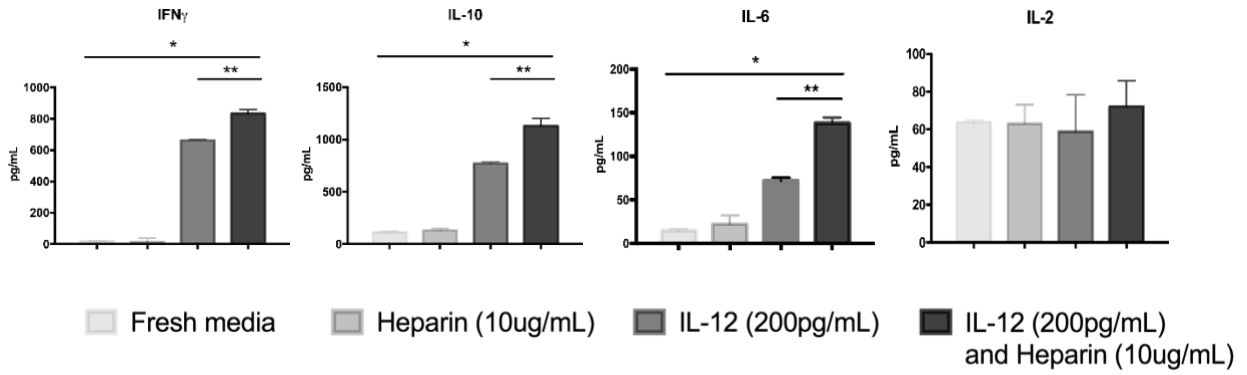
B
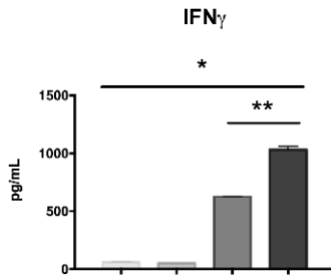
C
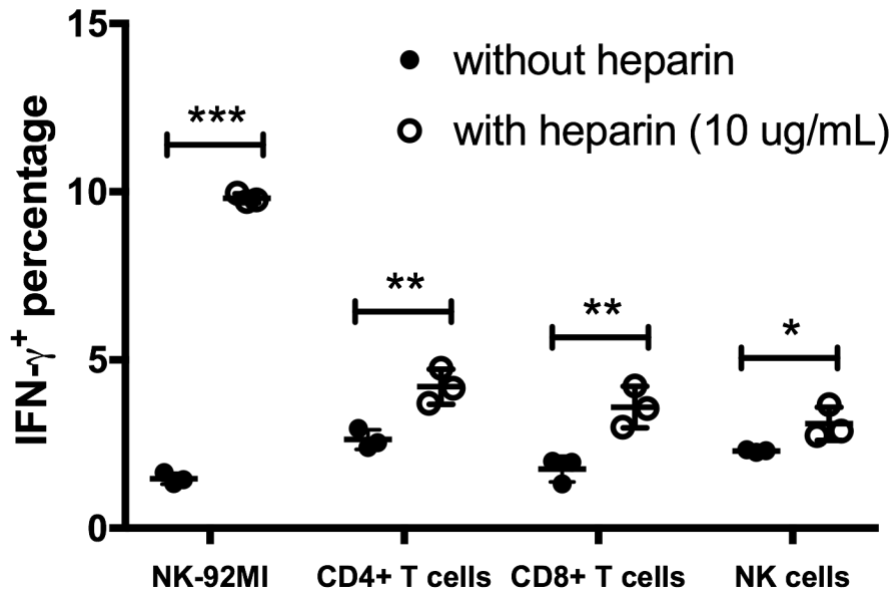
**Figure 3.2. Heparin amplifies hIL-12-induced cytokine profiles.**

D
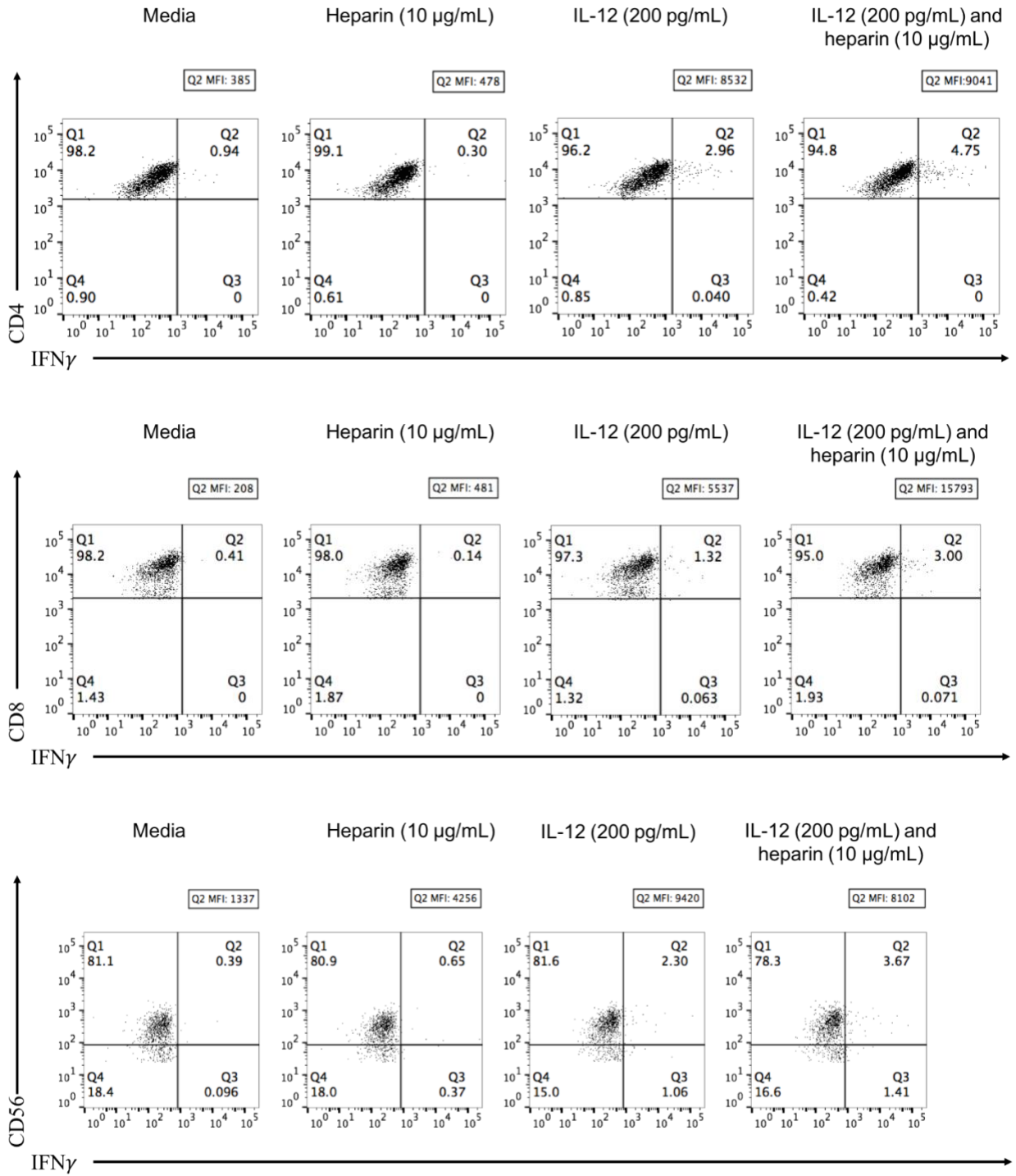
Figure 3.2. Heparin amplifies hIL-12-induced cytokine profiles.

E
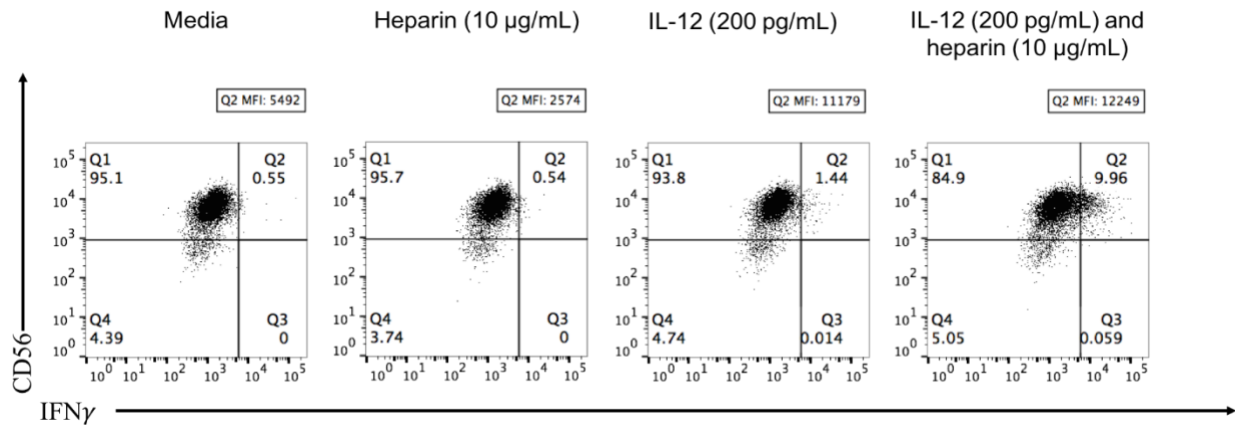
Figure 3.2. Heparin amplifies hIL-12-induced cytokine profiles. The secretion of prototypical

Th1, Th2 and Th17 cytokines by (A) NK-92MI cells and (B) activated T cells in response to hIL-

12 (200 pg/mL) in the presence and absence of heparin (10 µg/mL) were analyzed via a BD

CBA kit. Heparin alone does not alter baseline cytokine production while the addition of heparin

to hIL-12 increases the amount, but does not alter the type, of cytokine expressed by NK or T

cells. Columns represent mean ± standard deviation of triplicate measurements. (A), (B) *p<0.05

for one-way ANOVA comparing all treatment groups. **p<0.05 for Tukey's posttest comparing

hIL-12 alone and hIL-12 plus heparin. (C) Dot plots describe positive percentages of intracellular

IFN-γ in NK-92MI cells, CD4^{+} T cells, CD8^{+} T cells, and NK cells for comparison of hIL-12

alone and hIL-12 plus heparin (*p<0.05, **p<0.01, ***p<0.0001 via two-tailed t test). (D) Dot

plots show representative intracellular expression of IFN-γ by gated CD3^{+}CD4^{+} T cells,

CD3^{+}CD8^{+} T cells, and CD3^{-}CD56^{+} NK cells from PBMCs in four experimental groups (fresh

media, heparin, hIL-12, hIL-12 plus heparin). (E) Dot plots show representative intracellular

expression of IFN-γ by gated CD56^{+} NK92-MI cells in four experimental groups (media,

heparin, hIL-12, hIL-12 plus heparin). Experiments were performed in triplicate and repeated

three times with similar results.

A

B

C

○ No heparin ■ With heparin (10 μg/mL)
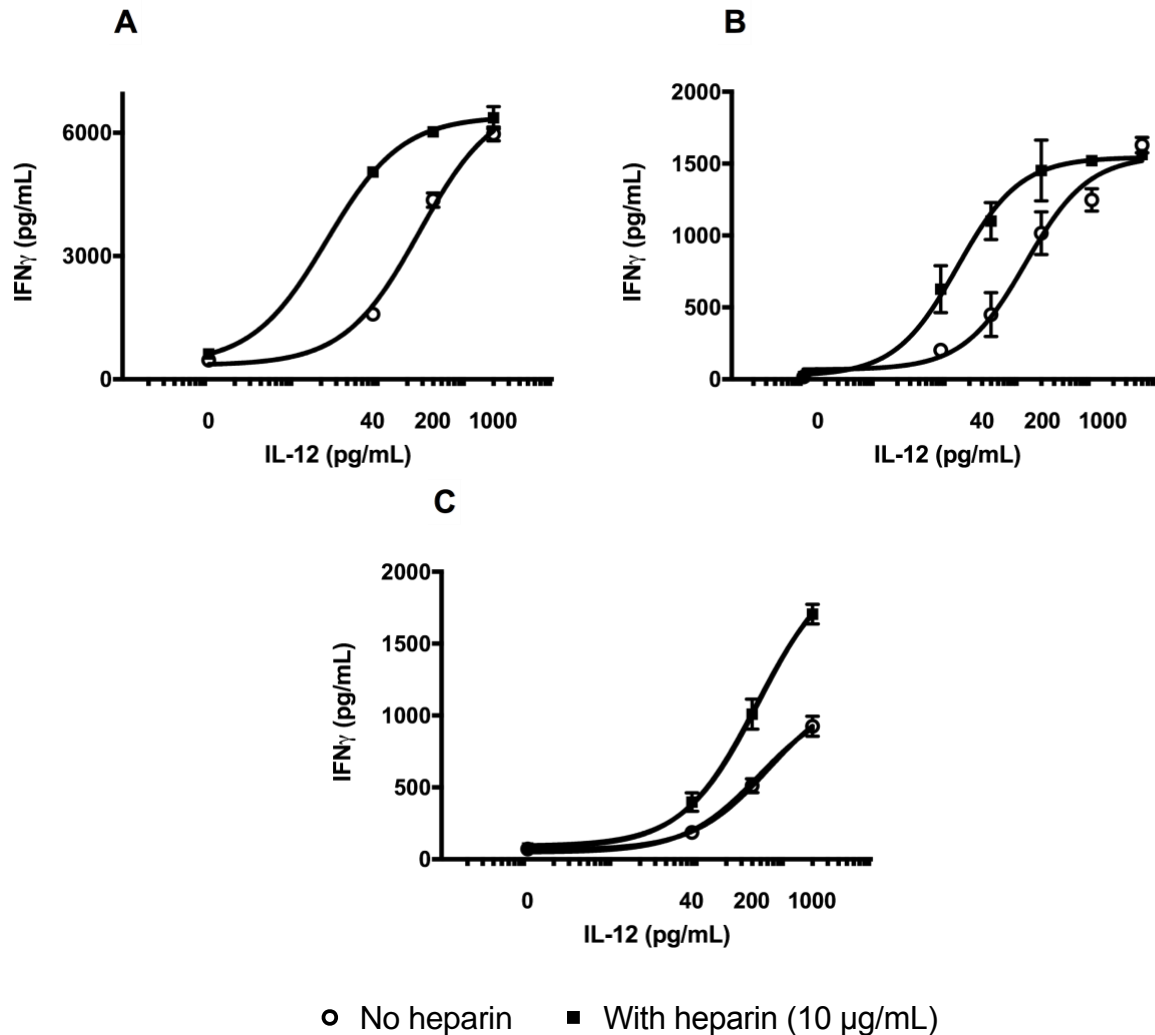
Figure 3.3. Heparin decreases the EC$_{50}$ value of hIL-12. hIL-12 bioactivity curves showing the IFN-γ production by **(A)** NK-92MI cells, **(B)** human PBMCs, and **(C)** human T cells exposed to increasing hIL-12 in the presence and absence of heparin (10 μg/mL). The EC$_{50}$ values of hIL-12 for NK-92MI cells and human PBMCs were significantly decreased by heparin (p<0.0001 vs. hIL-12 alone via extra sum-of-squares F test). All data points represent mean ± standard deviation of triplicate measurements. Experiments were performed in triplicate and repeated three times with similar results.
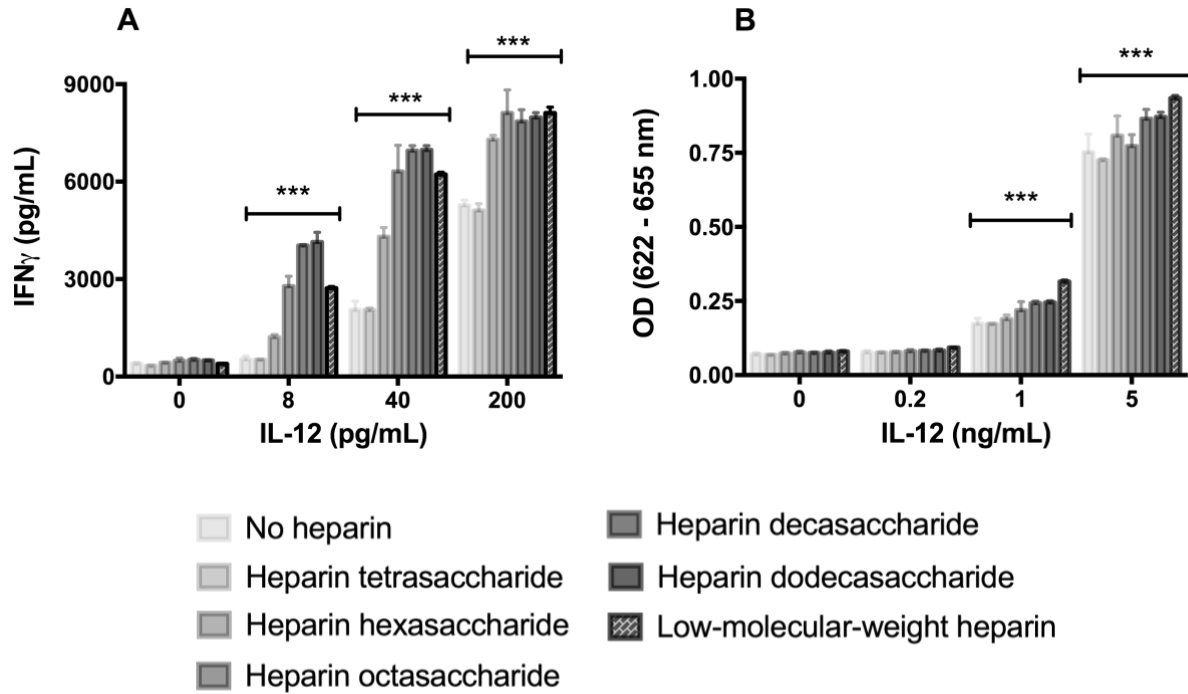
Figure 3.4. Modulatory activity is dependent on heparin chain length. hIL-12 activity as measured by (A) IFN-γ production by NK-92MI cells or (B) secreted alkaline phosphatase by HEK-Blue™ IL-12 cells was measured after co-culture with heparin oligosaccharides or LMWH (10 μg/mL). Heparin octasaccharide, decasaccharide, dodecasaccharide, and LMWH significantly increased the bioactivity of IL-12 in NK-92MI cells and HEK™ blue IL-12 cells (***p<0.0001 vs. hIL-12 alone via two-way ANOVA). Heparin tetrasaccharide did not increase the bioactivity of hIL-12 in NK-92MI cells (p>0.05 vs. hIL-12 alone via Tukey's posttest) and HEK™ blue IL-12 cells (p<0.0001 vs. hIL-12 alone via Tukey's posttest). Heparin hexasaccharide increased the bioactivity of hIL-12 in NK-92MI cells (p<0.0001 vs. hIL-12 alone, p<0.01 vs. hIL-12 plus LMWH via Tukey's posttest), and showed no effect on hIL-12 bioactivity in HEK™ blue IL-12 cells (p>0.05 vs. hIL-12 alone via Tukey's posttest). Columns represent mean ± standard deviation of triplicate measurements. Experiments were performed in triplicate and repeated three times with similar results.
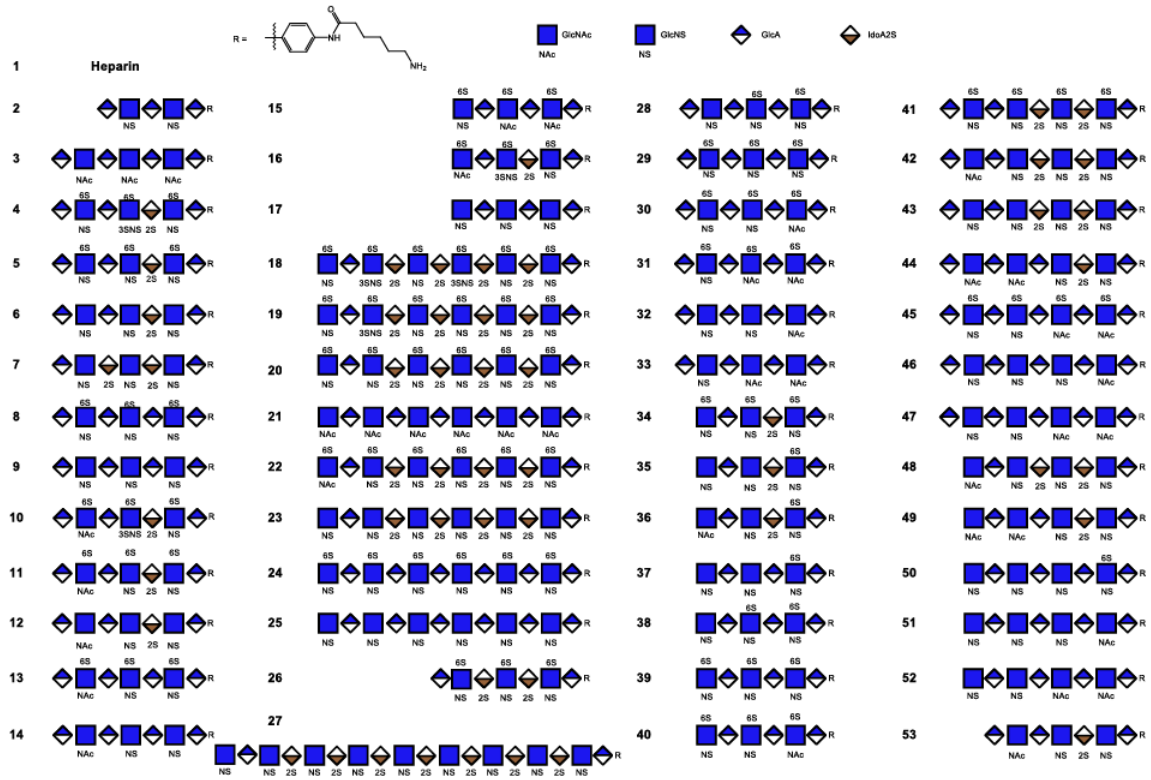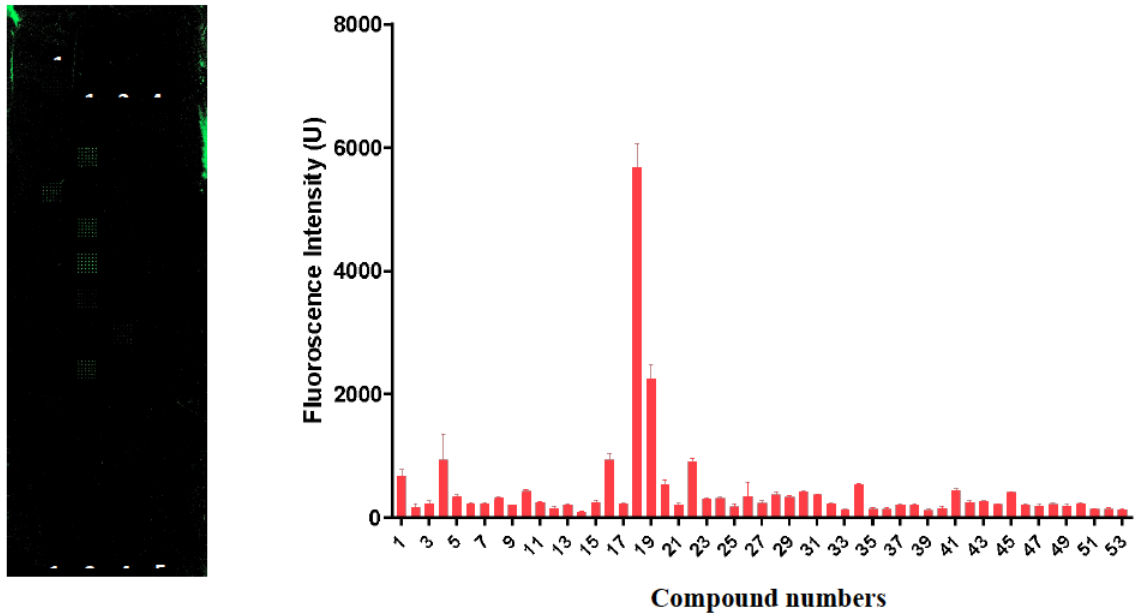
Figure 3.5. Heparin-induced enhancement of hIL-12 depends on sulfation level

106
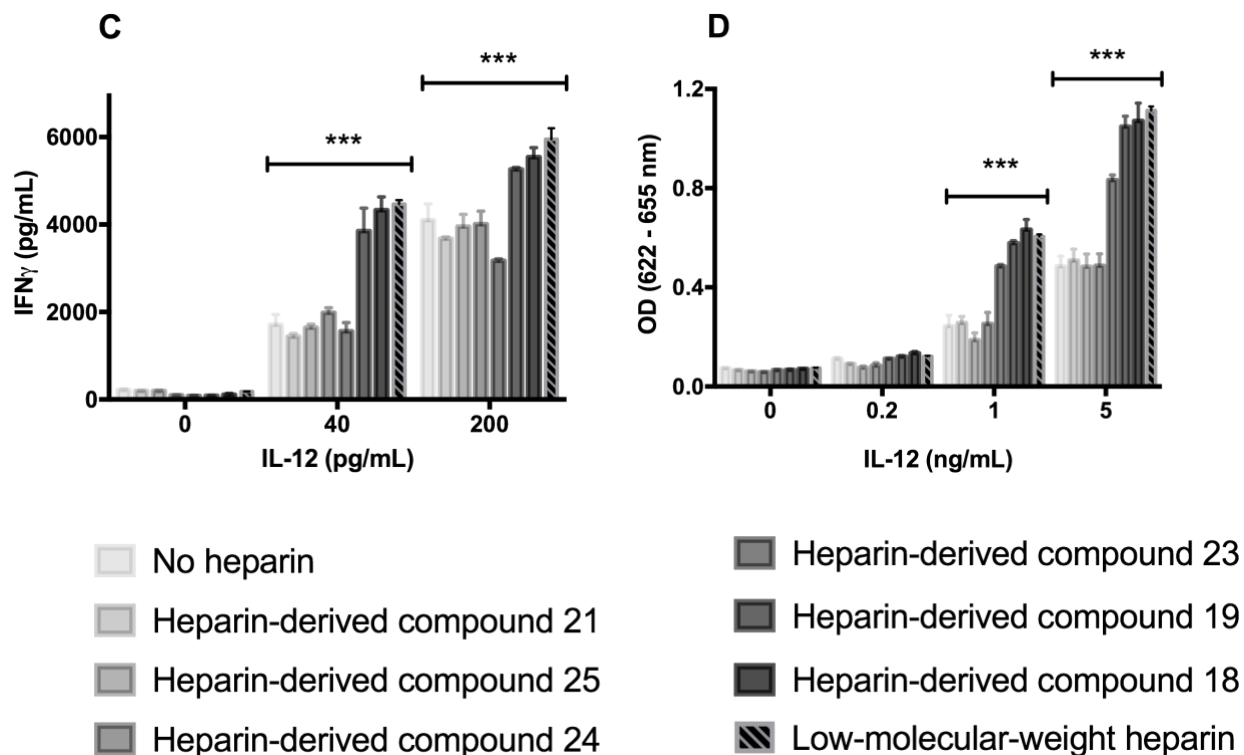
Figure 3.5. HS-induced enhancement of hIL-12 depends on sulfation level. hIL-12 binding to HS oligosaccharides was quantified via a novel microarray. (A) Fifty-three unique HS constructs were synthesized to provide a range of lengths and sulfation levels. Abbreviations: GlcNAc: N-acetylglucosamine; GlcNS: N-sulfated glucosamine; GlcA: glucuronic acid; IdoA2S: 2-O-sulfo-α-L-iduronic acid; 6S: 6-O-sulfate. (B) The binding of Alexa Fluor 488-labeled hIL-12 to the different heparin oligosaccharides was visualized and quantified via fluorescence microscopy. Six dodecasaccharides, including the high binding compounds 18 and 19, were selected for bioactivity studies. hIL-12 activity as determined by (C) IFN-γ production by NK-92MI cells or (D) secreted alkaline phosphatase by HEK-Blue™ IL-12 cells was measured after co-culture with heparin compounds 18, 19, 21, 23, 24, 25 or LMWH (10 μg/mL). Heparin compounds 18, 19, and LMWH significantly increased the bioactivity of hIL-12 in NK-92MI cells and HEK-

Blue^{TM} IL-12 cells (p<0.0001 vs. hIL-12 alone via Tukey's posttest). Heparin compounds 21, 24, 25 did not enhance the bioactivity of IL-12 in NK-92MI cells and HEK-Blue^{TM} IL-12 cells (p>0.05 vs. hIL-12 alone via Tukey's posttest). Heparin compound 23 did not enhance hIL-12 bioactivity in NK-92MI cells (***p<0.0001 vs. IL-12 alone via Tukey's posttest) and modestly enhance IL-12 bioactivity in HEK-Blue^{TM} IL-12 cells (p<0.0001 vs. IL-12 alone, p<0.0001 vs. IL-12 plus LMWH via Tukey's posttest). Data bars in the bioactivity studies represent mean ± standard deviation of triplicate measurements. Experiments were performed in triplicate and repeated three times with similar results.
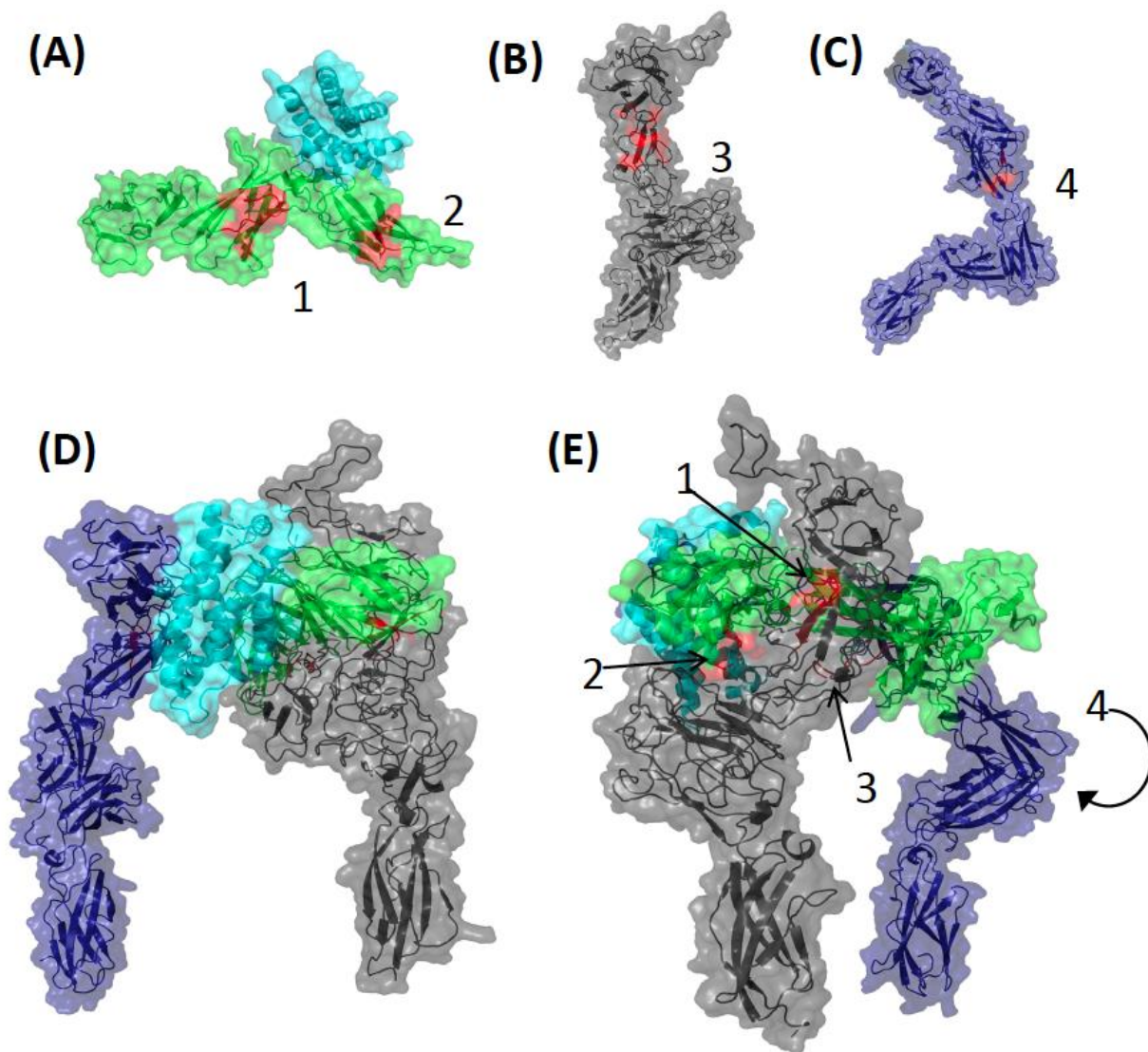
Heparin Binding Sites (IL-12 First)	Approx. Distance (Å)
1, 3	18
2, 3	14
1, 4	43
2, 4	75

Figure 3.6. Heparin may stabilize the interactions of hIL-12 with hIL-12Rβ1 and hIL-12Rβ2. (A) Heparin-binding motifs (red) on hIL-12 (PDB: 1F45) were identified in ClusPro as [117]LKDQKEPKNK[126] and [276]QVQGKSKREKK[286]. The ECD structures of (B) hIL-12Rβ1 and

(C) hIL-12Rβ2 were modeled in PyMOL. As with hIL-12, heparin-binding segments for each

receptor subunit were identified in ClusPro. The top scoring segment for each subunit is

highlighted (red). (D) A model of the hIL-12/hIL-12R complex was predicted using PyMOL and

ClusPro. Two views of the model, nearly 180 degrees rotated around the vertical axis, relate the

locations of the heparin binding segments (red). (E) Estimated distances from each of the heparin

binding sites on hIL-12 to the putative heparin binding sites on the receptor subunits were

calculated using PyMol's Measurement tool.
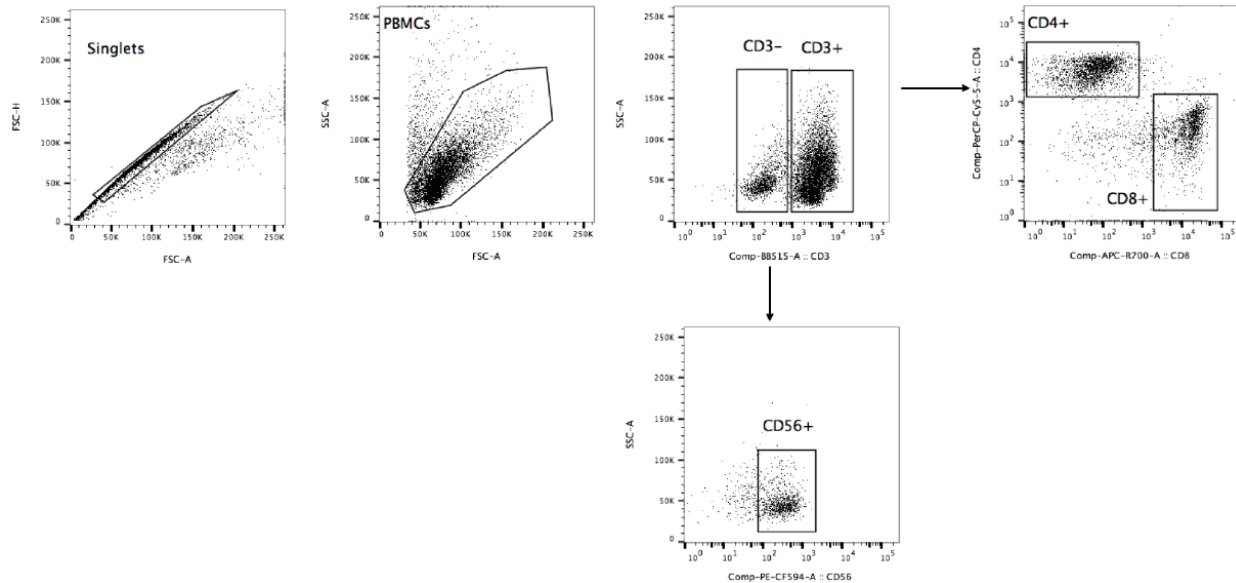
Supplementary Figure S.3.1. Gating strategies for CD4+ T cells, CD8+ T cells, CD56+ NK cells from PBMCs. Lymphocytes for analysis of CD4+ T cells, CD8+ T cells, and NK cells were gated based on using forward scatter (FSC)/side scatter (SSC) dot plots. Single cells were gated based on FSC-H and FSC-A dot plots. T cells were gated from lymphocytes based on dot plots SSC/CD3. From the T cell (CD3+) gate, CD4+ and CD8+ T cells were gated based on CD8/CD4 dot plots. From the non-T cell (CD3-) gate, NK cells (CD3-/CD56+) were gated based on SSC/CD56 dot plots.
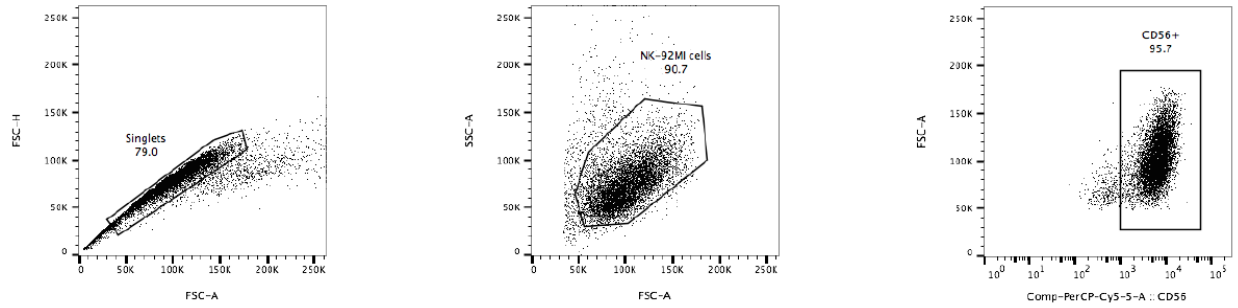
Supplementary Figure S.3.2. Gating strategy for NK-92MI cells. Single cells were gated

based on FSC-H and FSC-A dot plots. NK-92MI cells were gated based on using FSC-A/SSC-A

and FSC-A/CD56$^+$ dot plots.
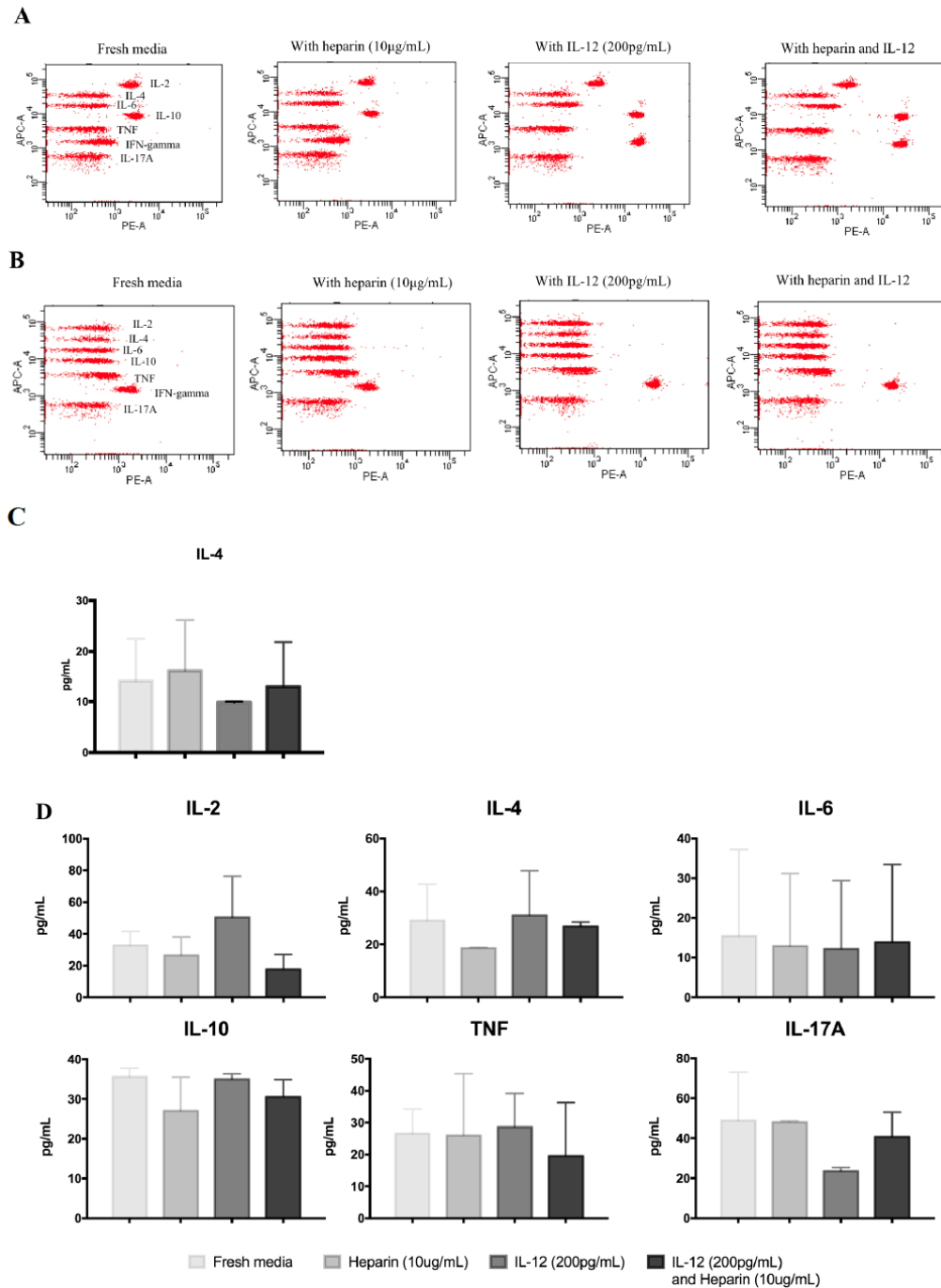
Supplementary Figure S.3.3. Cytokine profiles produced by NK-92MI cells and activated T cells in response to media alone, heparin alone, hIL-12 alone, or with both reagents. Cytometric bead array (CBA) dot plots showing the secretion of 7 cytokines including IL-2, IL-4, IL-6, IL-10, TNF, IFN-γ, and IL-17A from (A) NK-92MI cells or (B) Human T cells. Bar

graph showing the secretion of cytokines including IL-4 from (C) NK-92MI cells, and the

production of IL-2, IL-4, IL-6, IL-10, TNF and IL-17A from (D) Human T cells (p>0.05 in the

comparison of IFN-γ production induced by 4 conditions via one-way ANOVA).

A
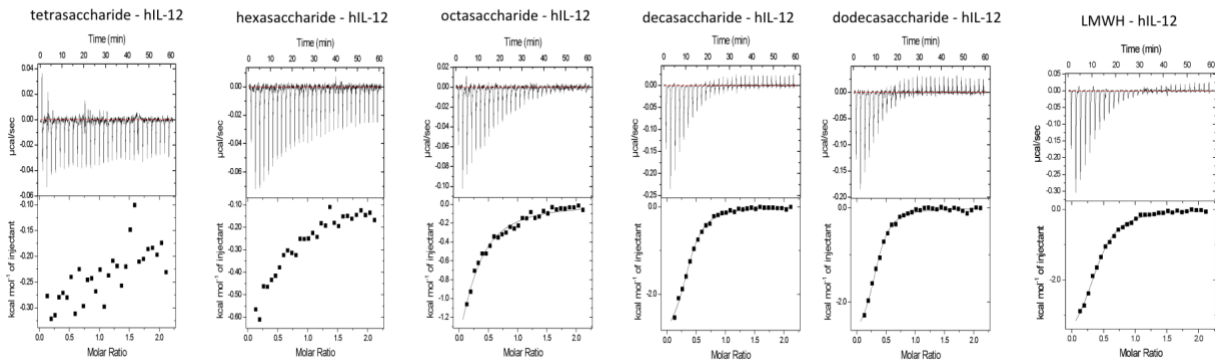
B
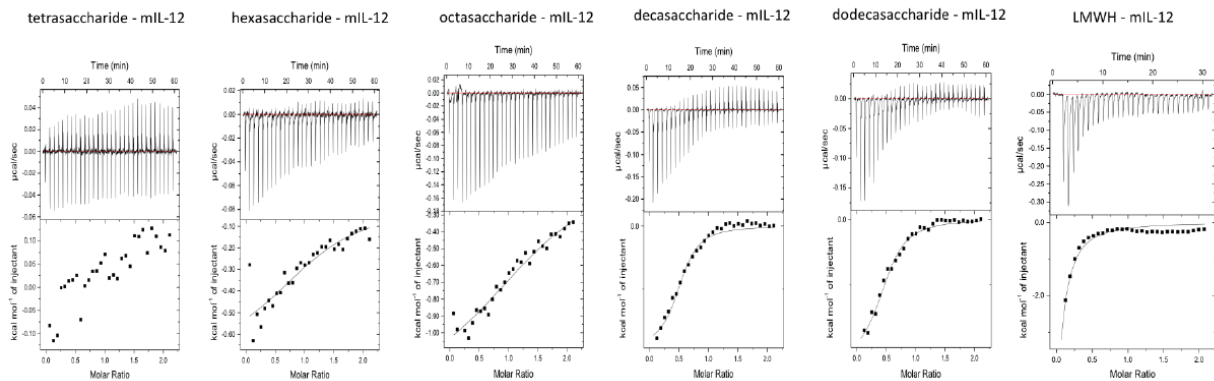
Supplementary Figure S.3.4. Isothermograms for hIL-12 or mIL-12 interactions with heparin. Isothermograms describe binding interactions between heparin and (A) hIL-12 or (B) mIL-12. The upper panel of each isothermogram shows the raw data obtained for each of the 30 injections. The lower panels display the best fit data to one-set of sites binding model using Origin™ v7.0 software.

REFERENCES

1. Hileman RE, Fromm JR, Weiler JM, Linhardt RJ. 1998. Glycosaminoglycan-protein interactions: definition of consensus sites in glycosaminoglycan binding proteins. *Bioessays* 20: 156-67

2. Ornitz DM, Yayon A, Flanagan JG, Svahn CM, Levi E, Leder P. 1992. Heparin is required for cell-free binding of basic fibroblast growth factor to a soluble receptor and for mitogenesis in whole cells. *Mol Cell Biol* 12: 240-7

3. Loo BM, Kreuger J, Jalkanen M, Lindahl U, Salmivirta M. 2001. Binding of heparin/heparan sulfate to fibroblast growth factor receptor 4. *J Biol Chem* 276: 16868-76

4. Fannon M, Forsten KE, Nugent MA. 2000. Potentiation and inhibition of bFGF binding by heparin: a model for regulation of cellular response. *Biochemistry* 39: 1434-45

5. Najjam S, Mulloy B, Theze J, Gordon M, Gibbs R, Rider CC. 1998. Further characterization of the binding of human recombinant interleukin 2 to heparin and identification of putative binding sites. *Glycobiology* 8: 509-16

6. Alvarez-Silva M, Borojevic R. 1996. GM-CSF and IL-3 activities in schistosomal liver granulomas are controlled by stroma-associated heparan sulfate proteoglycans. *J Leukoc Biol* 59: 435-41

7. Clarke D, Katoh O, Gibbs RV, Griffiths SD, Gordon MY. 1995. Interaction of interleukin 7 (IL-7) with glycosaminoglycans and its biological relevance. *Cytokine* 7: 325-30

8. Salek-Ardakani S, Arrand JR, Shaw D, Mackett M. 2000. Heparin and heparan sulfate bind interleukin-10 and modulate its activity. *Blood* 96: 1879-88

9. Hasan M, Najjam S, Gordon MY, Gibbs RV, Rider CC. 1999. IL-12 is a heparin-binding cytokine. *J Immunol* 162: 1064-70

10. Jayanthi S, Koppolu B, Smith SG, Jalah R, Bear J, Rosati M, Pavlakis GN, Felber BK, Zaharoff DA, Kumar TK. 2014. Efficient production and purification of recombinant human interleukin-12 (IL-12) overexpressed in mammalian cells without affinity tag. *Protein Expr Purif* 102: 76-84

11. Garnier P, Mummery R, Forster MJ, Mulloy B, Gibbs RV, Rider CC. 2018. The localisation of the heparin binding sites of human and murine interleukin-12 within the carboxyterminal domain of the P40 subunit. *Cytokine* 110: 159-68

12. Jayanthi S, Koppolu BP, Nguyen KG, Smith SG, Felber BK, Kumar TKS, Zaharoff DA. 2017. Modulation of Interleukin-12 activity in the presence of heparin. *Sci Rep* 7: 5360

13. Leonard JP, Sherman ML, Fisher GL, Buchanan LJ, Larsen G, Atkins MB, Sosman JA, Dutcher JP, Vogelzang NJ, Ryan JL. 1997. Effects of single-dose interleukin-12 exposure on interleukin-12-associated toxicity and interferon-gamma production. *Blood* 90: 2541-8

14. Soares da Costa D, Reis RL, Pashkuleva I. 2017. Sulfation of Glycosaminoglycans and Its Implications in Human Health and Disorders. *Annu Rev Biomed Eng* 19: 1-26

15. Xu X, Takano R, Nagai Y, Yanagida T, Kamei K, Kato H, Kamikubo Y, Nakahara Y, Kumeda K, Hara S. 2002. Effect of heparin chain length on the interaction with tissue factor pathway inhibitor (TFPI). *Int J Biol Macromol* 30: 151-60

16. Rezaie AR. 2007. Heparin chain-length dependence of factor Xa inhibition by antithrombin in plasma. *Thromb Res* 119: 481-8

17. Hochart H, Jenkins PV, Preston RJ, Smith OP, White B, O'Donnell J. 2008. Concentration-dependent roles for heparin in modifying lipopolysaccharide-induced activation of mononuclear cells in whole blood. *Thromb Haemost* 99: 570-5

18. Jalah R, Rosati M, Ganneru B, Pilkington GR, Valentin A, Kulkarni V, Bergamaschi C, Chowdhury B, Zhang G-M, Beach RK, Alicea C, Broderick KE, Sardesai NY, Pavlakis GN, Felber BK. 2013. The p40 Subunit of IL-12 Promotes Stabilization and Export of the p35 Subunit: Implications for Improved IL-12 Cytokine Production. *J Biol Chem* 288: 6763-76

19. Xu Y, Cai C, Chandarajoti K, Hsieh PH, Li L, Pham TQ, Sparkenbaugh EM, Sheng J, Key NS, Pawlinski R, Harris EN, Linhardt RJ, Liu J. 2014. Homogeneous low-molecular-weight heparins with reversible anticoagulant activity. *Nat Chem Biol* 10: 248-50

20. Xu Y, Chandarajoti K, Zhang X, Pagadala V, Dou W, Hoppensteadt DM, Sparkenbaugh EM, Cooley B, Daily S, Key NS, Severynse-Stevens D, Fareed J, Linhardt RJ, Pawlinski R, Liu J. 2017. Synthetic oligosaccharides can replace animal-sourced low-molecular weight heparins. *Sci Transl Med* 9

21. Yang J, Hsieh PH, Liu X, Zhou W, Zhang X, Zhao J, Xu Y, Zhang F, Linhardt RJ, Liu J. 2017. Construction and characterisation of a heparan sulphate heptasaccharide microarray. *Chem Commun (Camb)* 53: 1743-6

22. Comeau SR, Gatchell DW, Vajda S, Camacho CJ. 2004. ClusPro: an automated docking and discrimination method for the prediction of protein complexes. *Bioinformatics* 20: 45-50

23. Comeau SR, Gatchell DW, Vajda S, Camacho CJ. 2004. ClusPro: a fully automated algorithm for protein–protein docking. *Nucleic Acids Res* 32: W96-W9

24. Kozakov D, Brenke R, Comeau SR, Vajda S. 2006. PIPER: an FFT-based protein docking program with pairwise potentials. *Proteins* 65: 392-406

25. Kozakov D, Hall DR, Xia B, Porter KA, Padhorny D, Yueh C, Beglov D, Vajda S. 2017. The ClusPro web server for protein–protein docking. *Nat Protoc* 12: 255

26. Schrodinger L. The PyMOL molecular graphics system. 2010. *Version* 1: r1

27. Kelley LA, Mezulis S, Yates CM, Wass MN, Sternberg MJE. 2015. The Phyre2 web portal for protein modeling, prediction and analysis. *Nat Protoc* 10: 845

28. Chua AO, Chizzonite R, Desai BB, Truitt TP, Nunes P, Minetti LJ, Warrier RR, Presky DH, Levine JF, Gately MK. 1994. Expression cloning of a human IL-12 receptor component. A new member of the cytokine receptor superfamily with strong homology to gp130. *J Immunol* 153: 128-36

29. Presky DH, Yang H, Minetti LJ, Chua AO, Nabavi N, Wu C-Y, Gately MK, Gubler U. 1996. A functional interleukin 12 receptor complex is composed of two β-type cytokine receptor subunits. *Proc Natl Acad Sci U S A* 93: 14002-7

30. Mehrotra PT, Donnelly RP, Wong S, Kanegane H, Geremew A, Mostowski HS, Furuke K, Siegel JP, Bloom ET. 1998. Production of IL-10 by human natural killer cells stimulated with IL-2 and/or IL-12. *J Immunol* 160: 2637-44

31. Tam YK, Maki G, Miyagawa B, Hennemann B, Tonn T, Klingemann HG. 1999. Characterization of genetically altered, interleukin 2-independent natural killer cell lines suitable for adoptive cellular immunotherapy. *Hum Gene Ther* 10: 1359-73

32. Choijilsuren G, Jhou RS, Chou SF, Chang CJ, Yang HI, Chen YY, Chuang WL, Yu ML, Shih C. 2017. Heparin at physiological concentration can enhance PEG-free in vitro infection with human hepatitis B virus. *Sci Rep* 7: 14461

33. Scott JE, Bosworth TR, Cribb AM, Gressner AM. 1994. The chemical morphology of extracellular matrix in experimental rat liver fibrosis resembles that of normal developing connective tissue. *Virchows Arch* 424: 89-98

34. McKee RF, Hodson S, Dawes J, Garden OJ, Carter DC. 1992. Plasma concentrations of endogenous heparinoids in portal hypertension. *Gut* 33: 1549-52

35. Casanova JL, Abel L. 2002. Genetic dissection of immunity to mycobacteria: the human model. *Annu Rev Immunol* 20: 581-620

36. Fieschi C, Bosticardo M, de Beaucoudrey L, Boisson-Dupuis S, Feinberg J, Santos OF, Bustamante J, Levy J, Candotti F, Casanova JL. 2004. A novel form of complete IL-12/IL-23 receptor beta1 deficiency with cell surface-expressed nonfunctional receptors. *Blood* 104: 2095-101

37. Vignali DA, Kuchroo VK. 2012. IL-12 family cytokines: immunological playmakers. *Nat Immunol* 13: 722-8

CHAPTER 4: CONCLUSIONS AND FUTURE DIRECTIONS

4.1. Significant findings of this dissertation

Previous work from our lab has shown that IL-12 is a specific heparin-binding protein (1). The overarching goal of this research was to investigate if the interaction between heparin and IL-12 influenced the immunobiology of IL-12. In particular, we sought to explore the molecular consequences of heparin-IL-12 interaction, the biological outcomes of the interaction as well as the mechanisms responsible for these outcomes. The completed research has led to the following significant findings: [1] heparin increases IL-12 activity in human but not mouse lymphocytes; [2] heparin modestly protects IL-12 from proteolytic degradation; [3] heparin canonically amplifies IL-12-induced cytokine production by activated lymphocytes; [4] heparin-induced modulation of IL-12 bioactivity is dependent on heparin concentration, chain length and sulfation; [5] heparin likely stabilizes the interaction between IL-12 and IL-12R for which we have developed a model of stabilization; and [6] heparin is capable of enhancing IL-12 signaling in IL-12Rβ1deficient cells. Each of these findings is detailed below.

4.1.1. Heparin increases IL-12 activity in human but not mouse

IL-12 plays central role in the immune system by connecting the activities of innate and adaptive immunity (2). Due to this potent activity, IL-12 has been used in clinical trials for the treatment of cancer and HIV infection (3-5). We and others have identified likely heparin binding-domains on the p40 subunit of IL-12 (1, 6). Recently, we found that heparin binds to IL-12 with low micromolar affinity (Table 2.1) (1, 7). Thus, we first questioned if the binding between IL-12 and heparin plays a role in the physiological function of hIL-12 – a

powerful proinflammatory cytokine with immunoregulatory abilities. Our data revealed that heparin increased the biological activity of hIL-12 by up to 6 fold (7). Significantly, the enhancing effect of heparin on IL-12 bioactivity only occurred in human cells (NK-92MI cells, human T cells, human PBMCs, and HEK-Blue^TM cells), but not in murine cells (2D6 cells and splenocytes isolated from C57BL/6J mice). Interestingly, heparin was found to bind to both mIL-12 and hIL-12 with similar binding affinity (Table 3.1). Thus, we suspect that the mIL-12/mIL-12R interaction is of sufficient affinity such that heparin does not further enhance the interaction. On the other hand, the affinities of mIL-12 for hIL-12R and hIL-12 for hIL-12R are likely much lower than the affinity of mIL-12 for mIL-12R. Therefore, the benefit of adding heparin to stabilize the potentially 'loose' mIL-12/hIL-12R and hIL-12/hIL-12R complex resulted in a robust enhancement of mIL-12 activity. Planned research will test this hypothesis by producing recombinant proteins of the extracellular domain of human and mouse IL-12R in order to measure the binding affinities of 3 complexes including mIL-12/mIL-12R, mIL-12/hIL-12R, and hIL-12/hIL-12R in the presence and absence of heparin.

4.1.2. Heparin binds to IL-12 and prevents IL-12 from proteolytic degradation

In collaboration with Dr. Suresh Kumar's lab at the University of Arkansas-Fayetteville, we examined the molecular consequences of heparin-hIL-12 binding by several biochemical approaches. Using isothermal calorimetry to analyze the interaction of hIL-12 and heparin/heparan sulfate, we demonstrated that hIL-12 likely contains a single distinct, accessible binding pocket for heparin/heparan sulfate which could lead to dimerization of hIL-12. Other interleukins are able to increase the binding affinity to their receptors when cytokines form dimer or tetramer structures. For instance, homodimer forms of IL-5 are able to bind its extracellular domain of IL-5Rα and arrange in a critical "wrench-like" structural conformation (8). Similarly,

121

dimers or tetramers of IL-22 were shown to arrange into a V-shaped conformation binding to IL-22R1 receptor (9).

Furthermore, heparin has been shown to protect proteins from the proteolytic degradation of proteases present in the extracellular environment (10-13). We exposed hIL-12, with and without heparin, to various levels of proteolytic degradation from proteases in spent media to a protease cocktail containing trypsin, chymotrypsin, thrombin and thermolysin. For using spent media as a source of proteases, hIL-12 was not significantly degraded in spent media while heparin was found to prevent the proteolytic degradation of IL-12 in the protease cocktail by up to 14% within 30 minutes of incubation. Although heparin can slightly prevent hIL-12 from strong proteolytic degradation, this is unlikely to explain the enhanced hIL-12 biological activity *in vitro* that we discovered.

4.1.3. Heparin canonically amplifies IL-12 activity

Data in Chapter 2 highlight the ability of heparin to recover IL-12 bioactivity in cells expressing mutant forms of IL-12 receptors that were poorly active (Fig. 2.5). We proposed that heparin's interactions with IL-12 could activate a novel signaling pathway leading to the enhanced production of IFN-γ as well as other cytokines. Using a cytometric bead array (CBA) to measure production of the prototypical cytokines produced by the three major T helper cell classes, we showed that heparin only amplifies the bioactivity of IL-12, and does not trigger another signaling pathway. One limitation of this study is that the CBA assay evaluates only 7 cytokines related to Th1, Th2 and Th17 responses. Other cytokines and signaling pathways may be altered in the presence of heparin. For a more comprehensive analysis, higher level multiplex assays, such as Luminex RNA-sequencing and/or kinase profiling can be employed.

4.1.4. Heparin-induced modulation of IL-12 bioactivity is dependent on heparin concentration, chain length and sulfation

We have shown that sulfated GAGs including heparin and heparan sulfate could bind and enhance biological activity of hIL-12 (1, 7). However, the exact molecular mechanisms of this modulation still remain unclear. Thus, we extended our previous study to investigate characteristics of heparin that play essential roles in its modulation to hIL-12 bioactivity. In Chapter 3, we investigated three characteristics of heparin that might play a role in modulating IL-12 bioactivity including heparin concentration, chain length, and sulfation level. First, we found that concentrations of heparin ranging from 10 µg/mL to 25 µg/mL produce maximal effect on the enhancement of IL-12 bioactivity. The next investigation of heparin characteristics showed that heparin molecules less than a threshold of 6 saccharide units do not influence hIL-12 activity, while those above 8 saccharide units induce a bioactivity plateau that is similar to low molecular weight heparin. Likewise, heparins with less than 3 sulfate groups per disaccharide do not significantly improve hIL-12 bioactivity. In contrast, heparin molecules containing 3 sulfate groups showed improved hIL-12 binding and bioactivity. Interestingly, the inability of poorly sulfated heparins to enhance hIL-12 bioactivity agreed with our previous data in chapter 2 demonstrating that poorly or non-sulfated GAGs, e.g. chondroitin sulfate and hyaluronic acid, has no effect on hIL-12 bioactivity (7).

4.1.5. The development of a working model of stabilization showing the interaction of heparin – IL-12 and IL-12R

We have shown that heparin clearly increases the concentration of hIL-12 at cell surfaces by using a flow cytometry analysis of hIL-12 conjugated with a fluorescent tag (7). This result suggested that exogenous heparin is able to maintain a reservoir of hIL-12 at the cell surface. To elucidate how heparin could retain high concentrations of IL-12 at cell surfaces, we proposed a

working model capable of describing how heparin interacts with IL-12 and IL-12 receptors. Using an *in silico* analysis, we point out 4 putative binding sites of heparin on hIL-12 and hIL-12 receptors with 2 sites located in p40 subunit of hIL-12, 1 site located in hIL-12Rβ1, and 1 site located in hIL-12Rβ2. Thus, we proposed that heparin serves as a co-receptor of IL-12 and IL-12 receptors by simultaneously binding to heparin-binding sites on both ligand and receptors. By using this working model, we could explain the effect of heparin chain length on IL-12 bioactivity. When IL-12 is bound to IL-12R, the distances between heparin-binding domains located on different proteins ranging from 14 to 75 Å. A tetrasaccharide, with a maximum distance of approximately 16-17 Å between sulfate groups, would therefore have a lower probability of binding to and stabilizing the hIL-12/hIL-12R interactions than an octasaccharide or LMWH.

4.1.6. Heparin is capable of enhancing IL-12 signaling in IL-12Rβ1deficient cells

In Chapter 2, we showed that heparin is able to recover the bioactivity of IL-12 in cells expressing mutant forms of IL-12R that were poorly active. With the model of stabilization proposed in Chapter 3, we sought to explore the mechanism of IL-12 recovery in the presence of heparin. Thus, we investigated the effect of heparin on IL-12 activity in 2 cell-based models that lack normal IL-12Rβ1 expression including IL-12Rβ1 deficient PBMCs from MSMD patients as well as IL-12Rβ1 mutant NK-92MI cells. We showed that heparin enhanced the production of IFN-γ in response to IL-12 in PBMCs isolated from 4 of 6 MSMD patients. We also found that heparin recovers the bioactivity of IL-12 in multiple clones of IL-12Rβ1 mutant NK-92MI cells. However, the effect of heparin plus IL-12 in these cell clones still remains unclear because although IL-12Rβ1 expression was reduced, a wild-type sequence was found in all developed clones while a CRISPR-induced mutation could not be verified. Furthermore, we could not rule

out the possibility of off-target effects induced by CRISPR/Cas9. Studies of heparin induced IL-12 acitivty in IL-12Rb1-deficient cells produced two hypotheses. First, the IL-12Rb1 cells in which IL-12 activity is enhanced by heparin are 'leaky' and contain low levels of wild type IL-12Rβ1. Second, all IL-12 signaling is mediated through IL-12Rβ2 alone. These data as well as the above analyses are provided in the Appendix 1 of this dissertation.

4.2. Concluding remarks

Results from these studies clearly show a physiological function of heparin in IL-12 immunobiology. The observation of increased hIL-12 bioactivity by heparin is rare among other interleukins, for which heparin binding is typically more inhibitory/neutral than augmentative. A plausible physiological explanation for interaction of IL-12 and heparin is to retain IL-12 at specific sites. IL-12 is recognized to induce life-threatening adverse events when systemically administered (14). Heparin is released by mast cells and basophils that are typically recruited to inflammation sites (15-17). Thus, the localization of IL-12 and enhancement of its bioactivity by heparin at inflammation sites may provide a way to limit the systemic toxicity of this powerful cytokine. There are lines of evidence showing that other pro-inflammatory cytokines, e.g. TNF-α, IL-1, or GM-CSF, are able to bind to heparin (18-20). Thus, these findings support the paradigm of heparin-induced localization of proinflammatory cytokines at inflammation sites. The fact that heparin also makes IL-12 more effective at these sites may represent a positive feedback mechanism for cell-mediated immune responses.

4.3. Future directions

Our future research will address three unanswered questions including: [1] does heparin stabilize the complex of IL-12 and IL-12R? [2] how does heparin recover IL-12 bioactivity in

IL-12Rβ1 deficient cells including MSMD patient cells and engineered NK-92MI cells? [3] is heparin-induced modulation of IL-12 bioactivity physically relevant?

First, to investigate if heparin stabilizes the complex of IL-12 and IL-12R, we are planning to produce recombinant proteins of the extracellular domains (ECDs) of human and murine IL-12Rβ1 and IL-12Rβ2. These ECDs will help us to determine the binding strength of IL-12 to its receptors in the presence or absence of heparin via ITC. Moreover, we can compare the binding affinity of 2 complexes consisting of heparin/hIL-12/hIL-12Rβ1/hIL-12Rβ2 and heparin/mIL-12/mIL-12Rβ1/mIL-12Rβ2 that could explain why heparin binds to both mIL-12 and hIL-12, but only helps increasing the bioactivity of hIL-12 and mIL-12 on human derived cells. Related to this work, we are also pursuing crystallography work, in collaboration with Dr. Lars Pedersen at the National Institute of Environmental Health Sciences, to visualize and confirm the interaction between IL-12 receptors and IL-12 and/or heparin at an atomic level. X-ray crystallographic studies will show how the proteins interact with heparin, and any differences in the conformation of the IL-12 receptors when bound by IL-12 in the presence or absence of heparin. In addition, this study will be the first to provide atomic-level resolution of ECDs of IL-12 receptors.

Second, we seek to explore the molecular mechanisms underlying heparin-induced recovery of IL-12 bioactivity in MSMD patient cells. As mentioned above, studies to date have generated two hypotheses that can account for heparin-enhanced IL-12 activity in IL-12Rβ1 deficient cells. Because we hypothesized that heparin and IL-12 might signal through IL-12β2 receptor, thus we will investigate the downstream signaling of IL-12Rβ2. We will measure the phosphorylation of JAK2 and STAT4 in IL-12 plus heparin-induced MSMD patient cells because these two proteins are downstream targets of IL-12Rβ2 (21). To determine if heparin

126

can facilitate IL-12 signaling through IL-12Rβ2 alone, a cell line containing only IL-12Rβ2 can be generated. Similar cell lines have been created by our collaborators at Rockefeller University. There are several precedents of heterodimeric cytokines that can signal through single subunit chain receptors, whereas they conventionally bind to 2 different subunit receptors (9, 23). To evaluate the potential 'leakiness' of IL-12Rβ1 mutant cells, intracellular staining of activated T cells from responding MSMD patients can be used to sort IFN-γ expressing cells. The mRNA from these cells can then be isolated, amplified and sequenced to determine if wild-type constructs are indeed produced.

Even though CRISPR-induced IL-12Rβ1 mutations were not confirmed in mutant NK-92MI cells, this cell line remains valuable for future exploration. Future studies will focus on using CRISPR/Cas9 homology-directed repair to create a library of mutant NK-92MI with IL-12Rβ1 mutations matching the breadth of those observed in MSMD patients. By using Cas9 protein instead of Cas9 encoded plasmids, we can reduce the possibility of continuous expression of Cas9 that results in introduction of undesired off-targets and mutations. Using a homology template, specific mutations can be introduced to the IL-12Rβ1 gene with high accuracy. Mutations matching those discovered in MSMD patients can be developed. Furthermore, this technology can also be used to disrupt and determine the influence of the heparin binding domains on IL-12Rβ1 or IL-12Rβ2.

Lastly, the interaction of IL-12 and heparin are likely to help retain IL-12 at a site of inflammation rather than allowing potentially toxicity systemic dissemination of IL-12. To explore this possibility, the presence of endogenous heparin and heparin sulfate at inflammation sites must be quantified. Mast cells, the primary producers of heparin, have been found to accumulate in tumors during cancer progression (24). The mast cell-deficient mouse model most

widely used is WBB6F$_1$- Kit$^{W/W-v}$; these mice are commercially available (25). Thus, the production of heparin in tumors in wild-type mouse model and mast cell-deficient mice can be compared. If a difference in heparin production between these mouse models is found, then the local retention and bioactivity of injected IL-12 in these tumors can be explored. If there is no difference in heparin or heparan sulfate concentrations in tumors of wild-type and mast cell deficient mice, then other types of infection and inflammation can be explored.

REFERENCES

1. Jayanthi S, Koppolu B, Smith SG, Jalah R, Bear J, Rosati M, Pavlakis GN, Felber BK, Zaharoff DA, Kumar TK. 2014. Efficient production and purification of recombinant human interleukin-12 (IL-12) overexpressed in mammalian cells without affinity tag. *Protein Expr Purif* 102: 76-84

2. Trinchieri G. 2003. Interleukin-12 and the regulation of innate resistance and adaptive immunity. *Nat Rev Immunol* 3: 133-46

3. Atkins MB, Robertson MJ, Gordon M, Lotze MT, DeCoste M, DuBois JS, Ritz J, Sandler AB, Edington HD, Garzone PD, Mier JW, Canning CM, Battiato L, Tahara H, Sherman ML. 1997. Phase I evaluation of intravenous recombinant human interleukin 12 in patients with advanced malignancies. *Clin Cancer Res* 3: 409-17

4. Jacobson MA, Hardy D, Connick E, Watson J, DeBruin M. 2000. Phase 1 trial of a single dose of recombinant human interleukin-12 in human immunodeficiency virus-infected patients with 100-500 CD4 cells/microL. *J Infect Dis* 182: 1070-6

5. Motzer RJ, Rakhit A, Schwartz LH, Olencki T, Malone TM, Sandstrom K, Nadeau R, Parmar H, Bukowski R. 1998. Phase I trial of subcutaneous recombinant human interleukin-12 in patients with advanced renal cell carcinoma. *Clin Cancer Res* 4: 1183-91

6. Hasan M, Najjam S, Gordon MY, Gibbs RV, Rider CC. 1999. IL-12 is a heparin-binding cytokine. *J Immunol* 162: 1064-70

7. Jayanthi S, Koppolu BP, Nguyen KG, Smith SG, Felber BK, Kumar TKS, Zaharoff DA. 2017. Modulation of Interleukin-12 activity in the presence of heparin. *Sci Rep* 7: 5360

8. Kusano S, Kukimoto-Niino M, Hino N, Ohsawa N, Ikutani M, Takaki S, Sakamoto K, Hara-Yokoyama M, Shirouzu M, Takatsu K, Yokoyama S. 2012. Structural basis of interleukin-5 dimer recognition by its alpha receptor. *Protein Sci* 21: 850-64

9. de Oliveira Neto M, Ferreira JR, Jr., Colau D, Fischer H, Nascimento AS, Craievich AF, Dumoutier L, Renauld JC, Polikarpov I. 2008. Interleukin-22 forms dimers that are recognized by two interleukin-22R1 receptor chains. *Biophys J* 94: 1754-65

10. Saksela O, Moscatelli D, Sommer A, Rifkin DB. 1988. Endothelial cell-derived heparan sulfate binds basic fibroblast growth factor and protects it from proteolytic degradation. *J Cell Biol* 107: 743-51

11. Clarke D, Katoh O, Gibbs RV, Griffiths SD, Gordon MY. 1995. Interaction of interleukin 7 (IL-7) with glycosaminoglycans and its biological relevance. *Cytokine* 7: 325-30

12. Webb LM, Ehrengruber MU, Clark-Lewis I, Baggiolini M, Rot A. 1993. Binding to heparan sulfate or heparin enhances neutrophil responses to interleukin 8. *Proc Natl Acad Sci U S A* 90: 7158-62

13. Mummery RS, Rider CC. 2000. Characterization of the heparin-binding properties of IL-6. *J Immunol* 165: 5671-9

14. Leonard JP, Sherman ML, Fisher GL, Buchanan LJ, Larsen G, Atkins MB, Sosman JA, Dutcher JP, Vogelzang NJ, Ryan JL. 1997. Effects of single-dose interleukin-12 exposure on interleukin-12-associated toxicity and interferon-gamma production. *Blood* 90: 2541-8

15. Lim GB. 2017. Milestone 1: Discovery and purification of heparin. *Nat Rev Cardiol*

16. Holgate ST. 2000. The role of mast cells and basophils in inflammation. *Clin Exp Allergy* 30 Suppl 1: 28-32

17. Wedemeyer J, Galli SJ. 2000. Mast cells and basophils in acquired immunity. *Br Med Bull* 56: 936-55

18. Sebollela A, Cagliari TC, Limaverde GS, Chapeaurouge A, Sorgine MH, Coelho-Sampaio T, Ramos CH, Ferreira ST. 2005. Heparin-binding sites in granulocyte-macrophage colony-stimulating factor. Localization and regulation by histidine ionization. *J Biol Chem* 280: 31949-56

19. Kenig M, Gaberc-Porekar V, Fonda I, Menart V. 2008. Identification of the heparin-binding domain of TNF-alpha and its use for efficient TNF-alpha purification by heparin-Sepharose affinity chromatography. *J Chromatogr B Analyt Technol Biomed Life Sci* 867: 119-25

20. Ramsden L, Rider CC. 1992. Selective and differential binding of interleukin (IL)-1 alpha, IL-1 beta, IL-2 and IL-6 to glycosaminoglycans. *Eur J Immunol* 22: 3027-31

21. Vignali DA, Kuchroo VK. 2012. IL-12 family cytokines: immunological playmakers. *Nat Immunol* 13: 722-8

22. van de Vosse E, Haverkamp MH, Ramirez-Alejo N, Martinez-Gallo M, Blancas-Galicia L, Metin A, Garty BZ, Sun-Tan C, Broides A, de Paus RA, Keskin O, Cagdas D, Tezcan I, Lopez-Ruzafa E, Arostegui JI, Levy J, Espinosa-Rosales FJ, Sanal O, Santos-Argumedo L, Casanova JL, Boisson-Dupuis S, van Dissel JT, Bustamante J. 2013. IL-12Rbeta1 deficiency: mutation update and description of the IL12RB1 variation database. *Hum Mutat* 34: 1329-39

23. Collison LW, Delgoffe GM, Guy CS, Vignali KM, Chaturvedi V, Fairweather D, Satoskar AR, Garcia KC, Hunter CA, Drake CG, Murray PJ, Vignali DA. 2012. The composition and signaling of the IL-35 receptor are unconventional. *Nat Immunol* 13: 290-9

24. Maciel TT, Moura IC, Hermine O. 2015. The role of mast cells in cancers. *F1000Prime Rep* 7: 09

25. Reber LL, Marichal T, Galli SJ. 2012. New models for analyzing mast cell functions in vivo. *Trends Immunol* 33: 613-25

APPENDIX 1: EFFECTS OF HEPARIN ON IL-12 BIOACTIVITY IN IL-12 RECEPTOR SUBUNIT BETA 1 DEFICIENT CELLS

Introduction

IL-12 is a heterodimeric cytokine comprised of two disulfide-linked glycoprotein subunits, p35 and p40 (1-3). The IL-12 receptor similarly consists of heterodimeric subunits with the IL-12 receptor β1 (IL-12Rβ1) chain binding p40 and the IL-12 receptor β2 (IL-12Rβ2) chain binding p35 (4, 5). Binding of IL-12 by IL-12R activates Janus kinase 2 (JAK2) and tyrosine kinase 2 (TYK2), leading to the phosphorylation of signal transducers and activators of transcription 3 (STAT3) and STAT4. Homodimers of phosphorylated STAT4 (pSTAT4) translocate to the nucleus where they bind to promoters of IL-12-responsive genes, including IFN-γ.

Molecular defects in the IL-12 signaling pathway lead to defects in IFN-γ production which hinders an individual's ability to mount cell-mediated immune responses. Patients with inborn errors in IL-12/IFN-γ immunity have difficulty controlling intracellular microorganisms and are diagnosed with Mendelian susceptibility to mycobacterial disease (MSMD). MSMD is categorized by vulnerability to poorly virulent mycobacterial infections such as BCG vaccines and environmental mycobacteria (6, 7). The severity of MSMD varies widely from asymptomatic, subclinical infections to severe, disseminated disease which can be lethal (8). A clinical study of 141 MSMD patients from 30 countries around the world revealed that the mortality rate was 29.78% and the mean age at death was 7.5 years in the 40 patients who died (ranges from 1.2 to 37.7 year, standard deviation 8.1 year) (9). The causes of death were disseminated BCG infection, nontuberculous mycobacteria, tuberculosis, or salmonellosis, concurrent *M. avium* and *Salmonella* infections, severe electrolyte disorder following diarrhea (9).

132

IL-12Rβ1 deficiency is the most frequent known genetic etiology of MSMD. MSMD patients whose cells are deficient in IL-12Rβ1 expression poorly respond to IL-12 and only release low amounts of IFN-γ in response to IL-12 (8, 9). Each subunit of IL-12R exhibits similar affinity for its respective IL-12 subunit. The affinity of p40 for IL-12Rβ1 and p35 for IL-12Rb2 are strong - K_d = 6 nM and 5 nM, respectively. However, when the IL-12 heterodimer is bound to both receptor subunits, the affinity is enhanced two orders of magnitude (K_d = 65 pM) (10). Thus, loss of IL-12Rβ1 results in poor binding of IL-12 to IL-12Rβ2 leading to impairment of IL-12 signaling.

Our previous work demonstrated that heparin binds to and enhances the bioactivity of IL-12 (11, 12). This effect was limited to heparin molecules longer than 4 disaccharide units. The requirement of longer chain lengths implied that heparin could simultaneously bind two proteins, e.g. IL-12 and IL-12R, thus stabilizing their interaction. Using an *in silico* analysis, we identified 4 putative binding sites of heparin located in IL-12 and IL-12 receptors (2 sites on the p40 subunit of IL-12, 1 site on IL-12Rβ1, and 1 site on IL12Rβ2). Using the published structure of IL-12 and predicted structures for each receptor subunit, we developed a model of the IL-12/IL-12R complex (Fig. 3.6). By measuring distances between heparin binding domains on different subunits, we determined that only longer chains of heparin could span multiple domains. This finding agreed with our bioactivity studies and suggests that heparin may be facilitating enhanced bioactivity by stabilizing the IL-12/IL-12R complex.

In addition to enhancing IL-12 activity on wild-type cells, our previous work also showed that heparin can rescue IL-12 signaling in cells producing mutant forms of IL-12 receptors (12). Therefore, bioactivity data in both wild-type and mutant cells imply that heparin serves as a co-receptor for IL-12.

Previous studies have shown that IL-12Rβ1 is the subunit mainly accountable for binding of IL-12, whereas IL12Rβ2 plays a vital role in triggering the signaling functions of IL-12 (13, 14). Indeed, by using Ba/F3 cell line as the host cell for expression of IL-12Rβ1, IL-12Rβ2 or IL-12Rβ1 and IL-12Rβ2 receptors, IL-12 was shown to signal through the single expression of IL-12Rβ2 but not IL-12Rβ1 (10). In another study supporting cytokine signaling through a single chain, , IL-22 was shown to form dimers/tetramers and bind to two single IL-22R1 receptor chains (15), whereas this cytokine conventionally binds to two heterodimeric receptors, IL-10R1 and IL-22R1 (16). Yet another study showed that IL-35, a member of IL-12 family, was able to signal through a single receptor chain, with IL-12Rβ2 alone inducing phosphorylated STAT4, or gp130 alone inducing phosphorylated STAT1 (17).

Based on our data demonstrating that heparin facilitates IL-12 signaling in IL-12Rβ1 deficient cells as well as the single receptor chain signaling studies cited above, we developed two hypotheses: (1) heparin stabilizes binding between IL-12 and mutant expressed forms of IL-12Rβ1; and (2) heparin enhances binding between IL-12 and IL-12Rβ2 allowing IL-12 to signal through only one receptor subunit.

To test these hypotheses, we investigated the effect of heparin on IL-12 bioactivity in 2 cell-based models including engineered NK-92MI cells producing mutant forms of IL-12Rβ1 and MSMD patient cells that are deficient in IL-12Rβ1 expression. Engineered NK-92MI cells producing mutant forms of IL-12Rβ1 are necessary for this study because: [1] we can have an unlimited supply of mutant cells that are essential for numerous planned studies, [2] we can have a library of IL-12Rβ1 mutations that are important for determining the specific effect of heparin on IL-12 bioactivity in each type of mutation, and [3] we can correlatively compare the effect of heparin on IL-12 bioactivity between engineered NK-92MI cells and MSMD patient cells. IL-

12Rβ1 mutant NK-92MI cells were generated via CRISPR/Cas9 genomic editing technology. Loss of functional IL-12Rβ1 and subsequent restoration of IL-12 signaling in the presence of heparin was confirmed in IL-12 bioactivity assays. IL-12Rβ1 expression in different clones were examined via flow cytometry. Polymerase chain reaction (PCR) and Sanger sequencing were employed to characterize CRISPR/Cas9 induced mutations. IL-12 bioactivity, in the presence and absence of heparin, in peripheral blood T cells from 6 MSMD patients was also evaluated.

Materials and Methods

Cell culture and activation of MSMD peripheral blood mononuclear cells (PBMCs)

The IL-2-independent, IL-12-responsive human natural killer cell line, NK-92MI (ATCC; CRL-2408TM), was cultured in complete media consisting of Alpha MEM supplemented with 12% FBS, 12% horse serum, 100 U/mL penicillin/streptomycin, 0.2 mM inositol, 0.02 mM folic acid, and 0.1 mM 2-mercaptoethanol.

PBMCs from 9 MSMD patients were kindly provided by Dr. Jean-Laurent Casanova (Rockefeller University, NY). Mutations in IL12Rβ1 coding genes of those patients are described in Table A1.1 and Fig. A.1.1.

PBMCs were activated by incubating 10^6 cells/ml with anti-CD3, anti-CD28 coated superparamagnetic beads (Dynabeads® Human T-Activator CD3/CD28; ThermoFisher) in culture media at a bead:cell ratio of 1:1 for 3 days.

CRISPR/Cas9-mediated deletion of IL12Rβ1

A 20-bp guide sequences (5'- GGAGCACTCGTAACGATCAC -3') targeting DNA within the exon 3 of IL12Rβ1 gene was selected from "The CRISPR design tool" provided by Zhang lab, MIT (http://crispr.mit.edu/). Exon 3 of IL-12Rβ1 gene was targeted for knocking-out this gene because it codes for the cytokine binding region of IL12Rβ1 gene that plays important

role in the interaction of IL-12 and its receptors. The single-guide RNA was picked based on the high quality of guiding to IL12Rβ1 coding gene and minimized off-target binding on other sites in the human genome. Then, a plasmid containing this single-guide RNA was purchased from Origene (pCas-Guide-EF1a-GFP, Origene). Plasmids were amplified by *E. coli* and then purified using QIAGEN Plasmid Maxi Kit.

NK-92MI cells ($2x10^6$ cells) were re-suspended in 100 μl of electroporation buffer (Harvard Apparatus, Holliston, MA) and added to an electroporation cuvette. Plasmid (10 μg) was added to the electroporation cuvette and mixed well by pipetting. The cell suspension was electroporated with 250 volts, 25 ohms, and 750 μF in a 2 mm cuvette using the electroporation system ECM630 (Harvard Apparatus, Holliston, MA). Electroporated cells were then transferred to pre-warmed 1 ml culture media in a well of 6-well plate. These cells were cultured at 37°C for 72 hours.

NK-92MI transfected cells were harvested by centrifugation and diluted to a concentration of $2x10^6$ cells/ml in PBS. Then, the cells were filtered through a 50μm filter into a FACS tube. The transfected cells were sorted using FACS Aria III system (BD Biosciences). Only the top 5% of GFP-positive cells were collected to ensure high transfection levels of CRISPR/Cas9 complexes.

Cloning and sub-cloning selection of IL-12Rβ1 engineered mutant NK-92MI cells

Transfected cells were first cloned using a limiting dilution-based method. Cells were seeded in a 24-well plate with cell numbers of 50 cells/well. This concentration was used because the viability of this cell line is significantly reduced when they are seeded at extreme low density. Cells were cultured at 37°C, 5% CO_2 for 10 - 14 days. Colonies were picked and dispersed into the appropriate liquid growth medium for further expansion and testing.

136

For sub-cloning selection, cells were added to a mixture of base methylcellulose medium ClonaCell Flex (#03818, Stemcell Technologies) and culture media with the concentration of 100 cells/mL. Using a 12 mL syringe and a 16-gauge Blunt-End Needle (Catalog #28110), cell suspension was plated into a 100 mm Petri dishes and cultured at 37°C in a humidified atmosphere containing 5% CO_2 for 10 - 14 days without disturbing the plates. Colonies were picked and dispersed into the appropriate liquid growth medium for further expansion and testing.

IL-12 bioactivity assay

To assess the effect of heparin on IL-12 bioactivity in IL-12Rβ1 deficient cells, MSMD patient PBMCs, parental NK-92MI and IL12Rβ1 mutant cells were cultured with fixed or increasing concentrations of IL-12 (0, 200, 1000, 5000 pg/mL) ± 10 μg/ml heparin for 24 hours or 48 hours. IFN-γ production was quantified by ELISA.

Polymerase chain reaction and Sanger sequencing analysis of IL12Rβ1

Genomic DNA (gDNA) was extracted using QIAamp DNA Mini Kit (51304, Qiagen). Fifty nanograms of gDNA was then used for polymerase chain reaction (PCR) to amplify the sequence of exon 3, IL12Rβ1 gene. The sequence of primers used were as follows: (1) exon 3 – IL12Rβ1 → forward primer 5'- GGAGGGTTTAGGCTGAGGTG-3' and reverse primer 5'- ATCACGCATCCGAGAGTAGG-3'; (2) 2871 base pairs (bp) amplicon → forward primer: 5' - GAGGGCTGATGATCACTTGG - 3' and reverse primer: 5' - GCTAGTAGTATCAAGTCCCTTGCC - 3'; (3) 9499 bp amplicon → forward primer: 5' - CCTTGCTCAGCTTCAATGTG - 3' and reverse primer 5' - GGGACAGATGCAGAGATGG (18). PCR products were submitted to NCSU Genomic Sciences Laboratory for Sanger sequencing.

Flow cytometry analysis

Expression of CD56 and IL-12Rβ1 were analyzed using flow cytometry. Mutant and wild-type NK-92MI cells were stained with 1 μg/10^6 cells of PerCP-Cy5.5 mouse anti-human CD56, clone B159 (560842, BD Biosciences) or PerCP-Cy5.5-conjugated mouse IgG1, k isotype control (550795, BD Biosciences); APC mouse anti-human IL12Rβ1, clone 2.4E6 (558708; BD Biosciences), or APC-conjugated mouse IgG1, k isotype control (550854; BD Biosciences). Cells were rinsed twice in cold PBS and read on a BD FACSCelesta. Data were analyzed using FlowJo v10 software package (Flow Jo LLC, Ashland, OR).

For intracellular staining, protein transport inhibitor containing monensin (554724, BD Biosciences) was added to the cells during treatment with media alone, heparin alone (10 μg/mL), IL-12 alone (200 pg/mL), or IL-12 (200 pg/mL) plus heparin (10 μg/mL). Cells were fixed in Fixation/Permeabilization Solutions (554714 or 554655, BD Biosciences) using the manufacturer's recommended protocols. Anti-human IFNγ BV421 (clone: B27) or mouse anti-Stat4 (pY693) PE (clone 38/p-Stat4) were used for intracellular IFNγ and pSTAT4 staining. For pSTAT4 staining, permeabilization was performed using Perm Buffer III (558050, BD Biosciences). Data were acquired using a BD FACSCelesta flow cytometer (BD Biosciences) and analyzed using FlowJo software package (Flow Jo LLC, Ashland, OR).

Results

Generation of IL-12Rβ1 functionally deleted NK-92MI cells

Because IFN-γ is the primary downstream product of IL-12, we measured IFN-γ production as a readout of IL-12 bioactivity. Initial studies showed that 4 different clones of IL-12Rβ1 mutant NK-92MI cells responded to IL-12 (Fig. A.1.2) by producing different levels of IFN-γ. Clone 6 was selected for further study due to its low responsiveness to IL-12. Although

138

studies with 200 pg/ml indicated that IL-12Rβ1 was completely non-functional, when IL-12 concentration was increased (1000 pg/mL), higher levels of IFN-γ production were observed. This indicated that clone 6 may not be a true clonal population, but rather a mixture of knocked-out cells and wild-type cells. Therefore, we decided to subclone clone 6 using semi-solid methylcellulose medium. Most of the 9 subclones obtained did not respond to IL-12 at the dose of 200 pg/mL and only produced IFN-γ in response to IL-12 at 1000 pg/mL (Fig. A.1.3A). Subclone 7 did not respond to IL-12 even at the higher dose, however, this subclone produced a modest level of IFN-γ (266.748 ± 3.45 pg/mL) when treated with 5000 pg/mL of IL-12 (Fig. A.1.3B). In contrast, the wild-type NK-92MI cells produced 1271.61 ± 60.86 pg/ml of IFN-γ in response to 200 pg/mL of IL-12. For all IL-12Rβ1 mutant cells, heparin appeared to at least partially recover the bioactivity of IL-12.

Immunophenotyping studies revealed that subclone 7 expressed lower levels of not only IL-12Rβ1, but also CD56, pSTAT4, and IFN-γ compared to wild-type NK-92MI cells (Fig. A.1.4).The CRISPR/Cas9 approach used in this study, utilized non-homologous end-joining to rejoin DNA strands after double strand breaks. Thus, Sanger sequencing was employed to determine the nature of the mutations induced by CRISPR/Cas9. The amplification of a 319 bp region around the Cas9 cut site in exon 3 of the gene encoding IL-12Rβ1, from each of the subclones, produced a single clear band visualized by gel electrophoresis (Fig. A.1.5A). Sequencing PCR products revealed that exon 3, in mutant clones was intact and identical to wild-type cells (Fig. A.1.5B). In an attempt to look for larger insertion or deletions, PCR of exon 3 from subclone 7 cells was repeated using additional primers. These primers produced amplicons of 2871 bp and 9499 bp with no other significant gene PCR products. Thus, sequencing and PCR

analyses were unsuccessful at identifying a significant genomic alteration compared to wild-type cells (Fig. A.1.5C).

Effect of heparin on IL-12 bioactivity in PBMCs isolated from MSMD patients

Activated PBMCs from 6 out of 9 MSMD patients were evaluated for IFN-γ production in response to IL-12 alone or IL-12 plus heparin. Three patient samples were not evaluable due to insufficient cell numbers or contamination. Four of the six evaluable samples tested demonstrated a measurable increase in IFN-γ when heparin was included (Fig. A.1.6). Increases ranged from 17.76% in patient 006193 to 40.3% in patient 04893. Heparin had no effect on two MSMD patient samples. A cursory analysis relating the type or location of mutation (Table A.1.1) and the heparin-enhanced IL-12 activity revealed no obvious correlation.

Discussion

The data presented above confirmed our previous data that heparin can enhance IL-12 signaling in IL-12Rβ1 deficient cells. However, neither of the hypothetical mechanisms for the enhanced activity could be confirmed or refuted.

IL-12 bioactivity studies in IL-12Rβ1 mutant NK-92MI cells demonstrated that different clones responded differently to IL-12. Our initial interpretation of these data was that CRISPR/Cas9 randomly induced mutations in the sequence of exon 3 of IL-12Rβ1 which led to the expression of various IL-12Rβ1 mutant receptors. Cells with minor mutations in IL-12Rβ1 were expected to have higher levels of responsiveness to IL-12. However, PCR and sequencing experiments could not detect a mutation in the region of exon 3 of IL-12Rβ1. Because CRISPR/Cas9 might produce large insert/deletion fragments around exon 3, we tried to broaden the amplification around the exon 3 cut site using different primers. Unfortunately, the results of these amplifications did not reveal any differences in PCR products between mutant cells and

wild-type cells. In addition, sequencing data indicated that exon 3 in all subclones was identical to the wild-type version.

Although PCR and sequencing could not detect a mutation, IL-12Rβ1 expression levels, as assessed via flow cytometry were markedly reduced. As such, these mutant cells may still be considered as IL-12Rβ1-deficient. Given that CD56 and phosphorylated STAT4 were also decreased in NK-92MI mutants, it is possible that the CRISPR/Cas9 protocol induced unknown off-target effects. Nevertheless, heparin was still able to partially recover IL-12 signaling in these cells.

Studies of IL-12 bioactivity in MSMD patient cells revealed that heparin enhanced IL-12-induced production of IFN-γ in 4 of 6 patients. Notably, 2 of the patient samples that exhibited improved IL-12 signaling in the presence of heparin contained a point mutation which induced transcription of a stop codon. For instance, the genetic sequence of patient 004893 indicates substitution of a stop codon in exon 3 instead of a glutamine at position 32. Patient 013315 has a similar stop codon in exon 7. These mutations are located in the extracellular domain of IL-12Rβ1 and produce undetectable expression of IL-12Rβ1 as confirmed by other groups (8, 19). A complete IL-12Rβ1 knockout would seem to favor our second hypothesis that heparin facilitates IL-12 signaling through IL-12Rβ2 exclusively. However, according to Dr. J.-L. Casanova, a leading expert in MSMD and the provider of these cells, it is possible for cells to 'read through' the stop codon, thus producing the wild-type IL-12Rβ1. This 'leakiness' is very rare but could happen in a very small percentage of cells, likely less than 1 percent, that would not be detectable or impart clinical benefit. Nevertheless, a small number of 'leaky' cells could account for heparin-enhanced IL-12 signaling and does not allow for exclusion of any of our previous hypotheses.

The above discussion pertains to mutations in which a stop codon terminates the translation of IL-12Rβ1 thus resulting no expression of the receptor subunit. It should be noted that a subset of MSMD patients have mutations resulting in truncated IL-12Rβ1. We have requested, but have not received, MSMD patient samples with specific truncated forms of IL-12Rβ1, to determine if heparin can rescue IL-12 activity in patients with this genotype.

Conclusions and Future Studies

This study was our initial attempt to explain the effect of heparin on IL-12 bioactivity in IL-12Rβ1 deficient cells. We showed that heparin slightly recovered the production of IFN-γ in response to IL-12 in PBMCs isolated from 4 of 6 MSMD patients. This result appears to support the hypothesis that recovery of IL-12-induced IFN-γ production in MSMD patient PBMCs by heparin likely occurred by signaling via the intact IL-12Rβ2 receptor. However, due to the potential 'leakiness' of wild-type IL-12Rb1 expression, we could not confirm this hypothesis.

We also found that heparin helped recover the bioactivity of IL-12 in multiple clones of IL-12Rβ1 engineered mutant NK-92MI cells. However, the effect of heparin plus IL-12 in these cell clones was not definitive because impairment of IL-12 signaling in these cells were possibly explained by the off-target activity of CRISPR/Cas9. In this study, we delivered DNA plasmids coding for CRISPR/Cas9 complex that was not ideal for precise genome editing. Continuous expression of Cas9 nuclease by DNA plasmid increased the potential for undesired off-targets and mutations. Moreover, there was a high possibility that DNA plasmids might be integrated within the chromosome leading to stable expression of Cas9. In future experiments, Cas9 protein or Cas9 mRNA can be introduced to reduce off-target effects. Furthermore, we can improve the editing fidelity of CRISPR/Cas9 technology by using homology-directed repair (HDR) that provides a DNA template with homology to the sequence flanking double strand break (DSB)

location. HDR is a more precise mechanism for double strand break editing due to the use of

higher sequence homology between the damaged and intact donor strands of DNA. Using the

HDR approach will also allow for the generation of a library of mutants with known mutations at

various locations in the IL-12Rβ1 gene. Some of these mutations will be matched with known

mutations in MSMD patients. Additional future studies are described in Chapter 4.

Table A.1.1. Genetic status of MSMD patient samples

Patient code[$]	Gender	Origin	Gene	Phenotype	Genetic status
004893	F	France	IL-12Rβ1	Patient	p.Q32X/p.Q32X
006193	M	Morocco	IL-12Rβ1	Patient	c.1791+2T>G/c.1791+2T>G
009203	M	Poland	IL-12Rβ1	Patient	p.Q32*/WT and c.1189+2T>A/WT
013315	M	Morocco	IL-12Rβ1	Patient	p.R211X/p.R211X
004013	F	Mexico	IL-12Rβ1	Patient	deletion exon 8/WT and p.R521X/WT
012183	M	N/A	IL-12Rβ1	Patient	c.783+1G>A/c.783+1G>A
001043	F	Turkey	IL-12Rβ1	Patient	p.R486X/R486X
004632	M	Turkey	IL-12Rβ1	Patient	p.R486X/p.R486X
008404	M	France	IL-12Rβ1	Patient	p.Q32X/c.1623_1624delinsT

[$] Bold and italic font: Patient cells that responded with IL-12 and heparin

Italic font: Patient cells that did not respond with IL-12 and heparin

Underline font: Patient cells that did not expand after stimulation
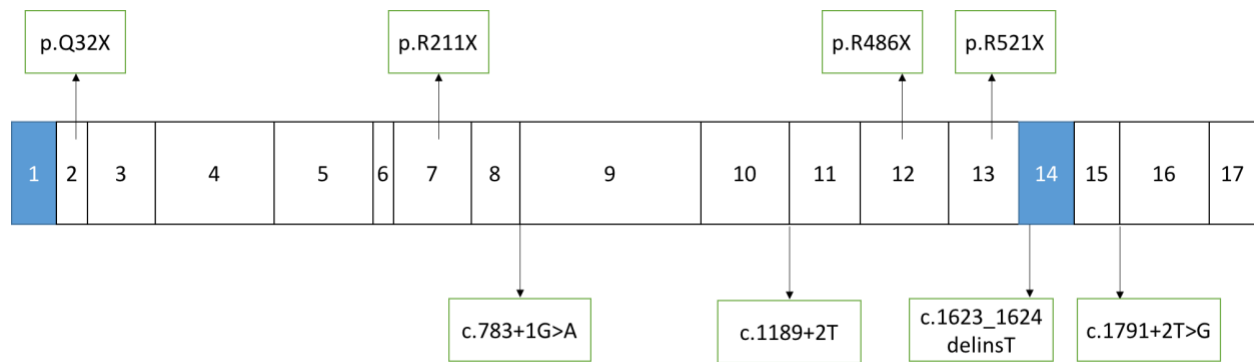
Figure A.1.1. Mutation locations in IL-12β1 gene of MSMD patients. Green boxes show mutation locations in IL-12Rβ1 gene of MSMD patients used in this study. IL-12Rβ1 gene includes 17 exons (numbered 1 to 17 in this graph), in which exon 1 codes for a signal peptide, exon 2 – 13 code for the extracellular domain, exon 14 codes for the transmembrane domain, exon 15 – 17 code for the intracellular domain.

A
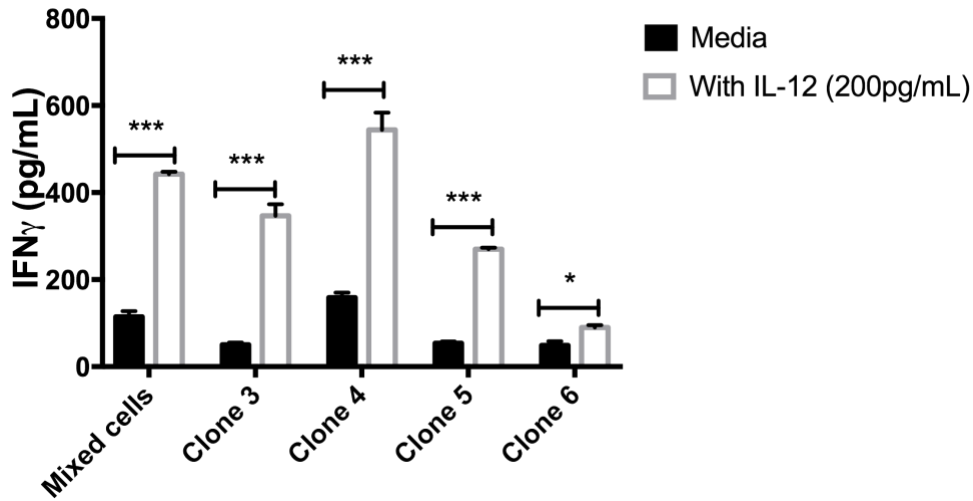
B
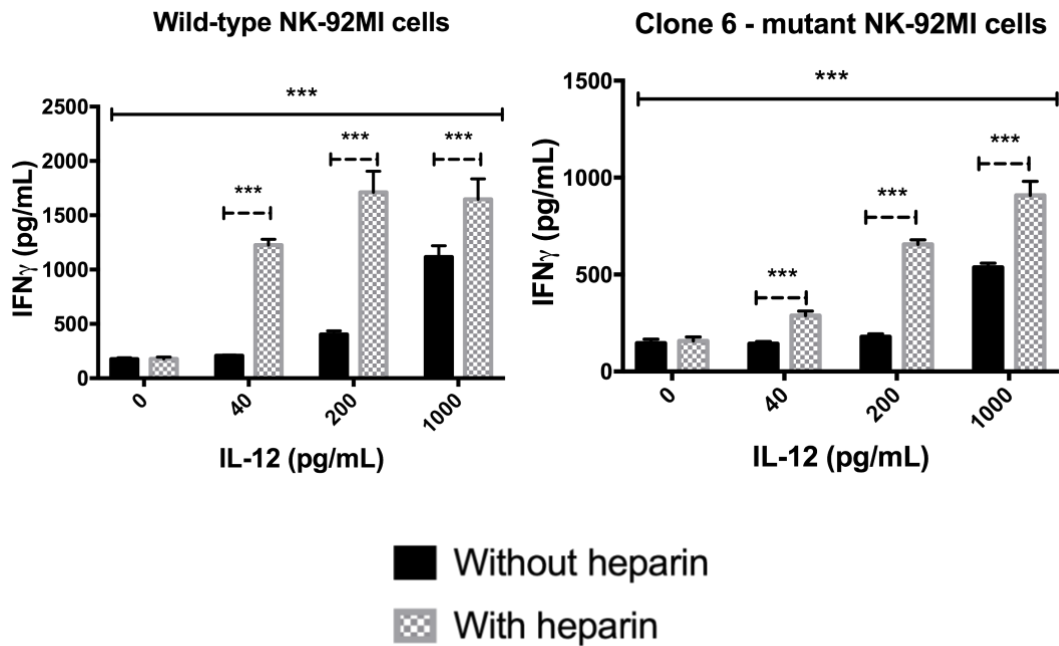
Figure A.1.2. IL-12 bioactivity assays on NK-92MI cells (clones and wild-type cells).

The production of IFN-γ by (A) NK-92MI cell clones or (B) NK-92MI clone 6 cells vs. wild-

type cells was measured after 24-hour exposure to a fixed concentration of IL-12, 200 pg/ml for

(A) or increasing doses of IL-12 for (B). Heparin concentration was used at a fixed concentration

146

of 10 μg/mL. IFNγ concentrations were measured via ELISA. (A) The comparison of IL-12 responsiveness in mutant NK-92MI cell clones to media vs. IL-12 alone via t test (***$p<0.0001$, *$p<0.05$ via t-test). (B) Heparin enhanced the bioactivity of IL-12 in mutant NK-92MI cells and wild-type NK-92MI cells (***$p<0.0001$ via two-way ANOVA). Tukey's posttest was used to distinguish the difference of IL-12 activity in specific concentration of IL-12 vs. IL-12 plus heparin (dashed line, ***$p<0.0001$). Data points represent mean ± standard deviation of triplicate measurements. Experiments were performed in triplicate and repeated three times with similar results.

A
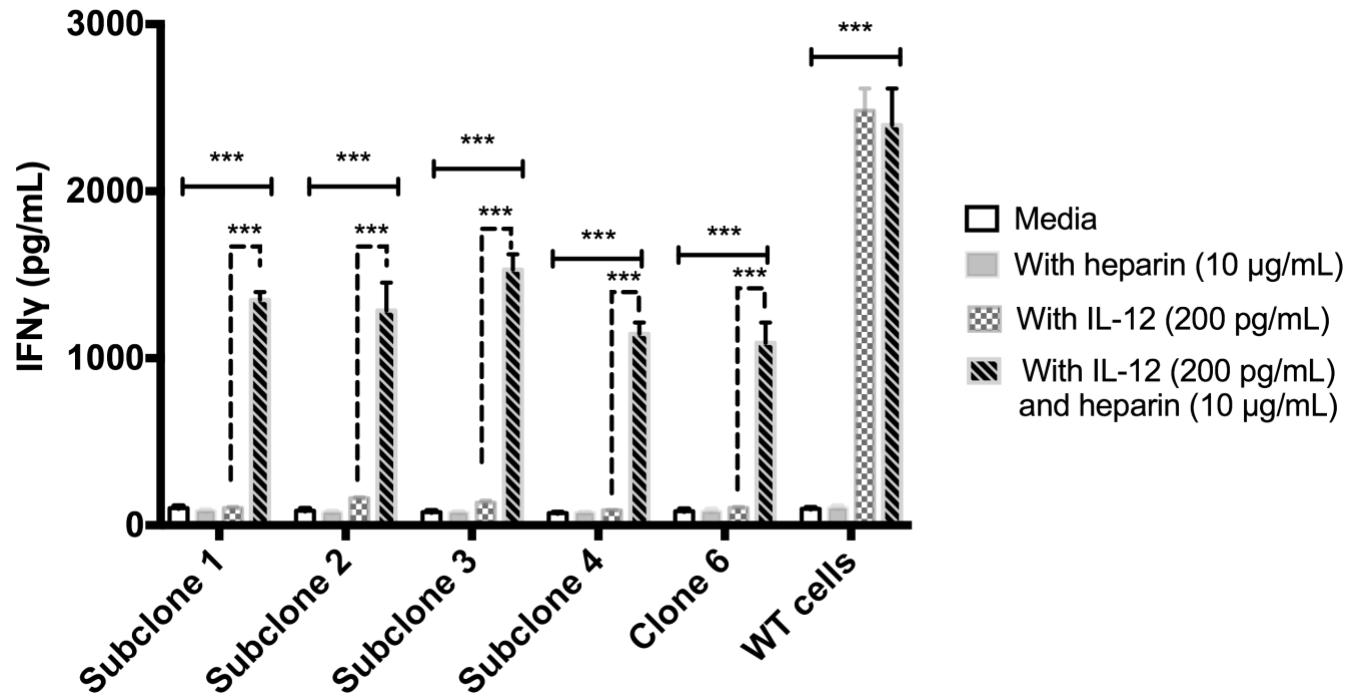
B
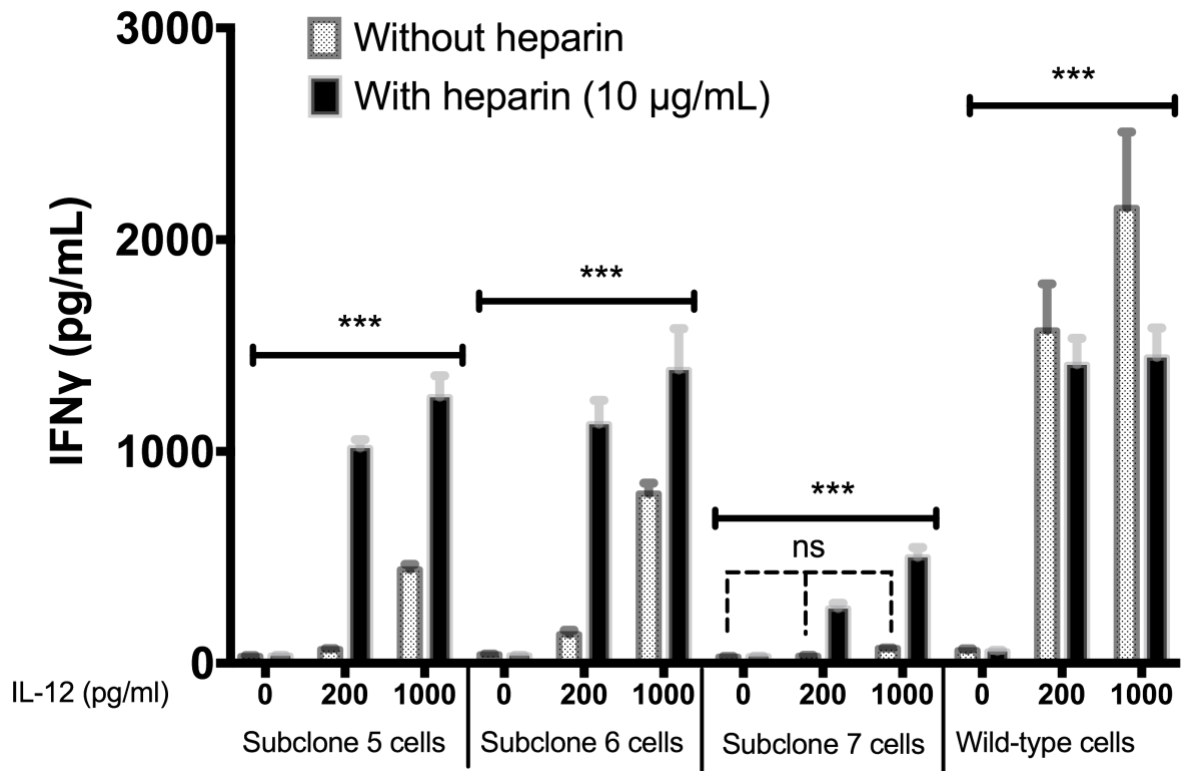
C
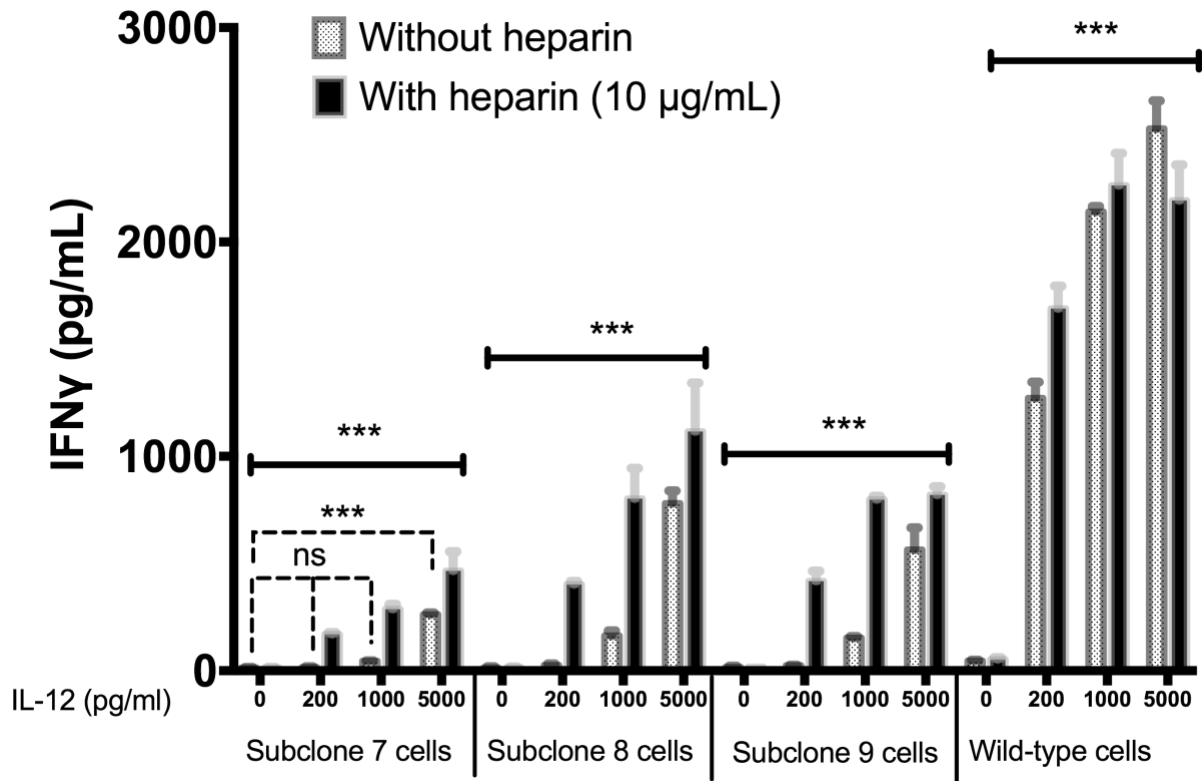

Figure A.1.3. IL-12 bioactivity assays on NK-92MI cells (sub clones and wild-type

cells). The production of IFN-γ by NK-92MI subcloned cells vs. wild-type cells was measured

after 24-hour exposure to (A) fixed dose of IL-12 (200 pg/mL) or (B) and (C) increasing doses of

IL-12 from 0 pg/mL to 1000 pg/mL (B) or from 0 pg/mL to 5000 pg/mL (C). Heparin

concentration was used at a fixed concentration of 10 μg/mL. IFNγ concentrations were

measured via ELISA. For statistical analyses, heparin enhanced the bioactivity of IL-12 in

mutant NK-92MI cells (***p<0.0001 vs. IL-12 alone via two-way ANOVA, solid line). Tukey's

posttest was used to compare the production of IFN-γ in response to IL-12 alone vs. IL-12 plus

heparin at each specific IL-12 concentration (dashed line, ***p<0.0001), ns: not significant. Data

points represent mean ± standard deviation of triplicate measurements. Experiments were

performed in triplicate and repeated three times with similar results.

A
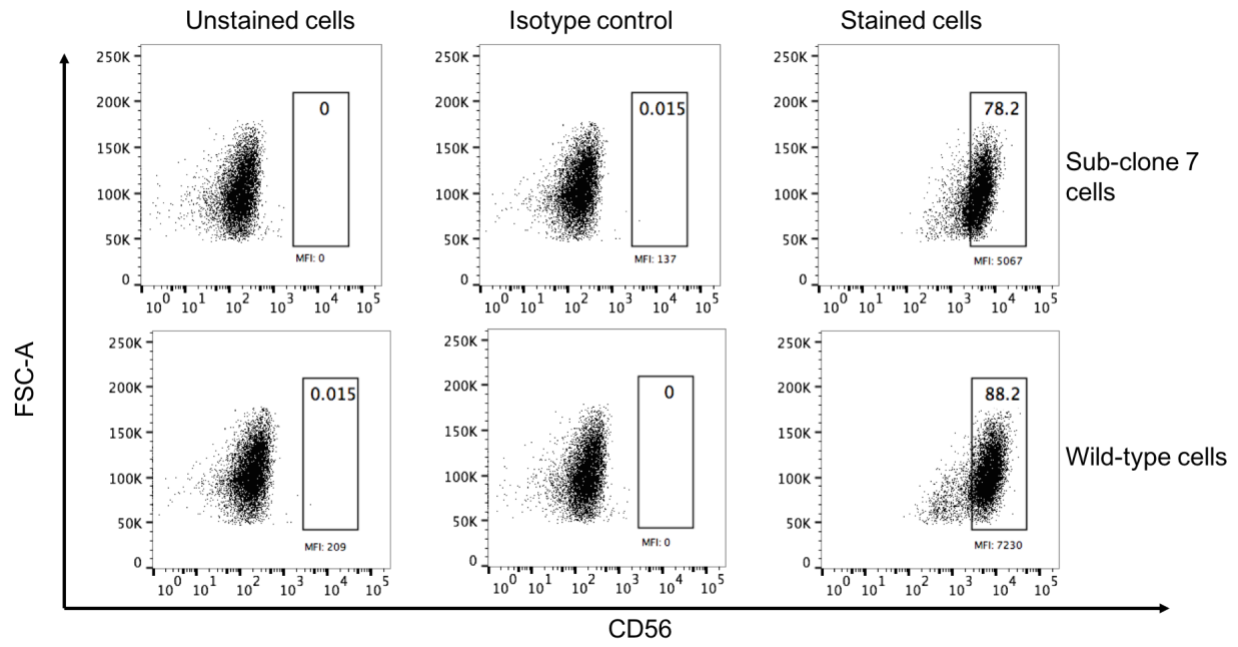
B
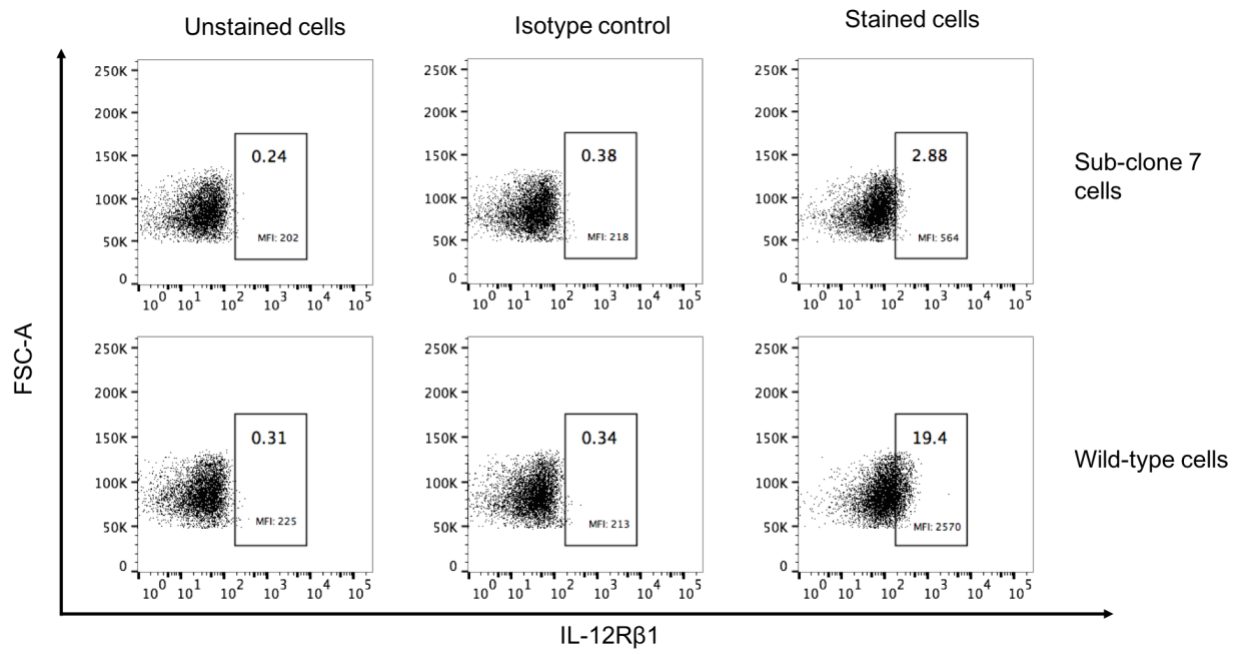
C
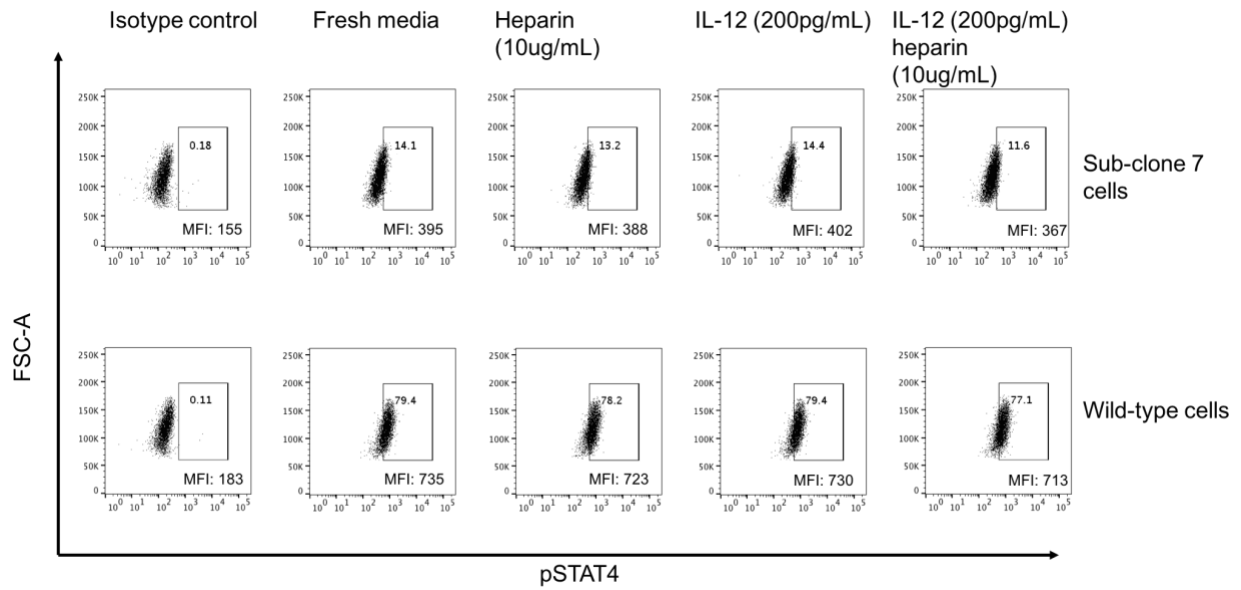
D
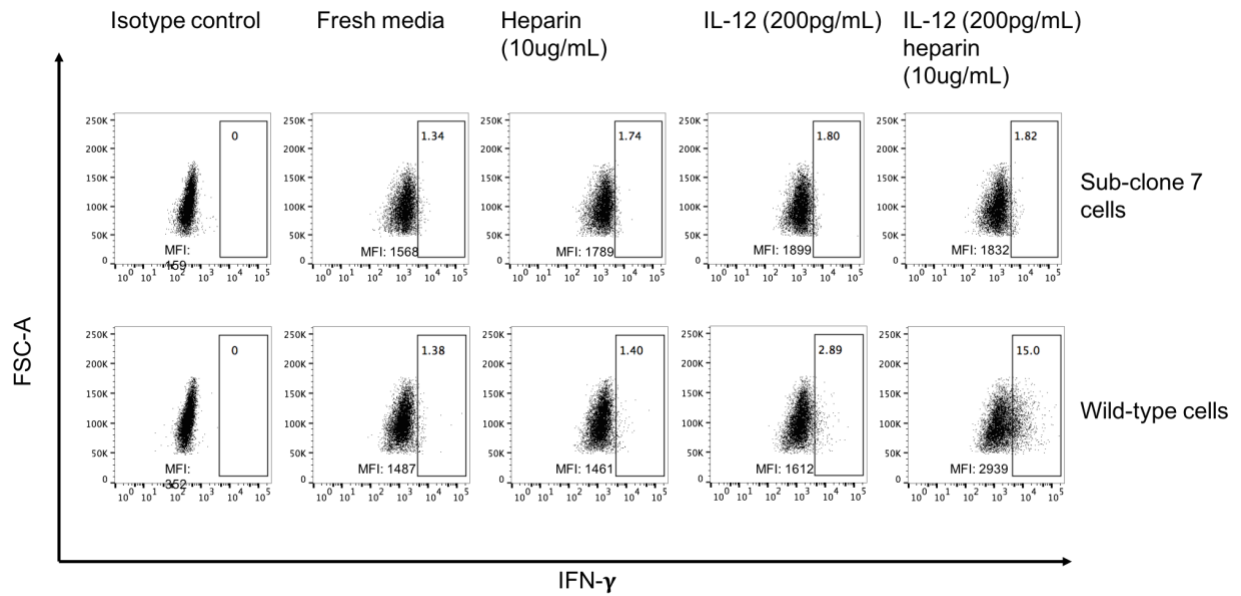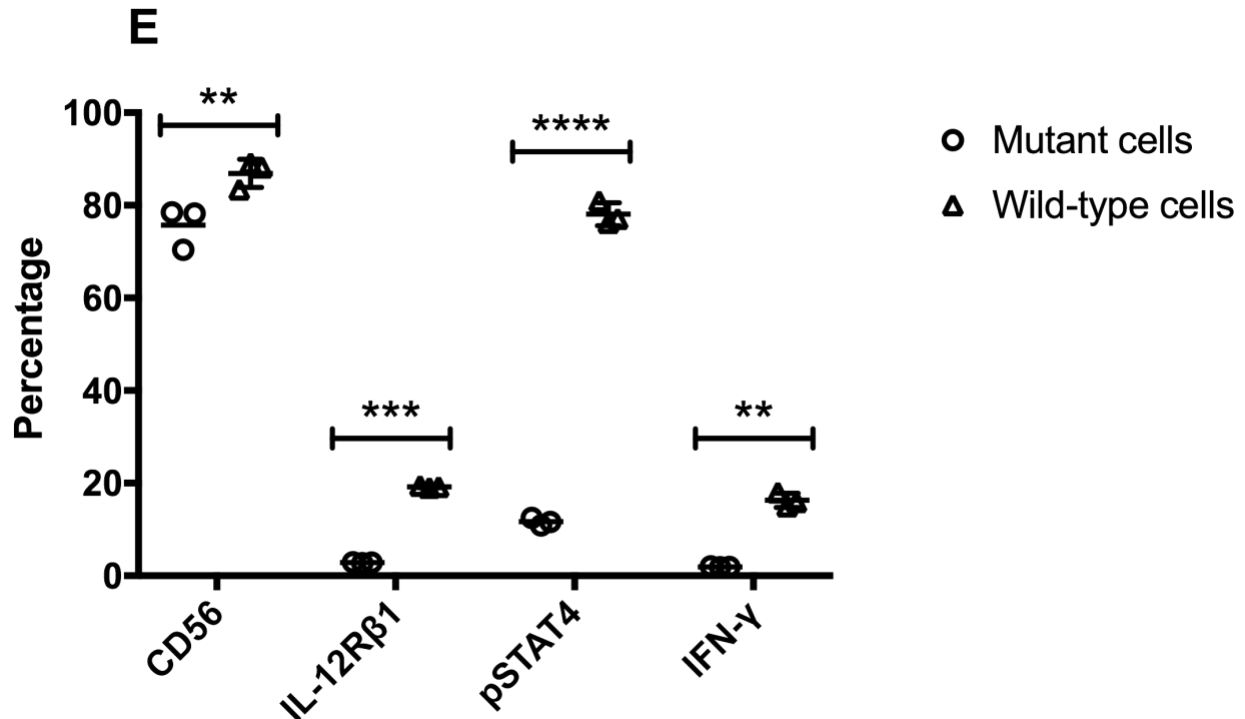
Figure A.1.4. Expression of CD56, IL-12Rβ1, pSTAT4, IFN-γ in mutant (subclone 7) and wild-type NK-92MI cells. Dot plots show representative expression of (A) CD56, (B) IL12Rβ1, (C) pSTAT4, (D) IFN-γ by mutant NK-92MI cells and wild-type NK-92MI cells. (A) Cells were stained using PerCP-Cy5.5 mouse anti-human CD56 (clone B159) or PerCP-Cy5.5-conjugated mouse IgG1, k isotype control. (B) Cells were stained using APC mouse anti-human IL12Rβ1, (clone 2.4E6) or APC-conjugated mouse IgG1, k isotype control. (C). Cells were stained using PE mouse anti-Stat4 (pY693) (clone 38/p-Stat4) or PE-conjugated mouse IgG2b, k isotype control. (D) Cells were stained using BV421 mouse anti-human IFNγ (clone: B27) or BV421-conjugated mouse IgG1, k isotype control. In (C) and (D), cells were stimulated by media, heparin alone (10 μg/mL), IL-12 alone (200 pg/mL), or both IL-12 (200pg/mL) and heparin (10 μg/mL) for 15 minutes (C) or 12h (D) before performing intracellular staining. (E) Dot plots describe positive percentages of CD56, IL-12Rβ1, pSTAT4 (under induction of IL-12 and

heparin), and IFN-γ (under induction of IL-12 and heparin) in mutant NK-92MI cells (subclone

7) and wild-type NK-92MI cells (**p<0.01, ***p<0.001, ****p<0.0001 via two-tailed t test).

Data were acquired using a FACSCelesta cytometer, and analyzed by FlowJo software.

Experiments were performed in triplicate and repeated three times with similar results.
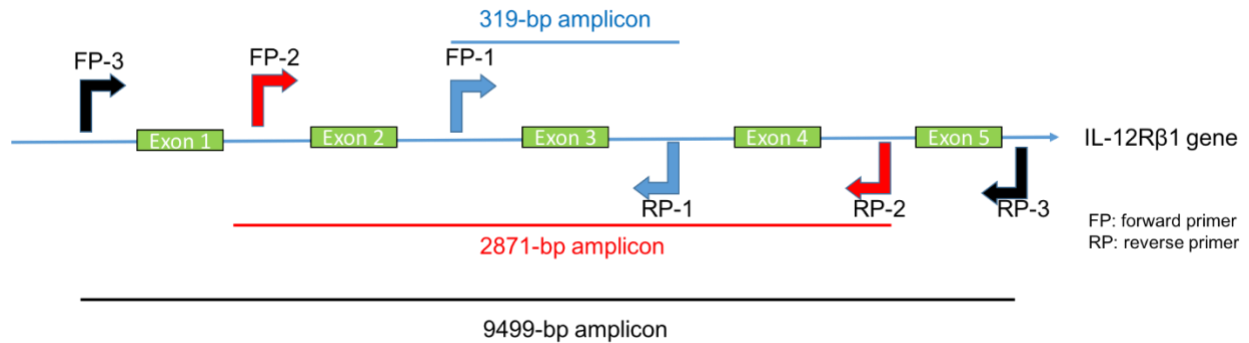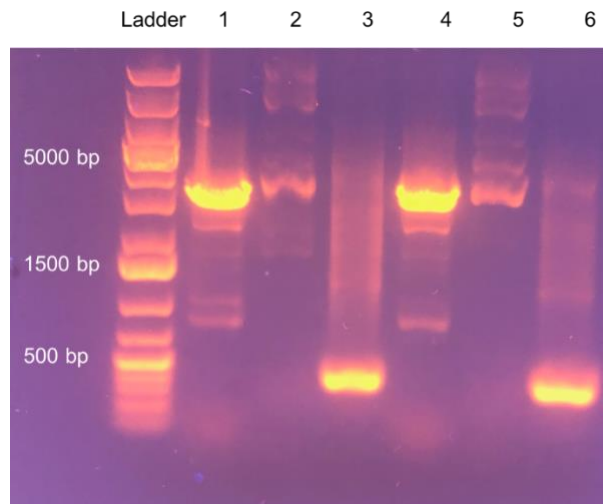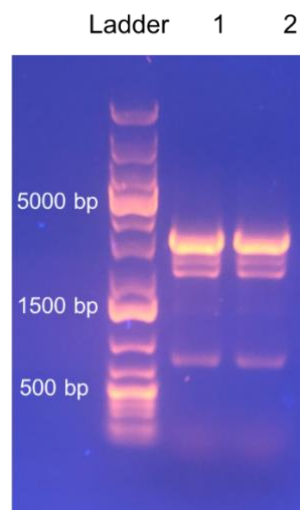
A
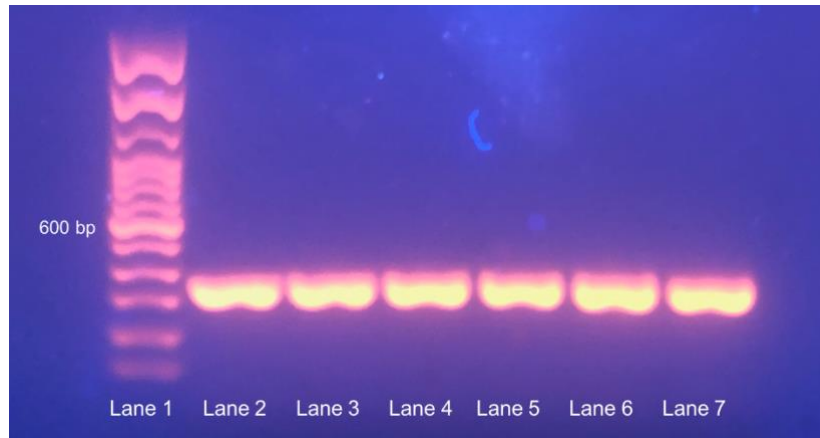
B
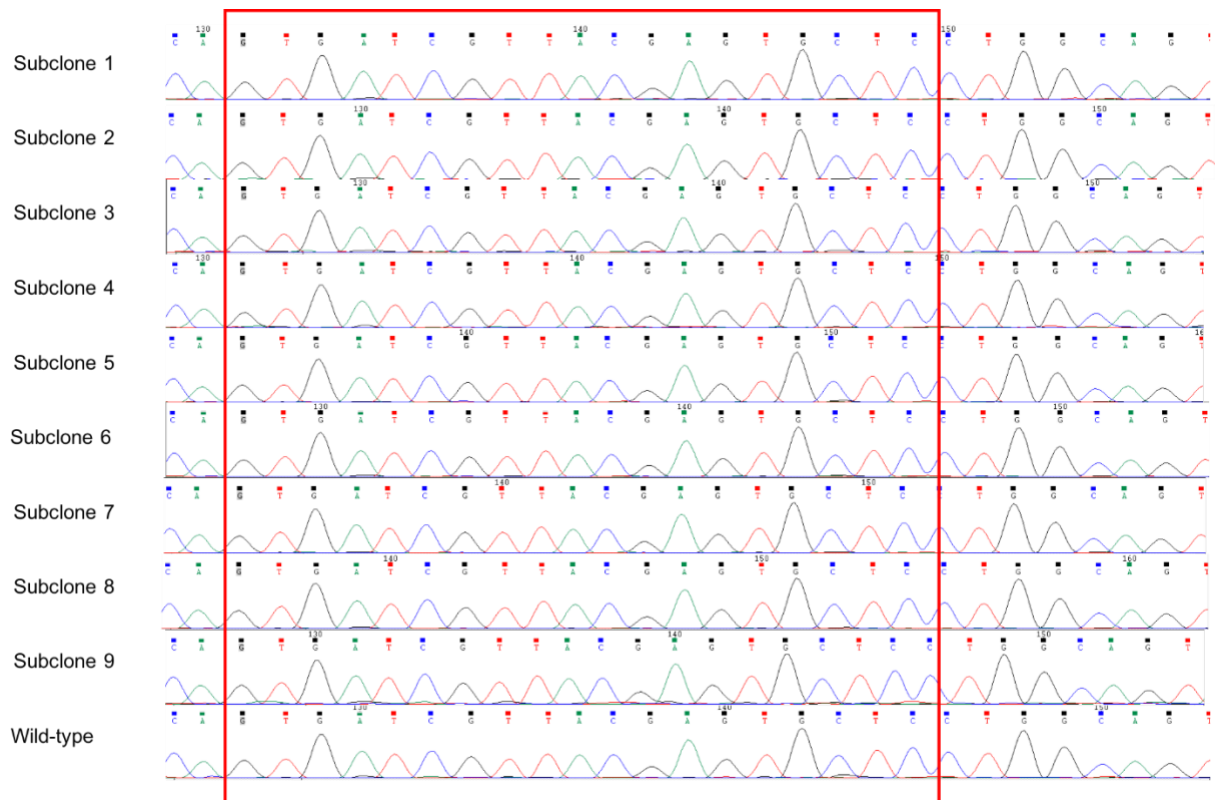
C

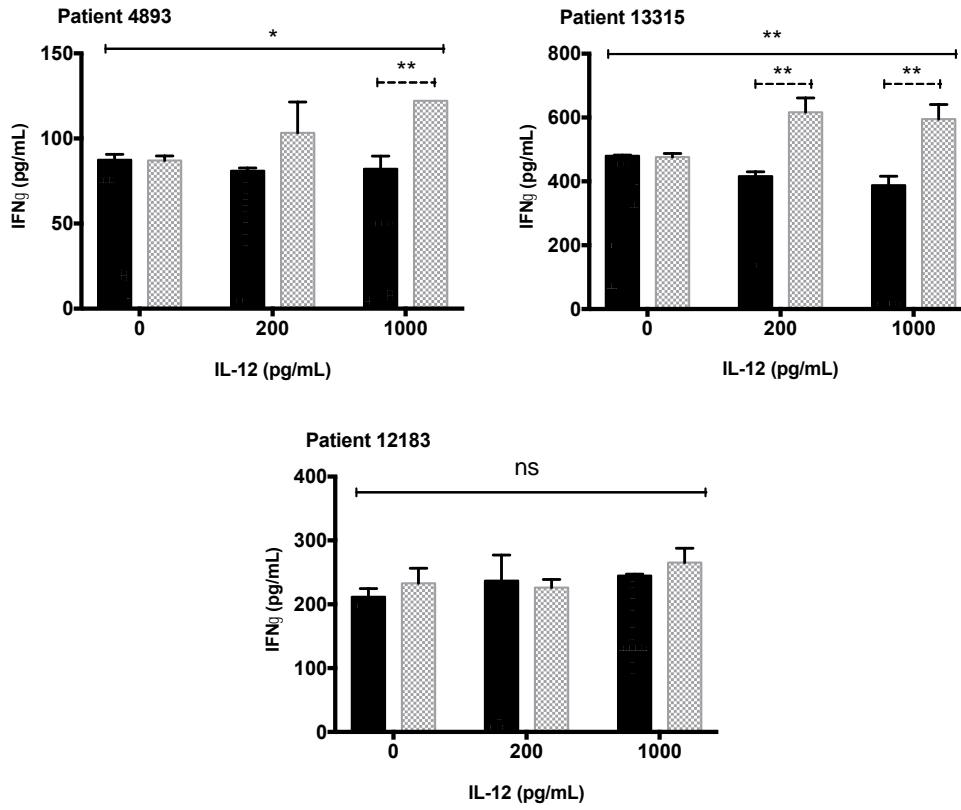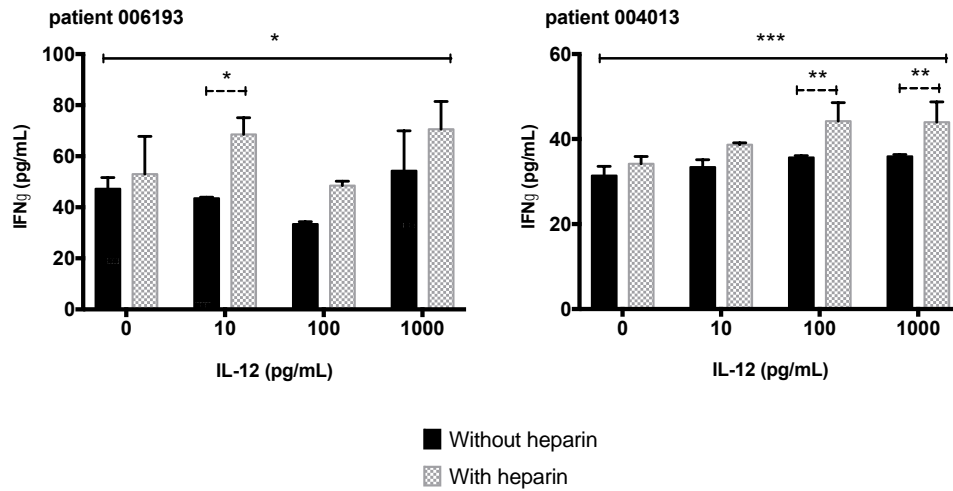**D**   **E**

Figure A.1.5. Amplification and sequencing of exon 3, IL12Rβ1 gene of mutant and wild-type NK-92MI cells. (A) PCR products of exon 3, IL12Rβ1 amplified from genomic DNA of subclone 5 (lane 2), subclone 6 (lane 3), subclone 7 (lane 4), subclone 8 (lane 5), clone 6 (lane 6), and wild-type cells (lane 7). (B) Sequencing comparison at CRIPSR/Cas9-targeting sequences (5'-GTGATCGTTACGAGTGCTCC-3') located on exon 3, IL-12Rβ1 gene of subclone cells and wild-type cells. (C) Map of amplifications in IL-12Rβ1 gene. (D) PCR products of 2871-bp (lane 1 and lane 4), 9499 bp (lane 2 and lane 5), and 319 bp (lane 3 and lane

6) amplifications in exon 3, IL-12Rβ1 gene of subclone 7 (lane 1 - 3) and wild-type cells (lane 4

- 6). (E) PCR products of 2871-bp amplification in exon 3, IL-12Rβ1 gene of subclone 7 (lane 1)

and wild-type cells (lane 2). (D) annealing temperature was set at 62.4 C. (E) annealing

temperature was set at 64.4 C.

A

Patient 4893

Patient 13315

Patient 12183

B

patient 006193

patient 004013

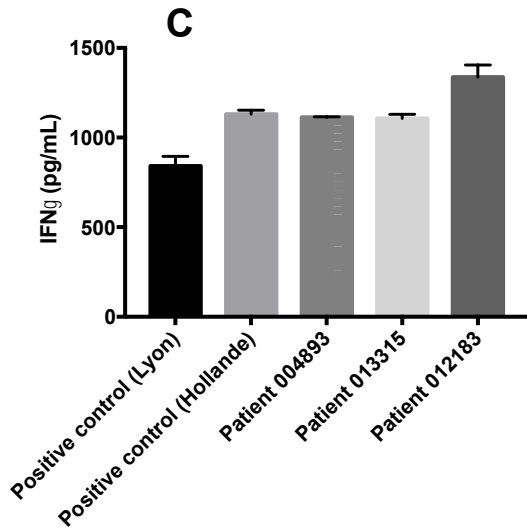■ Without heparin
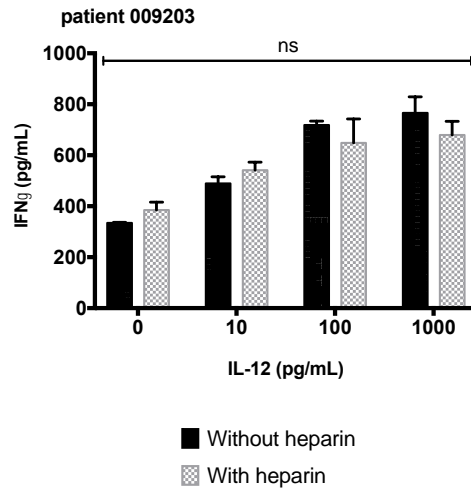▨ With heparin

157

B (cont.)

Figure A.1.6. The effect of heparin on IL-12 bioactivity on MSMD patient PBMCs. The

production of IFN-γ produced by MSMD patient PBMCs in response to IL-12 alone and IL-12

plus heparin in (A) the first batch (patient 4893, 13315, and 12183) or (B) the second batch

(patient 6193, 4013, 9203). (C) The production of IFN-γ 2 healthy donors and 3 MSMD patients

of the first batch that were induced by PMA/Ionomycin. IFN-γ production was measured after

48-hour exposure to increasing concentrations of IL-12 for (A and B) or a fixed concentration of

PMA/Ionomycin (0.08 μM PMA and 1.34 μM Ionomycin) for (C). Heparin concentration was fixed at 10 μg/mL. IFN-γ concentrations were measured via ELISA. For global response of patients, treatment of heparin and IL-12 showed no recovery of IL-12 bioactivity in comparison with IL-12 alone ($p>0.5$ via two-way ANOVA, solid line). For particular analysis on each patient, heparin slightly recovered the bioactivity of IL-12 in PBMCs isolated from two MSMD patients (*$p<0.05$ vs. IL-12 alone via two-way ANOVA, solid line – patient 4893 and **$p<0.01$ vs. IL-12 alone via two-way ANOVA, solid line – patient 13315, *$p<0.05$ vs. IL-12 alone). Tukey's posttest was used to compare the production of IFN-γ in response to IL-12 alone vs. IL-12 plus heparin at each specific IL-12 concentration (dashed line, *$p<0.05$, **$p<0.01$). Heparin did not recover IL-12 bioactivity in patient 12183 and patient 9203 ($p>0.05$ vs. IL-12 alone via two-way ANOVA, solid line). Data points represent mean ± standard deviation of triplicate measurements. Three experiments were repeated with similar results.

REFERENCES

1. Gubler U, Chua AO, Schoenhaut DS, Dwyer CM, McComas W, Motyka R, Nabavi N, Wolitzky AG, Quinn PM, Familletti PC, et al. 1991. Coexpression of two distinct genes is required to generate secreted bioactive cytotoxic lymphocyte maturation factor. *Proc Natl Acad Sci U S A* 88: 4143-7

2. Wolf SF, Temple PA, Kobayashi M, Young D, Dicig M, Lowe L, Dzialo R, Fitz L, Ferenz C, Hewick RM, et al. 1991. Cloning of cDNA for natural killer cell stimulatory factor, a heterodimeric cytokine with multiple biologic effects on T and natural killer cells. *J Immunol* 146: 3074-81

3. Schoenhaut DS, Chua AO, Wolitzky AG, Quinn PM, Dwyer CM, McComas W, Familletti PC, Gately MK, Gubler U. 1992. Cloning and expression of murine IL-12. *J Immunol* 148: 3433-40

4. Chizzonite R, Truitt T, Desai BB, Nunes P, Podlaski FJ, Stern AS, Gately MK. 1992. IL-12 receptor. I. Characterization of the receptor on phytohemagglutinin-activated human lymphoblasts. *J Immunol* 148: 3117-24

5. Desai BB, Quinn PM, Wolitzky AG, Mongini PK, Chizzonite R, Gately MK. 1992. IL-12 receptor. II. Distribution and regulation of receptor expression. *J Immunol* 148: 3125-32

6. Casanova JL, Abel L. 2002. Genetic dissection of immunity to mycobacteria: the human model. *Annu Rev Immunol* 20: 581-620

7. Bustamante J, Boisson-Dupuis S, Abel L, Casanova JL. 2014. Mendelian susceptibility to mycobacterial disease: genetic, immunological, and clinical features of inborn errors of IFN-gamma immunity. *Semin Immunol* 26: 454-70

8. Fieschi C, Bosticardo M, de Beaucoudrey L, Boisson-Dupuis S, Feinberg J, Santos OF, Bustamante J, Levy J, Candotti F, Casanova JL. 2004. A novel form of complete IL-12/IL-23 receptor beta1 deficiency with cell surface-expressed nonfunctional receptors. *Blood* 104: 2095-101

9. de Beaucoudrey L, Samarina A, Bustamante J, Cobat A, Boisson-Dupuis S, et al. 2010. Revisiting human IL-12Rbeta1 deficiency: a survey of 141 patients from 30 countries. *Medicine (Baltimore)* 89: 381-402

10. Presky DH, Yang H, Minetti LJ, Chua AO, Nabavi N, Wu CY, Gately MK, Gubler U. 1996. A functional interleukin 12 receptor complex is composed of two beta-type cytokine receptor subunits. *Proc Natl Acad Sci U S A* 93: 14002-7

11. Jayanthi S, Koppolu B, Smith SG, Jalah R, Bear J, Rosati M, Pavlakis GN, Felber BK, Zaharoff DA, Kumar TK. 2014. Efficient production and purification of recombinant human interleukin-12 (IL-12) overexpressed in mammalian cells without affinity tag. *Protein Expr Purif* 102: 76-84

12. Jayanthi S, Koppolu BP, Nguyen KG, Smith SG, Felber BK, Kumar TKS, Zaharoff DA. 2017. Modulation of Interleukin-12 activity in the presence of heparin. *Sci Rep* 7: 5360

13. Wu C, Ferrante J, Gately MK, Magram J. 1997. Characterization of IL-12 receptor beta1 chain (IL-12Rbeta1)-deficient mice: IL-12Rbeta1 is an essential component of the functional mouse IL-12 receptor. *J Immunol* 159: 1658-65

14. Wu C, Wang X, Gadina M, O'Shea JJ, Presky DH, Magram J. 2000. IL-12 receptor beta 2 (IL-12R beta 2)-deficient mice are defective in IL-12-mediated signaling despite the presence of high affinity IL-12 binding sites. *J Immunol* 165: 6221-8

15. de Oliveira Neto M, Ferreira JR, Jr., Colau D, Fischer H, Nascimento AS, Craievich AF, Dumoutier L, Renauld JC, Polikarpov I. 2008. Interleukin-22 forms dimers that are recognized by two interleukin-22R1 receptor chains. *Biophys J* 94: 1754-65

16. Jones BC, Logsdon NJ, Walter MR. 2008. Structure of IL-22 bound to its high-affinity IL-22R1 chain. *Structure* 16: 1333-44

17. Collison LW, Delgoffe GM, Guy CS, Vignali KM, Chaturvedi V, Fairweather D, Satoskar AR, Garcia KC, Hunter CA, Drake CG, Murray PJ, Vignali DA. 2012. The composition and signaling of the IL-35 receptor are unconventional. *Nat Immunol* 13: 290-9

18. Turner AJ, Aggarwal P, Miller HE, Waukau J, Routes JM, Broeckel U, Robinson RT. 2015. The introduction of RNA-DNA differences underlies interindividual variation in the human IL12RB1 mRNA repertoire. *Proc Natl Acad Sci U S A* 112: 15414-9

19. Gokturk B, Reisli I, Caliskan U, Oleaga-Quintas C, Deswarte C, Turul-Ozgur T, Burgucu D, Migaud M, Casanova JL, Picard C, Bustamante J. 2016. Infectious diseases, autoimmunity and midline defect in a patient with a novel bi-allelic mutation in IL12RB1 gene. *Turk J Pediatr* 58: 331-6

APPENDIX 2: THE ENHANCING EFFECT OF HEPARIN ON MOUSE IL-23 BIOACTIVITY
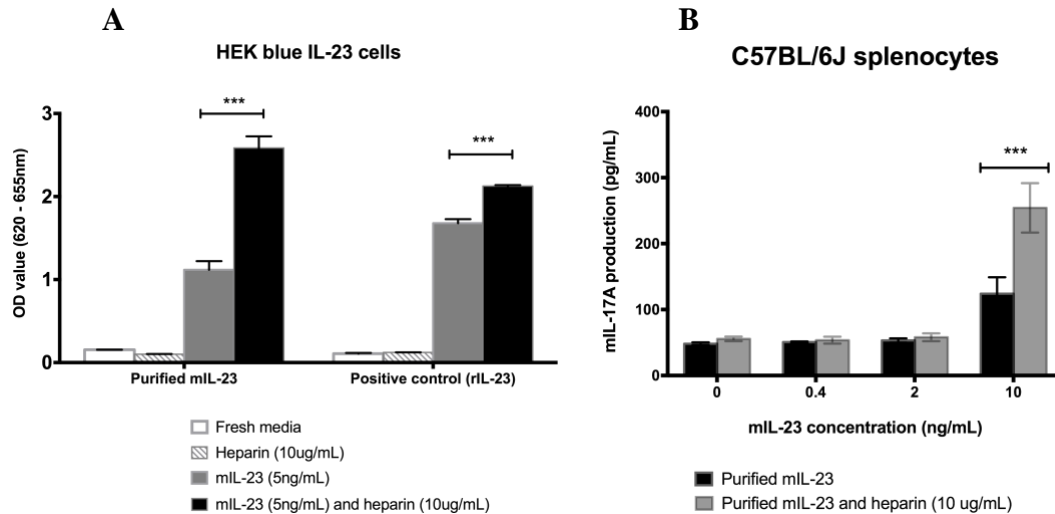
Appendix 2. The enhancing effect of heparin on mouse IL-23 bioactivity. The production of (A) alkaline phosphatase by HEK-Blue[TM] IL-23 cells or (B) mouse IL-17A by splenocytes isolated from C57BL/6J mouse was measured after exposure to a fixed concentration of mIL-23 (5 ng/mL) for (A) or a range of mouse IL-23 concentration for (B). Heparin was used at a fixed concentration of 10 μg/mL. Purified mouse IL-23 is the recombinant protein purified by our lab. Positive control of mouse IL-23 (rIL-23) is the commercial recombinant protein from market place. Production of alkaline phosphatase was measured by a colorimetric assay that detects the colored product converted by alkaline phosphatase. Mouse IL-17A was measured via ELISA. Heparin enhances the bioactivity of mouse IL-23 in HEK-Blue[TM] IL-23 cells and C57BL/6J splenocytes (***$p < 0.05$ via two-tailed t test).

APPENDIX 3: THE INHIBITORY EFFECT OF P40 ON IL-12 BIOACTIVITY IS REDUCED BY HEPARIN
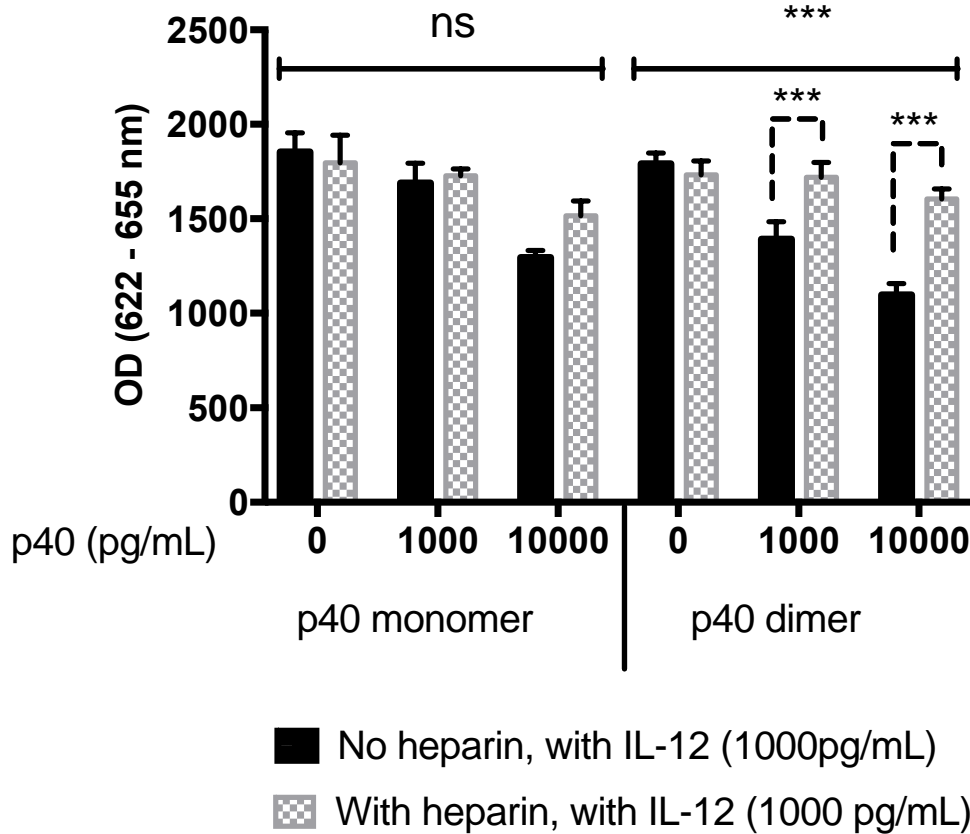
Appendix 3. The inhibitory effect of p40 on IL-12 bioactivity is reduced by heparin. The production of (A) alkaline phosphatase by HEK-Blue[TM] IL-12 cells was measured after exposure to a fixed concentration of IL-12 (1000 pg/mL) and a fixed concentration of heparin (10 μg/mL) with a range concentrations of mouse p40 monomer, p40 dimer. Production of alkaline phosphatase was measured by a colorimetric assay that detects the colored product converted by alkaline phosphatase. Heparin reduced the inhibitory effect of p40 on IL-12 bioactivity in HEK-Blue[TM] IL-23 cells (***$p<0.0001$ via two-way ANOVA, solid line), ns: not significant. Tukey's posttest was used to compare the reduction of p40 inhibitory effect on IL-12 bioactivity by heparin at specific p40 concentration (dashed line, ***$p<0.0001$).